NISTIR 5177

The ENDF/B-VI Neutron Cross Section Measurement Standards

A. D. Carlson
W. P. Poenitz*
G. M. Hale**
R. W. Peelle***
D. C. Dodder**
C. Y. Fu***
W. Mannhart****

U.S. DEPARTMENT OF COMMERCE
Technology Administration
National Institute of Standards
and Technology
Gaithersburg, MD 20899

*Argonne National Laboratory-West
**Los Alamos National Laboratory
***Oak Ridge National Laboratory
****Physikalisch-Technische Bundesanstalt

Sponsored in part by the
U. S. Department of Energy

NIST

NISTIR 5177

The ENDF/B-VI Neutron Cross Section Measurement Standards

A. D. Carlson
W. P. Poenitz*
G. M. Hale**
R. W. Peelle***
D. C. Dodder**
C. Y. Fu***
W. Mannhart****

U.S. DEPARTMENT OF COMMERCE
Technology Administration
National Institute of Standards
and Technology
Gaithersburg, MD 20899

*Argonne National Laboratory-West
**Los Alamos National Laboratory
***Oak Ridge National Laboratory
****Physikalisch-Technische Bundesanstalt

Sponsored in part by the
U. S. Department of Energy

May 1993

U.S. DEPARTMENT OF COMMERCE
Ronald H. Brown, Secretary

NATIONAL INSTITUTE OF STANDARDS AND TECHNOLOGY
Raymond G. Kammer, Acting Director

PREFACE

The Standards Subcommittee of the U.S. Cross Section Evaluation Working Group (CSEWG) encourages, performs, coordinates, oversees and approves evaluations of cross section measurement standards for the Evaluated Nuclear Data Files (ENDF/B). This report describes the process used to obtain the standards evaluations for the sixth version of ENDF/B. New evaluations have been produced for each of the cross section standards and the spontaneous fission neutron spectrum for ^{252}Cf.

ABSTRACT

This document provides information on the neutron cross section standards placed in the ENDF/B-VI library. The H(n,n), ^{3}He(n,p), and C(n,n) cross sections were each obtained from well established R-matrix analysis techniques. The additional standards, i.e., the ^{6}Li(n,t), ^{10}B(n,α), ^{10}B(n,α_1), Au(n,γ), and ^{235}U(n,f) cross sections, were obtained with a new method. The new method involves combining the results of a simultaneous evaluation and R-matrix analyses. Contained herein is a discussion of the development of the method, a description of the evaluation process, some information on the various experiments used in the analyses, comparisons of the R-matrix, simultaneous evaluation and combination results, and comparisons to ENDF/B-V. Tables of numerical data are given for each of the cross section standards. Also the new ENDF/B-VI evaluation for the spontaneous fission neutron spectrum for ^{252}Cf is given.

KEYWORDS: Au(n,γ); ^{10}B(n,α); ^{10}B(n,α_1); C(n,n); combining procedure; ENDF/B-VI Neutron Cross Section Standards; H(n,n); ^{3}He(n,p); ^{6}Li(n,t); R-matrix; simultaneous evaluation; standard; ^{235}U(n,f); ^{252}Cf spontaneous fission neutron spectrum

Table of Contents

List of Tables

1. INTRODUCTION

The measurement of neutron cross sections can often be significantly simplified by using a cross section standard which eliminates the need for a direct measurement of the neutron fluence. A cross section measurement is then made by placing both the sample which is used for the cross section determination and the sample utilizing the cross section standard in the same neutron beam. For thin samples the ratio of counting rates is proportional to the ratio of the cross section to be measured to that of the standard. The accuracy of such a cross section measurement is limited by the uncertainty in the standard cross section relative to which it is measured. Normally such standards apply only in certain energy regions, where their cross sections are relatively smooth and well known. Improvements in the standard cause all cross sections measured relative to that standard to be improved. This is the reason for the emphasis on increasing the quality of the neutron cross section standards. This also explains why they must be evaluated prior to completion of a new version of an evaluated nuclear data file such as ENDF/B. The standards include H(n,n), ^{3}He(n,p), ^{6}Li(n,t), ^{10}B(n,α), ^{10}B(n,α_1), C(n,n), Au(n,γ), and ^{235}U(n,f).

2. EVALUATION METHODS

Measurement programs have continuously improved the data base of the standards. Evaluations have also improved with time; however, there have been significant weaknesses in earlier evaluations. In some cases evaluations have been performed by qualitatively or semi-quantitatively combining different kinds of data sets by simply drawing smooth curves through the existing data. Such evaluations are difficult to document and it is not clear how to determine meaningful uncertainties and covariance information.

In previous evaluations for ENDF/B, a hierarchical approach was followed. The lighter element cross section standards were generally considered to be better known. The H(n,n) cross section was considered the best known standard and was evaluated first and independently of the other standards. This standard is considered so well known that measurements relative to it are often called absolute measurements. The ^{6}Li(n,t) cross section evaluation was performed next. The only ^{6}Li(n,t) data which were used were absolute measurements or those measured relative to the H(n,n) standard which were converted to cross sections using the adopted hydrogen evaluation. Then the ^{10}B+n standard cross sections were evaluated. The only ^{10}B data which were used were absolute measurements and those relative to H(n,n) and ^{6}Li(n,t) which were converted using the new hydrogen and lithium evaluations. This process was continued for each of the standards. This method for using ratio measurements does not use all the information available. It does not include absolute and ratio data on the same basis as they were measured. For example, a ratio of the ^{10}B(n,α) to the ^{6}Li(n,t) cross sections would be used in the ^{10}B(n,α) cross section evaluation but not in the ^{6}Li(n,t) evaluation.

The difficulties with the hierarchical evaluation procedure and the successes already realized using comprehensive objective data combination techniques [1] led to the seeking out of a more global approach for ENDF/B-VI than had been used earlier. With such "objective" techniques one relies on least-squares or similar procedures to combine the input data consistent with experimental uncertainties. Each experiment must be evaluated in detail to represent it fairly in this process. The method should be able to handle the full information content of the

data base. Thus data would be evaluated simultaneously to assure proper use of the available information. Ratio measurements of standard cross sections would have an impact on each of the cross sections in the ratio. Correlations among the experimental data would be taken into account in the simultaneous evaluation.

It was recognized that there are some absolute cross section measurements of similar quality which are not normally considered standards. For those cases where accurate ratio measurements of these cross sections to those of standards exist, the evaluation of that cross section should be performed simultaneously with the standards evaluation since it in principle will affect the values of the evaluated standards and their uncertainties. Thus the standards and other well-known cross sections would be evaluated with the same procedure. As a practical matter the addition of data from many nuclides can become a very immense problem though it can be handled. Very few cross sections would have any appreciable impact on the determination of a standard cross section except other standards. Including data on $^{238}U(n,\gamma)$, $^{238}U(n,f)$ and $^{239}Pu(n,f)$ could improve the quality of the standards evaluations since precise absolute measurements exist and many ratio measurements to the standards are available. There is of course the benefit that evaluations of these important nuclear reactor fuel cross sections will be obtained. It was also felt that the evaluation should include the use of average cross sections over selected energy intervals for appropriate heavy-element cross sections to take advantage of data sets that extend down to thermal energies.

The presence of shape measurements which extend to thermal energies in addition to absolute data imply that an evaluation of the standards will provide information on the thermal constants. In principle the thermal constants could be evaluated simultaneously with the standards. Including the results of a completed thermal constants evaluation, with the associated variance-covariance information, in the standards evaluation process is equivalent to this. Therefore either the thermal constants data base or the complete results of a thermal cross section evaluation should be used as input to this evaluation.

It was perceived that it is important to retain fits to theory in the evaluation of the light element standards. This could be implemented with R-matrix analyses. Such analyses can provide coupling to reaction theory and give a smooth meaningful analytical expression for the energy dependance of the cross sections. The accurate determination of R-matrix parameters does however require a rather large data base. Data in addition to angle integrated neutron cross sections such as differential cross sections, polarizations, and charged particle measurements involving the same compound nucleus can have a significant impact on the standard cross sections. In the R-matrix analysis, different reactions leading to the same compound nucleus are linked by unitarity to the standard cross section. This condition imposes constraints on the standard cross section which are particularly strong near resonances.

The ideal way to perform this evaluation would be to develop a single fitting program that would use all the experimental data involving these reactions. The evaluation should provide output covariance data which is consistent with a cross section evaluation that weights input data with the inverse of its variance-covariance matrix. The output for the light elements would be R-matrix parameters, while average cross sections at many energies would be output for the heavy element cross sections. It was decided that the H(n,n), $^{3}He(n,p)$ and C(n,n) cross sections would not be evaluated in this analysis. For H(n,n) the cross sections were considered very well known so that data on the other nuclides would have very little impact on it. This cross section

was thus treated as absolute in the evaluation. For ^{3}He(n,p) and C(n,n) very few ratio measurements to other standards exist so little would be gained by putting them into the evaluation. Separate R-matrix evaluations were performed at a later time for each of these standards.

The single fitting program was not implemented. Instead the decision was made that the evaluation would be the result of combining a simultaneous evaluation using generalized least squares with separate R-matrix analyses. This procedure took advantage of the strengths of the two different analysis modes which can make use of separate classes of experimental information to impact on the evaluation of the standard cross sections. It should be noted that under proper conditions a global fitting procedure could be achieved by combining the output of the simultaneous and R-matrix analyses.

3. EVALUATION PROCEDURE FOR H(n,n), ^{3}He(n,p), AND C(n,n)

For ENDF/B-VI, the hierarchical approach was retained for H(n,n) to the extent that measurements relative to it were treated as absolute. A nucleon-nucleon cross section evaluation by Dodder and Hale [2] was performed. This charge independent R-matrix evaluation, which was adopted for ENDF/B-VI, made use of a large data base of n-p and p-p experimental data at energies below 30 MeV. A summary of the channel configuration and data fitting characteristics of the analysis is given below.

Channel	Maximum Angular Momentum ℓ_{max}	Channel Radius a_c (fm)
n-p	3	3.26
p-p	3	3.26

Reaction	Number of Observable Types	Number of Data Points	χ^2
n-p scattering	3	448	407
p-p scattering	4	388	399
Totals:	7	836	806

Number of parameters = 33 $\Rightarrow$ χ^2 per degree of freedom = 1.004*

*Including recent corrections [3] to the 16.9 MeV n-p analyzing power data of Tornow *et al.* [4] reduces the overall χ^2 per degree of freedom of the fit to 0.9988.

This data base includes measurements not used in the Hopkins-Breit [5] phase-shift analysis which was the basis for the hydrogen evaluation for versions II, III, IV, and V of ENDF/B. This evaluation gives a representation of the n-p and p-p experimental data in the 0-30 MeV energy range that is comparable to or better than that of other recent work [6],[7]. The new analysis also gives reasonable results for newly measured quantities, such as the polarization transfer data from Karlsruhe [8].

The charge independent model used takes the isospin-1 reduced-width amplitudes in the R-matrix describing n-p scattering to be identically the same as those describing p-p scattering. The energy eigenvalues in the two systems are taken to differ only by an overall constant Coulomb energy shift. This simple model allows the p-p scattering data to influence the n-p fit. Where measurements of the cross section and analyzing powers for the p-p and n-p reactions are compared, the data are quite different at the same energy. These differences, coming primarily from Coulomb terms and symmetrization properties of the two systems, are well reproduced by the charge-independent calculation. The new data, including a coherent scattering length evaluation by Holden [9] leads to changes in the shapes of the angular distribution compared to those of ENDF/B-V.

Two quantities often used to characterize the center of mass n-p angular distribution near 14 MeV are the back-angle cross section, $\sigma(180°)$, and the asymmetry ratio $R = \sigma(180°)/\sigma(90°)$. The ENDF/B-VI evaluation gives for these quantities at $E_n = 14.1$ MeV:

$$\sigma(180°) = 58.89 \pm 0.60 \text{ mb} \quad , \quad R = 1.093 \pm 0.010 \quad .$$

The value of R is in agreement with most previous measurements. However, it disagrees with a measurement made after the completion of the evaluation by Ryves and Kolkowski [10], of $R = 1.053 \pm 0.015$, which is consistent with the ENDF/B-V value. The measurement of [10] was actually a determination at 14.47 MeV of the ratio of the 180° to 110° cross sections from which a value of R was derived. The ENDF/B-VI values of the back-angle cross section and asymmetry ratio, on the other hand, are in excellent agreement with an evaluation of the 14.1 MeV experimental data that was done in 1982 by Vincour, Bém, and Presperin [11].

The ENDF/B-VI total elastic cross section, its uncertainty and the Legendre coefficients for atomic hydrogen are given in tables 1 and 2. Use is confined to energies sufficiently high so that molecular binding effects do not alter the cross sections. Complete covariance files are not presently available for the H(n,n) cross section. In figure 1, measurements and the ENDF/B-V evaluation [5],[12] are compared with the ENDF/B-VI results for the angular distribution for neutron scattering at 14.1 MeV neutron energy. The difference in the cross sections at 180 degrees in the center of mass system between ENDF/B-VI and ENDF/B-V is significant. This angle corresponds to proton recoils at zero degrees in the laboratory system, which is commonly used for proton recoil detectors. In figure 2, precise hydrogen total cross section measurements and the ENDF/B-VI evaluation are compared with the ENDF/B-V evaluation. The new evaluation is in somewhat better agreement with the measurements than the ENDF/B-V results. There is also a reduction in the uncertainty of the total cross section in the new evaluation, compared with that of ENDF/B-V.

The evaluation of the ^{3}He(n,p) cross section which is in ENDF/B-V is really quite dated since it was originally performed in 1968. A new evaluation was recently done by Hale [13] using all possible two body reactions in the ^{4}He system. As can be seen in figure 3, the new evaluation is in much better agreement with the newer measurements than ENDF/B-V. The measurements shown in figure 3 were not included in the ENDF/B-VI evaluation. This cross section is tabulated in table 3 along with its uncertainty. Complete covariance files are not presently available for the ^{3}He(n,p) cross section.

The carbon standard is the scattering cross section for natural carbon for energies less than 1.8 MeV. In ENDF/B-V, the evaluation was based on an R-matrix analysis for ^{12}C using natural carbon data. In the use of this standard, one had to note that two resonances in ^{13}C could

cause problems since they are not included in the evaluation. A revision of the ENDF/B-V evaluation by Fu [14] was made to include the effects of these two resonances. The revision was also an R-matrix analysis based on the available data. This evaluation was accepted for use in ENDF/B-VI. In figure 4, the ENDF/B-VI carbon total cross section evaluation is shown compared with the data of Heaton [15] and the ENDF/B-V evaluation near the 152.9 keV resonance in ^{13}C. The Heaton data were obtained with a natural carbon sample. In figure 5, the ENDF/B-VI evaluation is compared with that of ENDF/B-V near the 1.736 MeV resonance. Though this structure is often referred to as one resonance, it is actually composed of a narrow d-wave resonance superimposed almost directly over a broader s-wave minimum. The carbon total elastic cross section, its uncertainty and the Legendre coefficients are given in tables 4 and 5. The changes between ENDF/B-V and ENDF/B-VI are small enough so that the covariance files from version V will be used for version VI.

4. GLOBAL EVALUATION PROCEDURE

Most of the standards and other important cross sections were evaluated by combining the results of a simultaneous evaluation and R-matrix analyses. An energy grid was defined for the evaluation which is the same for all cross sections involved in the evaluation and the fitting parameters are the values of the cross sections for these grid points.

It was decided that the generalized least squares program GMA, which is described in more detail in reference [1] would be used for the simultaneous evaluation. A related type of analysis had been used successfully for the evaluation of the $^{235}U(n,f)$ cross section for ENDF/B-V. For the GMA evaluation, the cross sections which were evaluated are $^{6}Li(n,t)$, $^{6}Li(n,n)$, $^{10}B(n,\alpha_0)$, $^{10}B(n,\alpha_1)$, $^{10}B(n,n)$, $Au(n,\gamma)$, $^{235}U(n,f)$, $^{238}U(n,f)$, $^{238}U(n,\gamma)$, and $^{239}Pu(n,f)$. The input data for this evaluation was composed of two independent subsets. One of these subsets is a large data base of pointwise measurements assembled at Argonne National Laboratory. The references for this data base are given in appendix A. This data base includes both shape and absolute cross section measurements and their ratios. Also total cross section measurements for ^{6}Li and ^{10}B are contained in the data base since the scattering and reaction data are interrelated in these measurements. Measurements of the ^{235}U and ^{239}Pu fission cross sections in the ^{252}Cf spontaneous fission neutron spectrum were also included in the data base. These data can be obtained with high accuracy and are only weakly dependent on the uncertainties in the ^{252}Cf spontaneous neutron fission spectrum. These data can have an important effect on the normalization of the evaluated cross sections. A considerable effort was directed at examining the various experiments looking for corrections, etc. which were not fully documented in the published papers. Ratio measurements other than those to the hydrogen standard which have been converted to cross section values were reinstated to the originally measured quantities. Measurements relative to hydrogen were converted using the ENDF/B-VI values for the total elastic cross section. Perhaps the most difficult part of this work was the determination for each experiment of the uncertainties and correlations in that experiment and correlations with other experiments. This information was used to form covariance matrices for the measurements so that a full covariance analysis could be performed for the evaluation. Rather than include the entire data base for the thermal constants, the results of the recent evaluation by Axton [16], with the associated variance-covariance data were used as the second independent data input subset to the GMA analysis. It should be noted that the $Au(n,\gamma)$ and $^{10}B(n,\alpha)$ cross sections at thermal were treated as constants in the Axton evaluation though they are parameters in the present evaluation procedure.

The evaluations of the ^{6}Li and ^{10}B cross sections for both versions IV and V of ENDF/B have been produced with the R-matrix coupled channel program EDA [17]. It was decided that this program would be a suitable R-matrix code for the present evaluation process if all experiments which are correlated and all ratio measurements (except those to the hydrogen standard) were put into the data base used for the simultaneous evaluation. The R-matrix fits were done at Los Alamos National Laboratory. In these analyses the experimental data are used as measured with weighting normally based on the quoted uncertainties. It is assumed that no correlations other than the overall normalization are present among the data from a particular experiment. The code uses automated search routines to minimize chi-square of the fits to the input data. In addition to the R-matrix parameters, derivatives of fitted cross sections with respect to these parameters and the covariance matrix are available as output. Following the fitting process, the cross sections were calculated for the same energy grid as is used for the simultaneous evaluation to permit the combination of the results. The parameters deduced from these analyses provide neutron cross sections well beyond the standards region. The $^{6}Li+n$ and $^{10}B+n$ analyses were each done separately with this code. For the ^{7}Li system the data base includes ^{6}Li total, $^{6}Li(n,n)$ integrated, $^{6}Li(n,n)$ differential, $^{6}Li(n,n)$ polarization, $^{6}Li(n,t)$ integrated, $^{6}Li(n,t)$ differential, $^{4}He(t,t)$ differential, and $^{4}He(t,t)$ polarization data. For the ^{11}B system the data base includes ^{10}B total, $^{10}B(n,n)$ integrated, $^{10}B(n,n)$ differential, $^{10}B(n,n)$ polarization, $^{10}B(n,\alpha_0)$ integrated, $^{10}B(n,\alpha_0)$ differential, $^{10}B(n,\alpha_1)$ integrated, $^{10}B(n,\alpha_1)$ differential, $^{7}Li(\alpha,\alpha_0)$ differential, $^{7}Li(\alpha,\alpha_1)$ differential, and $^{7}Li(\alpha,n)$ differential data. The references for the ^{7}Li and ^{11}B data bases are given in appendix B.

Altogether more than 10,000 data points were fit with 109 R-matrix parameters and 935 pointwise cross sections and parameters. The 935 pointwise cross sections and parameters include 406 pointwise cross sections for reactions other than with boron and lithium, 370 pointwise cross sections for boron and lithium reactions, 22 thermal constants, and 137 normalization values for shape data.

A procedure for combining the simultaneous and R-matrix evaluations was determined. It is described in appendix C. It is based on the observation that the individual fitting processes described above include computation of sums that can be combined to produce the same overall output parameters as would have been obtained from a global least squares fit of all the input data in terms of R-matrix parameters for the $^{6}Li+n$ and $^{10}B+n$ systems and pointwise values for the other cross sections. A program for performing the combination was written at Oak Ridge National Laboratory. Methods were studied to handle correlations between data sets used in the R-matrix and simultaneous evaluations. It was concluded that it would not be difficult to handle correlations if only a small amount of common data were present, but it would become increasingly difficult as more common data are present in the two evaluation processes. For simplicity then, the boron and lithium experimental data were separated into two uncorrelated groups, one to be used in the R-matrix analyses, called segment 1, and the other in the simultaneous analysis, called segment 2. All ratio measurements other than those to the hydrogen standard were used in the simultaneous evaluation. Experiments which are correlated were put into the segment 2 data base. The combining procedure makes use of the variance-covariance matrices from the separate fits as well as the derivatives with respect to the evaluation parameters of the fitted values corresponding to the input data elements. The input data sets are thus taken into account in a consistent manner. The output is adjusted R-matrix parameters for the $^{6}Li+n$ and $^{10}B+n$ systems and final point cross sections for the remaining reactions. The adjusted R-matrix parameters were used to calculate the $^{6}Li+n$ and $^{10}B+n$ cross sections for ENDF/B-VI.

For the combination process, the fitting variables in the least-squares minimization were small changes in the R-matrix parameters (e_{LR} and e_{BR}) for the lithium and boron reactions and small relative cross section changes (e_p) for the heavy elements. For simplicity in writing the equations below, the Axton set is not explicitly recognized and only the lithium R-matrix fit is represented. The least-squares equation [18] can be written for this case in terms of submatrices:

$$\left[\begin{pmatrix} Q_{1L} & 0 \\ 0 & 0 \end{pmatrix} + S^t\, Q_2\, S\right] \begin{pmatrix} \varepsilon_{LR} \\ \varepsilon_P \end{pmatrix} = S^t\, R_2 \quad . \tag{1}$$

The matrix Q_{1L} is the inverse of the R-matrix parameter covariance matrix for the Segment 1 lithium data.

$$R_2 = \begin{pmatrix} G_{2L}^t \\ G_{2P}^t \end{pmatrix} V_2^{-1}\, \eta_2 \quad , \quad S = \begin{pmatrix} S_L & 0 \\ 0 & 1 \end{pmatrix} \quad ,$$

and

$$Q_2 = \begin{pmatrix} G_{2L}^t \\ G_{2P}^t \end{pmatrix} V_2^{-1}\, (G_{2L},\, G_{2P}) \quad .$$

The matrix V_2 is the variance-covariance matrix of the Segment 2 input data. The elements of G_{2L} and G_{2P} are the partial derivatives of the approximation equations, corresponding to each Segment 2 reduced input datum, with respect to relative changes in the pointwise cross section parameters. The reduced data vector η_2 contains the differences between the experimental data, reduced to a fixed energy grid, and the initial estimates derived from the zero-order parameter values. Finally, the elements of S_L are the logarithmic derivatives of the pointwise interpolated cross sections for the ^{7}Li system with respect to its R-matrix parameters; these were obtained from the R-matrix equations at the Segment 1 solution point.

Equation (1) was solved for the 674 elements of e. The output covariance matrix propagating the input data uncertainties and correlations is the inverse of the matrix on the left side. The equivalents of the matrices Q_{1L}, S, Q_2, and R_2 in eq (1) were obtained from the EDA and GMA programs for their respective data segments as assumed in the formulation above. The lithium and boron results from the Segment 1 fits and the Axton output thermal parameters were used as initial estimates in the final Segment 2 iteration.

Since the R-matrix formulations were quite nonlinear for some of the parameter refinements, the final parameters for lithium and boron were obtained from R-matrix fits to the cross sections obtained from the combination output.

Due to the difficulties associated with the transfer of large data files among the participants of the evaluation process, an effort was made to select initial estimates of the output variables which were sufficiently close to the output values so that a single iteration would suffice. In a trial analysis, a non-optimum partitioning of the boron data base between the R-matrix and simultaneous analyses was performed [19]. There were significant differences between the R-matrix and simultaneous evaluations. Though the results of the combination process should be independent of the partitioning of the input data, the desire to run only one iteration led to a more favorable partitioning.

In one case, the combination of the R-matrix and simultaneous pointwise evaluations of the independent data segments was iterated. This was done for an early data set where a second iteration was performed by obtaining the R-matrix parameter covariance matrix for the parameters corresponding to the output of the first iteration. This matrix had one negative eigenvalue, but the iteration could proceed formally. The resulting cross section changes were substantially smaller than those in the first iteration, but the output data covariance matrix had many negative eigenvalues and the results were considered unusable. The underlying problem was that the R-matrix fits were quite nonlinear in some parameters over intervals comparable to the iteration increments, though the development of the combination equations and the tentatively quoted output uncertainties assume linearity. The one-pass combination results were accepted regardless of this inconsistency because they seemed to represent the input data.

5. UNCERTAINTIES

Few experimenters document their known experimental uncertainties with enough detail to allow an evaluator to fully determine the required input data covariance matrix [20],[21]. Also since some experimental uncertainties are unrecognized or underestimated, inconsistencies among input data commonly occur. Under these circumstances, there may be inconsistencies in the output from the evaluation process. Also the output uncertainties may be too small. To account in some sense for unknown systematic errors, separate factors of the square root of χ^2/(degree of freedom) were determined for the simultaneous evaluation, for the R-matrix evaluation of lithium and for the R-matrix evaluation of boron. Each of these factors were applied, to the analyses where they were determined, as a scale factor to increase the output uncertainties. Very unusual results can be obtained with discrepant correlated data. To remove problems associated with these discrepancies, data greater than three standard deviations away from the output results were down weighted in the GMA analysis. This had the effect of reducing the χ^2/(degree of freedom) quantity referred to above to essentially 1. This process was not performed for the R-matrix evaluations where this quantity was 4.00 for the lithium analysis and 1.25 for the boron analysis. The parameter covariance matrices from the EDA analyses were scaled by the χ^2/(degree of freedom) factors. Even after this increase in the uncertainties, they still appear small to the reviewers of the evaluation [22]. Concerns have been expressed that users would not use these uncertainties but instead would arbitrarily increase them to what they considered a more acceptable level. A strong statement has been made that the Standards Subcommittee should provide such expanded uncertainties since they have had the closest contact with the data base and could make better estimates of more "acceptable" values. Such expanded uncertainties were provided. These uncertainties [23] are qualitative estimates such that if a modern day experiment were performed today on a given standard using the best techniques, most of these results would be expected to fall within these expanded uncertainties. They were intended to take into account data inconsistencies and concerns about R-matrix parameters. These estimated (expanded) uncertainties are given in table 6. It is not assumed that these uncertainties are totally correlated within the energy ranges given. These expanded uncertainties will be put in file 1 for each standard. Complete covariance files for the combination output are available but are very large. Based on the number of experimental data points it is clear that the covariance matrix is much larger than necessary. Work is now being done to collapse the matrix. Preliminary results for ^{6}Li(n,t), ^{10}B(n,α), Au(n,γ), ^{235}U(n,f), ^{238}U(n,γ), ^{238}U(n,f), and ^{239}Pu(n,f) are available as part of the International Reactor Dosimetry File [24].

6. COMPARISONS OF THE R-MATRIX, SIMULTANEOUS EVALUATION, AND COMBINATION RESULTS

In figures 6-20, the combination output is compared with the Segment 1 and Segment 2 results for each of the cross sections in the evaluation process. In figures 6-11, the combination output and Segment 2 results are compared to the Segment 1 (R-matrix) results. For these cross sections the partitionings of the data bases were done to provide the highest quality data for the R-matrix analyses so that convergence could be more easily obtained for that work. Thus the Segment 2 (simultaneous evaluation) results are poorly defined, have large uncertainties and have a much smaller effect on the combination output than the Segment 1 results. In figures 12-20, the combination output and Segment 2 results are compared with the initial estimates for the final iteration of the Segment 2 data in GMA. The Segment 1 results impact on the combination results for these cases only through ratio measurements to the ^{6}Li and ^{10}B standard cross sections. Including the Segment 1 data reduces the uncertainties and causes some changes in the combination results. In figures 12-20, the results shown are those prior to smoothing.

7. SMOOTHING/FITTING OF OUTPUT DATA

The lithium and boron cross sections which are obtained from this evaluation process are smooth since they are calculated from R-matrix parameters. However the results obtained for the heavy element standards in some cases showed fluctuations that seemed unreasonable based on expectations from the theory of average cross sections. Significant fluctuations can occur, for example, if not all the output points in a neighborhood reflect the same input data sets and if unrecognized uncertainties existed. Possible methods for fitting the capture and fission cross sections were considered. However instead such methods were used only to provide insight on how to do the smoothing. In figures 21-25, the differences between the smoothed results and the original combination output are shown. The uncertainties shown are the output values from the combination procedure.

8. RESULTS

The cross sections and uncertainties for the standards which were obtained from the combination of the simultaneous and R-matrix analyses are given here in tables 7-11. The results are given only for the energy regions over which these cross sections are recommended as standards by the CSEWG standards subcommittee, but the user must decide where to use the standard based on the uncertainty information available. There may be situations where a standard can be used over a much larger energy interval. In some cases, data points have been added to the original evaluated output to improve the definition of the cross section shape and to ease in interpolation of the data. For the ^{10}B and ^{6}Li cross sections shown in tables 7-9, the results are point values at all energies. Though in some cases these cross sections were obtained in part with measurements having moderate neutron energy resolution, its effect on the evaluation is probably not significant. For the $Au(n,\gamma)$ and $^{235}U(n,f)$ cross sections shown in tables 10 and 11, the results are low resolution smooth point values.

In tables 7-11 not all of the cross section results from the evaluation process are given. Non-standard cross sections, data beyond the standards region for a standard and most of the thermal constants are not shown. For completeness the entire output listing from the cross

section evaluation process, as it was when it first became available, is given in appendix D. The 9.4 eV value for the ^{235}U fission cross section is the integral cross section over the range from 7.8 to 11 eV. For the heavy elements the cross sections shown for energies from 0.15 through 15 keV represent decimal interval average values labeled at the center energies for intervals starting at 0.1 to 0.2 keV and ending with the interval 10 to 20 keV.

The standard cross sections are shown in figures 26-30 as ratios of the ENDF/B-VI to ENDF/B-V values. For the $^{6}Li(n,t)$ cross section, shown in figure 26, the changes are relatively small below 100 keV which was the recommended maximum energy for use of this cross section as a standard for ENDF/B-V. The changes are however larger than expected based on the uncertainties of the two evaluations and the number of data sets in common for the evaluations. The inclusion of the simultaneous evaluation results in the ENDF/B-VI evaluation has only a small effect in this lower energy region. The structure near 250 keV may be largely due to effects associated with inconsistencies in both the energy scales and the width of that resonance. This cross section is recommended for use as a standard below 1 MeV. The comparisons of the ENDF/B-V and ENDF/B-VI boron cross sections are shown in figures 27 and 28. The standards are the $^{10}B(n,\alpha_1)$ and the $^{10}B(n,\alpha)$ cross sections and they are recommended as standards below 250 keV. Similar results are seen for these cross sections as for the $^{6}Li(n,t)$ reaction in the low energy region. The changes are relatively small but larger than anticipated based on the uncertainties of the evaluations. At the higher neutron energies, significant differences are observed. The $^{10}B(n,\alpha_0)$ measurements of Olson and Kavanagh [25] and Sealock [26] have had important effects on the ENDF/B-VI evaluation at these energies. Recent measurements of the branching ratio [27] are 10 to 30% lower than ENDF/B-VI in the 100 to 600 keV energy region. However new determinations [28] of the $^{10}B(n,\alpha_1)$ cross section agree well with ENDF/B-VI to above 1 MeV. The ENDF/B-VI $Au(n,\gamma)$ cross section which is shown in figure 29 is similar to that of ENDF/B-V. However it is somewhat lower at the lower and higher neutron energies. Below about 300 keV, there is structure in the present evaluation which is a result of including measurements [29],[30] taken with high enough resolution to see effects due to competition with inelastic scattering and fluctuations in the neutron widths and spacings of the compound nucleus levels. This cross section is recommended as a standard from 200 keV to 2.5 MeV. The $^{235}U(n,f)$ cross section is shown in figure 30. This cross section is a standard from 150 keV to 20 MeV. The ENDF/B-VI cross section is lower than that of ENDF/B-V by 1-2% below 3 MeV. New measurements [31] and the inclusion of the ^{252}Cf spectrum averaged $^{235}U(n,f)$ data, particularly [32] and [33], had a significant impact on lowering these values in the ENDF/B-VI evaluation. Above about 15 MeV the data base is rather poor so appreciable differences occur with changes in evaluation method. Recent measurements [34]-[35] indicate differences as large as 5% with ENDF/B-V and ENDF/B-VI.

In figures 31-33, the ratios of the results of this evaluation process to those of ENDF/B-V [37] are given for the $^{238}U(n,f)$, $^{238}U(n,\gamma)$, and $^{239}Pu(n,f)$ reactions.

A new evaluation of the ^{252}Cf spontaneous fission neutron spectrum has been completed by Mannhart [38]. This evaluation made use of recent time-of-flight measurements of this spectrum. From the information that was available, a complete covariance matrix was generated for each experiment. The data were combined by generalized least-squares techniques. The evaluation was carried out with 70 energy grid points between 25 keV and 19.8 MeV. The individual experimental data were extrapolated to these grid points by using the shape of a Maxwellian distribution appropriate for each experiment. The evaluation gave a value of χ^2 per degree of freedom of approximately unity and indicated no incompatibility between the

experiments. The resulting relative uncertainty of the evaluation is smaller than 2% between 180 keV and 9.3 MeV. A weighted spline interpolation between the discrete data points was used to generate a continuous shape of the evaluated neutron spectrum. The result of the evaluation has been compared with available theoretical descriptions of the ^{252}Cf neutron spectrum. None of the existing theories is compatible with the evaluation over the whole energy range. The values at the energy points chosen for the ENDF/B-VI evaluation are given in Table 12. The uncertainties which were obtained from the evaluation process are shown in Table 13. The complete covariance matrix is available but large so it is not shown in this document.

9. CONCLUSIONS AND RECOMMENDATIONS

The work described in this report has produced improved cross section standards which are self consistent. The methods employed are the most sophisticated that have been used since the ENDF/B system was introduced. There are however still a number of improvements to the evaluation process which should be considered before the next evaluation of the standards so that delays can be avoided.

There are some inconsistencies in the present work which should be handled properly. In the evaluation [16] of the thermal constants the Au(n,γ) and ^{10}B(n,α) cross sections which are standards for these measurements were treated as constants. The thermal constants from this evaluation were imported into the present evaluation where these standards were treated as variables. The effect of this transgression is small since the uncertainties on these cross sections at thermal are small.

The H(n,n) cross section was assumed to be so well known that the remaining standards would have little impact on it in this evaluation. Concerns about the hydrogen standard angular distribution for energies above a few MeV suggest that it may be valuable to include this cross section in the comprehensive combining process. Also the ^{3}He(n,p) and C(n,n) cross sections were not used in the combining process since few ratio measurements to these standards exist. For completeness, inclusion of the ^{3}He(n,p) data should be considered in the next evaluation.

Because of the success in using nuclear models in the evaluation of the ^{238}U(n,γ) cross sections [39], including such models in future standards evaluations of capture cross sections should be encouraged. More work should be done on models which could be used to fit fission data. This could possibly improve the quality of the evaluation and reduce or eliminate the need for smoothing of the output results.

Approaches should be considered for doing the evaluation so that the entire process could be done on one computer system. For the present formalism, the R-matrix and simultaneous evaluations and the procedure for combining them could then be iterated more easily.

An important problem encountered with the present evaluation was the uncertainties in the standard cross sections. Improved methods to increase the uncertainties based on the spread in the input values should be investigated. This effort could be eliminated if discrepancies in the data base could be resolved.

10. REFERENCES

[1] Poenitz, W.P., Proc. Conference on Nuclear Data Evaluation Methods and Procedures, Brookhaven National Laboratory, BNL-NCS-51363, Vol. 1 (1981), p. 249.

[2] Dodder, D.C. and Hale, G.M., private communication to CSEWG (Oct. 1987).

[3] Tornow, W., *et al.*, Phys. Rev. **C37**, 2326 (1988).

[4] Tornow, W., Lisowski, P., Byrd, R.C., and Walter, R.L., Phys. Rev. Lett. **39**, 915 (1977); and Nucl. Phys. **A340**, 34 (1980).

[5] Hopkins, J.C. and Breit, G., Nucl. Data **A9**, 137 (1971).

[6] Arndt, R.A., "N-N Phase-Shift Analysis," Interactive Computer Program SAID, private communication (1988).

[7] Nagels, M.N., Rijken, T.A., and deSwaart, J.J., Phys. Rev. **D17**, 768 (1978).

[8] Klages, H., *et al.*, Karlsruhe Polarization Transfer Measurements for n-p Scattering," private communication from W. Tornow, Duke University (1988).

[9] Holden, N.E., private communication (1987).

[10] Ryves, T.B. and Kolkowski, P., Ann. Nucl. Energy, **17**, 657 (1990).

[11] Vincour, J., Bém, P., and Presperin, V., in *Neutron Induced Reactions*, Proc. of Europhysics Topical Conference, Smolinice (1982), p. 413.

[12] Carlson, A.D. and Bhat, M.R., ENDF/B-V Cross Section Measurement Standards. Brookhaven National Laboratory Report BNL-NCS-51619 (October 1982).

[13] Hale, G.M., private communication (1987).

[14] Fu, C.Y., Nucl. Sci. Eng. **106**, 494 (1990).

[15] Heaton, II, H.T., Menke, J.L., Schrack, R.A., and Schwartz, R.B., Nucl. Sci. Eng. **56**, 27 (1975).

[16] Axton, E.J., Central Bureau for Nuclear Measurements, GE/PH/01/86; private communication (1986).

[17] Hale, G.M., NBS Spec. Pub. 493, 30 (1977): see also, G.M. Hale, NBS Spec. Publ. 425, 302 (1975); G.M. Hale, BNL-NCS-51363, 509 (1981).

[18] Peelle, R.W., in *Advances in Nuclear Science and Technology*, Vol. 14, J. Lewis and M. Becker eds., (1982), p. 37.

[19] Carlson, A.D., Poenitz, W.P., Hale, G.M., and Peelle, R.W., *Proc. Intern. Conf. Nucl. Data for Basic and Applied Science*, P. Young *et al.* eds., Gordon and Breach, Vol. 2 (1986), p. 1429.

[20] Poenitz, W.P., Proc. Advisory Group Meeting on Nuclear Standard Reference Data, International Atomic Energy Agency, IAEA-TECDOC-335 (1985), p. 426.

[21] Peelle, R.W., Proc. NEANDC/NEACRP Specialists Meeting of Fast Neutron Fission Cross Sections of ^{233}U, ^{235}U, ^{238}U, and ^{239}Pu, June 28-30, 1976, Argonne National Laboratory Report ANL-76-90 (1976) p. 421.

[22] Sowerby, M.G., AERE Harwell, private communication to A.D. Carlson following review of the proposed ENDF/B-VI standards file (1987).

[23] Dunford, C.L., Summary of CSWEG Meeting, May 8-10, 1990, Brookhaven National Laboratory (Enclosure 3A).

[24] Kocherov, N. and McLaughlin, P.K., International Reactor Dosimetry File (IRDF-90), IAEA-NDS-141, Vienna, Austria, (August 1990).

[25] Olson, M.D. and Kavanagh, R.W., Phys. Rev. **C30**, 1375 (1984).

[26] Sealock, R.M., *et al.*, Nucl. Phys. **A357**, 279 (1981).

[27] Weston, L.W. and Todd, J.H., Nucl. Sci. Eng. **109**, 113 (1991).

[28] Schrack, R.A., Wasson, O.A., Larson, D.C., Dickens, J.K., and Todd, J.H., Proc. International Conference on Nuclear Data for Science and Technology, Jülich, 1991, p. 507.
[29] Macklin, R.L., private communication.
[30] Kononov, V.N., Yurlov, B.D., Poletoev, E.D., and Timokhov, V.M., Sov. J. Nucl. Phys. **26**, 500 (1977).
[31] Carlson, A.D., Behrens, J.W., Johnson, R.G., and Cooper, G.E., Proc. Advisory Group Meeting on Nuclear Standard Reference Data, International Atomic Energy Agency, IAEA-TECDOC-335 (1985), p. 162.
[32] Heaton,II, H.T., Grundl, J.A., Spiegel, Jr., V., Gilliam, D.M., and Eisenhauer, C., NBS Spec. Publ. 425, (1979), *now* National Institute of Standards and Technology; also Trans. Am. Nucl. Soc. **44**. 533 (1983).
[33] Davis, M.C. and Knoll, G.F., Ann. Nucl. Energy **5**, 583 (1978).
[34] Alkhazov, I.D., *et al.*, Proc. International Conference on Nuclear Data for Science and Technology, Mito, Japan (1988), p. 145.
[35] Carlson, A.D., Proc. International Conference on Nuclear Data for Science and Technology, Jülich, 1991, p. 518.
[36] Lisowski, P.W., Gavron, A., Parker, W.E., Ullmann, J.L., Balestrini, S.J., Carlson, A.D., Wasson, O.A., and Hill, N.W., Proc. Specialists' Meeting on Neutron Cross Section Standards for the Energy Region Above 20 MeV, NEANDC-305 U, Uppsala, Sweden (1991), p. 177.
[37] Kinsey, R., ENDF-201, ENDF/B Summary Documentation, Brookhaven National Laboratory Report BNL-NCS-17541 (1979).
[38] Mannhart, W., Proc. Advisory Group Meeting on Properties of Neutron Sources, International Atomic Energy Agency, IAEA-TECDOC-410 (1987), 158; and Proc. Consultants Meeting on Physics of Neutron Emission in Fission, International Atomic Energy Agency, INDC(NDS)-220/L (1989) p. 305.
[39] Froehner, F.H., Nucl. Sci. Eng., **103**. 119 (1989).
[40] Rose, P.F., ENDF-201, ENDF/B-VI Summary Documentation, Brookhaven National Laboratory, BNL-NCS-17541, 4th Edition [ENDF/B-VI], October 1991.
[41] Carlson, A.D., Prog. Nucl. Energy **13**, 79 (1984).
[42] Priesmeyer, H.G., *et al.*, Prod. Conf. Nuclear Data for Basic and Applied Science, Santa Fe, 13-17 May 1985, Vol. 2, p. 1463; see also NEANDC(E)-272U.
[43] Borzakov, S.B., *et al.*, Sov. J. Nucl. Phys. **35**, 307 (1982); Yad. Fiz. **35**, 532 (1982).

Table 1. H(n,n) Cross Section
ENDF/B-VI, MAT 0125

Recommended as a standard from about 10 eV to 20 MeV

Log-log interpolation

Cross Section Values

E(ev)	σ(b)	E(eV)	σ(b)	E(ev)	σ(b)
1.000000-5	2.047800+1	2.530000-2	2.047800+1	1.000000+2	2.046400+1
1.000000+3	2.034400+1	5.000000+3	1.982700+1	1.000000+4	1.922200+1
2.000000+4	1.813000+1	3.000000+4	1.717300+1	4.000000+4	1.632500+1
5.000000+4	1.557100+1	6.000000+4	1.489400+1	7.000000+4	1.428300+1
8.000000+4	1.373000+1	9.000000+4	1.322600+1	1.000000+5	1.276500+1
1.200000+5	1.195100+1	1.400000+5	1.125500+1	1.600000+5	1.065200+1
1.800000+5	1.012500+1	2.000000+5	9.660900+0	2.200000+5	9.247800+0
2.400000+5	8.878000+0	2.600000+5	8.544700+0	2.800000+5	8.242800+0
3.000000+5	7.967800+0	3.200000+5	7.716200+0	3.400000+5	7.485000+0
3.600000+5	7.271800+0	3.800000+5	7.074500+0	4.000000+5	6.891200+0
4.200000+5	6.720500+0	4.400000+5	6.561100+0	4.600000+5	6.411700+0
4.800000+5	6.271500+0	5.000000+5	6.139600+0	5.500000+5	5.841200+0
6.000000+5	5.580500+0	6.500000+5	5.350400+0	7.000000+5	5.145300+0
7.500000+5	4.961100+0	8.000000+5	4.794500+0	8.500000+5	4.642900+0
9.000000+5	4.504200+0	9.500000+5	4.376500+0	1.000000+6	4.258600+0
1.100000+6	4.047100+0	1.200000+6	3.862500+0	1.300000+6	3.699200+0
1.400000+6	3.553300+0	1.500000+6	3.421900+0	1.600000+6	3.302500+0
1.700000+6	3.193400+0	1.800000+6	3.093100+0	1.900000+6	3.000300+0
2.000000+6	2.914200+0	2.100000+6	2.833900+0	2.200000+6	2.758800+0
2.300000+6	2.688300+0	2.400000+6	2.621900+0	2.500000+6	2.559200+0
2.600000+6	2.499900+0	2.700000+6	2.443600+0	2.800000+6	2.390200+0
2.900000+6	2.339300+0	3.000000+6	2.290700+0	3.200000+6	2.199900+0
3.400000+6	2.116600+0	3.600000+6	2.039800+0	3.800000+6	1.968600+0
4.000000+6	1.902400+0	4.200000+6	1.840600+0	4.400000+6	1.782800+0
4.600000+6	1.728600+0	4.800000+6	1.677500+0	5.000000+6	1.629400+0
5.500000+6	1.520200+0	6.000000+6	1.424400+0	6.500000+6	1.339600+0
7.000000+6	1.263900+0	7.500000+6	1.195900+0	8.000000+6	1.134500+0
8.500000+6	1.078600+0	9.000000+6	1.027700+0	9.500000+6	9.810600-1
1.000000+7	9.381600-1	1.050000+7	8.985700-1	1.100000+7	8.619400-1
1.150000+7	8.279300-1	1.200000+7	7.962800-1	1.250000+7	7.667600-1
1.300000+7	7.391500-1	1.350000+7	7.132900-1	1.400000+7	6.890000-1
1.450000+7	6.661500-1	1.500000+7	6.446200-1	1.550000+7	6.242900-1
1.600000+7	6.050700-1	1.700000+7	5.696100-1	1.800000+7	5.376400-1
1.900000+7	5.086600-1	2.000000+7	4.822700-1		

H(n,n) Total Cross Section Uncertainty
(at each point in the energy range)

Energy Range (keV)	Uncertainty (%)
(1.E-08) - 20000	0.2

Table 2. H(n,n) Center of Mass Legendre Coefficients

$$DSIGMA = \frac{SIGMA}{4\pi} \sum_{\ell=0}^{N} (2\ell+1)\, A_\ell\, P_\ell \quad , \quad A_0 = 1$$

Linear-linear interpolation

Legendre Coefficients

E(ev)	A_1	A_2	A_3	A_4	A_5	A_6
1.000000+3	-1.919300-6	2.09480-11	6.46600-16	1.75260-15	1.59600-15	6.75230-16
5.000000+3	-9.565900-6	5.32530-10	-2.28790-14	2.18920-15	2.91700-15	4.33020-16
1.000000+4	-1.905700-5	2.174000-9	-2.03730-13	1.04840-15	2.98240-15	2.67990-16
2.000000+4	-3.781800-5	9.040700-9	-1.63080-12	-7.69510-16	3.35790-15	3.78840-16
3.000000+4	-5.629700-5	2.109700-8	-5.44050-12	-1.55260-15	5.40630-15	-1.19990-15
4.000000+4	-7.450300-5	3.881400-8	-1.27190-11	-3.98810-16	7.24070-15	-1.26220-15
5.000000+4	-9.244800-5	6.264000-8	-2.44990-11	2.53870-15	5.79960-15	-3.97000-15
6.000000+4	-1.101400-4	9.300100-8	-4.17500-11	1.06790-14	7.25530-15	-4.26570-15
7.000000+4	-1.276000-4	1.303000-7	-6.53900-11	2.52870-14	9.05720-15	-3.84690-15
8.000000+4	-1.448200-4	1.749200-7	-9.62850-11	4.81870-14	9.60700-15	-4.50220-15
9.000000+4	-1.618200-4	2.272300-7	-1.35250-10	8.48110-14	1.11240-14	-5.19310-15
1.000000+5	-1.786000-4	2.875800-7	-1.83080-10	1.38780-13	1.13670-14	-6.18790-15
1.200000+5	-2.115600-4	4.336800-7	-3.08190-10	3.20310-13	1.40520-14	-6.60940-15
1.400000+5	-2.437500-4	6.156800-7	-4.77060-10	6.38410-13	1.68590-14	-8.54390-15
1.600000+5	-2.752400-4	8.358100-7	-6.94620-10	1.15700-12	1.70030-14	-9.83310-15
1.800000+5	-3.060700-4	1.096100-6	-9.65340-10	1.95720-12	1.78870-14	-1.34820-14
2.000000+5	-3.362900-4	1.398300-6	-1.293300-9	3.13180-12	2.07690-14	-1.23530-14
2.200000+5	-3.659500-4	1.744200-6	-1.682200-9	4.79110-12	2.32330-14	-1.40190-14
2.400000+5	-3.950900-4	2.135200-6	-2.135600-9	7.06500-12	2.61440-14	-1.49890-14
2.600000+5	-4.237300-4	2.572800-6	-2.656600-9	1.01010-11	2.87370-14	-1.63780-14
2.800000+5	-4.519300-4	3.058100-6	-3.248300-9	1.40680-11	3.29280-14	-1.76030-14
3.000000+5	-4.797000-4	3.592200-6	-3.913500-9	1.91510-11	3.93490-14	-1.76720-14
3.200000+5	-5.070800-4	4.176300-6	-4.655000-9	2.55590-11	4.33610-14	-1.99170-14
3.400000+5	-5.341100-4	4.811200-6	-5.475300-9	3.35230-11	4.96140-14	-2.11050-14
3.600000+5	-5.607900-4	5.497700-6	-6.377000-9	4.32970-11	5.70690-14	-2.19600-14
3.800000+5	-5.871600-4	6.236700-6	-7.362500-9	5.51500-11	6.51150-14	-2.37860-14
4.000000+5	-6.132400-4	7.028700-6	-8.434300-9	6.93850-11	7.69690-14	-2.27990-14
4.200000+5	-6.390500-4	7.874500-6	-9.594700-9	8.63200-11	9.00210-14	-2.41450-14
4.400000+5	-6.646000-4	8.774600-6	-1.084600-8	1.06300-10	1.06280-13	-2.59090-14
4.600000+5	-6.899300-4	9.729400-6	-1.219100-8	1.29700-10	1.25220-13	-2.65130-14
4.800000+5	-7.150300-4	1.073900-5	-1.363200-8	1.56910-10	1.47950-13	-2.69690-14
5.000000+5	-7.399400-4	1.180500-5	-1.517200-8	1.88350-10	1.74600-13	-2.81080-14
5.500000+5	-8.014300-4	1.471500-5	-1.946700-8	2.88460-10	2.63420-13	-3.07190-14
6.000000+5	-8.619700-4	1.797800-5	-2.443500-8	4.25570-10	3.95680-13	-3.07690-14
6.500000+5	-9.217400-4	2.159900-5	-3.011900-8	6.08420-10	5.84140-13	-3.09700-14
7.000000+5	-9.808800-4	2.557900-5	-3.656800-8	8.46840-10	8.46730-13	-2.92840-14
7.500000+5	-1.039500-3	2.991800-5	-4.383300-8	1.151800-9	1.20650-12	-2.44010-14
8.000000+5	-1.097800-3	3.461700-5	-5.197100-8	1.535300-9	1.68400-12	-1.79070-14
8.500000+5	-1.155800-3	3.967600-5	-6.104600-8	2.010600-9	2.31400-12	-4.71540-15
9.000000+5	-1.213600-3	4.509400-5	-7.112300-8	2.592200-9	3.12430-12	1.19130-14
9.500000+5	-1.271300-3	5.086800-5	-8.227600-8	3.295700-9	4.15800-12	3.94310-14
1.000000+6	-1.328900-3	5.699700-5	-9.458400-8	4.138000-9	5.45600-12	7.24780-14
1.100000+6	-1.444200-3	7.031000-5	-1.230100-7	6.312500-9	9.04730-12	1.80950-13
1.200000+6	-1.559900-3	8.501200-5	-1.571400-7	9.275900-9	1.43630-11	3.60870-13
1.300000+6	-1.676200-3	1.010700-4	-1.978300-7	1.320900-8	2.19700-11	6.50090-13
1.400000+6	-1.793400-3	1.184700-4	-2.460200-7	1.831400-8	3.25500-11	1.09330-12

Table 2 (Continued)

E(ev)	A_1	A_2	A_3	A_4	A_5	A_6
1.500000+6	-1.911600-3	1.371700-4	-3.027600-7	2.481500-8	4.69040-11	1.75150-12
1.600000+6	-2.030900-3	1.571400-4	-3.691900-7	3.295700-8	6.59660-11	2.70220-12
1.700000+6	-2.151500-3	1.783500-4	-4.465600-7	4.300700-8	9.08120-11	4.04220-12
1.800000+6	-2.273300-3	2.007700-4	-5.362000-7	5.525600-8	1.22660-10	5.89340-12
1.900000+6	-2.396400-3	2.243500-4	-6.395600-7	7.001700-8	1.62880-10	8.40060-12
2.000000+6	-2.520800-3	2.490800-4	-7.581600-7	8.762500-8	2.13020-10	1.17450-11
2.100000+6	-2.646500-3	2.749000-4	-8.936500-7	1.084400-7	2.74770-10	1.61410-11
2.200000+6	-2.773600-3	3.017900-4	-1.047700-6	1.328400-7	3.50000-10	2.18450-11
2.300000+6	-2.902000-3	3.297100-4	-1.222300-6	1.612300-7	4.40750-10	2.91530-11
2.400000+6	-3.031600-3	3.586300-4	-1.419100-6	1.940300-7	5.49240-10	3.84210-11
2.500000+6	-3.162500-3	3.885100-4	-1.640200-6	2.317100-7	6.77840-10	5.00540-11
2.600000+6	-3.294600-3	4.193200-4	-1.887700-6	2.747200-7	8.29130-10	6.45250-11
2.700000+6	-3.427900-3	4.510300-4	-2.163800-6	3.235600-7	1.005800-9	8.23760-11
2.800000+6	-3.562300-3	4.835900-4	-2.470700-6	3.787600-7	1.210800-9	1.04220-10
2.900000+6	-3.697800-3	5.169900-4	-2.810600-6	4.408400-7	1.447200-9	1.30760-10
3.000000+6	-3.834300-3	5.511800-4	-3.186100-6	5.103800-7	1.718200-9	1.62790-10
3.200000+6	-4.110200-3	6.218100-4	-4.053500-6	6.741500-7	2.377500-9	2.46990-10
3.400000+6	-4.389700-3	6.952500-4	-5.093600-6	8.749900-7	3.217400-9	3.65310-10
3.600000+6	-4.672300-3	7.712300-4	-6.327900-6	1.118100-6	4.268100-9	5.28250-10
3.800000+6	-4.957600-3	8.495200-4	-7.779400-6	1.409100-6	5.561500-9	7.48650-10
4.000000+6	-5.245200-3	9.299000-4	-9.471700-6	1.753900-6	7.129800-9	1.042000-9
4.200000+6	-5.534600-3	1.012100-3	-1.142900-5	2.158400-6	9.005600-9	1.426900-9
4.400000+6	-5.825500-3	1.096000-3	-1.367700-5	2.629300-6	1.122000-8	1.925200-9
4.600000+6	-6.117400-3	1.181300-3	-1.624200-5	3.173000-6	1.380400-8	2.562700-9
4.800000+6	-6.409900-3	1.267800-3	-1.915000-5	3.796500-6	1.678300-8	3.369400-9
5.000000+6	-6.702800-3	1.355300-3	-2.242900-5	4.506800-6	2.017900-8	4.380000-9
5.500000+6	-7.433800-3	1.577500-3	-3.242800-5	6.710700-6	3.059300-8	8.074200-9
6.000000+6	-8.158900-3	1.802300-3	-4.535600-5	9.620600-6	4.373800-8	1.409400-8
6.500000+6	-8.873400-3	2.027300-3	-6.165800-5	1.335800-5	5.919400-8	2.349800-8
7.000000+6	-9.573000-3	2.250400-3	-8.177900-5	1.804400-5	7.587300-8	3.766600-8
7.500000+6	-1.025400-2	2.469800-3	-1.061500-4	2.380200-5	9.178600-8	5.835400-8
8.000000+6	-1.091300-2	2.683900-3	-1.352000-4	3.075000-5	1.037700-7	8.775100-8
8.500000+6	-1.154700-2	2.891400-3	-1.693000-4	3.899900-5	1.071600-7	1.285300-7
9.000000+6	-1.215400-2	3.091200-3	-2.088200-4	4.865400-5	9.550800-8	1.838900-7
9.500000+6	-1.273100-2	3.282500-3	-2.540700-4	5.980900-5	6.016700-8	2.576000-7
1.000000+7	-1.327700-2	3.464700-3	-3.053300-4	7.254700-5	-1.005200-8	3.540700-7
1.050000+7	-1.379100-2	3.637400-3	-3.628100-4	8.693800-5	-1.293000-7	4.782900-7
1.100000+7	-1.427100-2	3.800500-3	-4.266800-4	1.030300-4	-3.150700-7	6.359500-7
1.150000+7	-1.471700-2	3.953900-3	-4.970100-4	1.208800-4	-5.886800-7	8.333400-7
1.200000+7	-1.512700-2	4.098000-3	-5.738300-4	1.404900-4	-9.756100-7	1.077400-6
1.250000+7	-1.550200-2	4.233300-3	-6.570900-4	1.618900-4	-1.506000-6	1.375600-6
1.300000+7	-1.584100-2	4.360400-3	-7.466400-4	1.850500-4	-2.215000-6	1.735800-6
1.350000+7	-1.614500-2	4.480300-3	-8.422500-4	2.099600-4	-3.143100-6	2.166600-6
1.400000+7	-1.641200-2	4.594000-3	-9.436200-4	2.365900-4	-4.336800-6	2.676400-6
1.450000+7	-1.664400-2	4.703100-3	-1.050300-3	2.648900-4	-5.848400-6	3.273900-6
1.500000+7	-1.684100-2	4.809100-3	-1.161800-3	2.948100-4	-7.736700-6	3.967600-6
1.550000+7	-1.700200-2	4.913900-3	-1.277500-3	3.262900-4	-1.006700-5	4.765600-6
1.600000+7	-1.713000-2	5.019600-3	-1.396600-3	3.592600-4	-1.291100-5	5.675100-6
1.700000+7	-1.728200-2	5.244000-3	-1.641500-3	4.295000-4	-2.046100-5	7.851600-6
1.800000+7	-1.730400-2	5.505700-3	-1.888000-3	5.052000-4	-3.109100-5	1.052300-5
1.900000+7	-1.719900-2	5.833900-3	-2.125200-3	5.864200-4	-4.559100-5	1.367200-5
2.000000+7	-1.697400-2	6.264600-3	-2.339400-3	6.737900-4	-6.481300-5	1.721100-5

Table 3. $^{3}He(n,p)$ Cross Section

ENDF/B-VI, MAT 0225

Recommended as a standard below 50 keV

Log-log interpolation

Cross Section Values

E (eV)	σ(b)
1.0000E-05	2.6745E+05
2.5300E-02	5.3160E+03
1.0000E-01	2.6733E+03
1.0000E+00	8.4453E+02
1.0000E+01	2.6622E+02
1.0000E+02	8.3357E+01
2.0000E+02	5.8590E+01
4.0000E+02	4.1081E+01
6.0000E+02	3.3326E+01
8.0000E+02	2.8705E+01
1.0000E+03	2.5552E+01
2.0000E+03	1.7733E+01
4.0000E+03	1.2216E+01
6.0000E+03	9.7779E+00
8.0000E+03	8.3288E+00
1.0000E+04	7.3426E+00
1.5000E+04	5.8163E+00
2.0000E+04	4.9128E+00
2.5000E+04	4.3006E+00
3.0000E+04	3.8520E+00
3.5000E+04	3.5058E+00
4.0000E+04	3.2288E+00
4.5000E+04	3.0012E+00
5.0000E+04	2.8100E+00

$^{3}He(n,p)$ Cross Section Uncertainty
(at each point in the energy range)

Energy Range (keV)	Uncertainty (%)
(1.E-08) - 0.1	0.3
0.1 - 1	0.7
1 - 10	2.0
10 - 50	5.0

Table 4. C(n,n) Cross Section
ENDF/B-VI, MAT 600

Recommended as a standard below 1.8 MeV

Linear-linear interpolation

Cross Section Values

E(ev)	σ(b)	E(eV)	σ(b)	E(ev)	σ(b)
1.000000-5	4.739200+0	2.530000-2	4.739200+0	5.000000+3	4.716100+0
1.000000+4	4.699100+0	1.500000+4	4.682100+0	2.000000+4	4.665300+0
2.500000+4	4.648600+0	3.000000+4	4.631900+0	3.500000+4	4.615400+0
4.000000+4	4.598900+0	4.500000+4	4.582500+0	5.000000+4	4.566200+0
7.500000+4	4.486200+0	1.000000+5	4.408400+0	1.250000+5	4.330100+0
1.300000+5	4.314800+0	1.350000+5	4.301200+0	1.400000+5	4.289100+0
1.425000+5	4.284800+0	1.450000+5	4.283800+0	1.475000+5	4.292400+0
1.487500+5	4.307000+0	1.500000+5	4.340000+0	1.510000+5	4.393700+0
1.520000+5	4.476500+0	1.529000+5	4.520600+0	1.540000+5	4.454500+0
1.550000+5	4.373100+0	1.560000+5	4.321000+0	1.580000+5	4.271000+0
1.600000+5	4.248400+0	1.612500+5	4.239300+0	1.625000+5	4.232000+0
1.650000+5	4.220400+0	1.700000+5	4.202100+0	1.750000+5	4.186100+0
1.800000+5	4.171200+0	2.000000+5	4.115900+0	2.250000+5	4.048400+0
2.500000+5	3.982800+0	2.750000+5	3.918200+0	3.000000+5	3.855100+0
3.250000+5	3.793700+0	3.500000+5	3.733800+0	3.750000+5	3.675300+0
4.000000+5	3.618200+0	4.250000+5	3.562600+0	4.500000+5	3.508200+0
4.750000+5	3.455100+0	5.000000+5	3.403300+0	5.250000+5	3.352700+0
5.500000+5	3.303200+0	5.750000+5	3.254900+0	6.000000+5	3.207600+0
6.250000+5	3.161500+0	6.500000+5	3.116300+0	6.750000+5	3.072200+0
7.000000+5	3.029000+0	7.250000+5	2.986800+0	7.500000+5	2.945400+0
7.750000+5	2.905000+0	8.000000+5	2.865400+0	8.250000+5	2.826700+0
8.500000+5	2.788800+0	8.750000+5	2.751700+0	9.000000+5	2.715400+0
9.250000+5	2.679800+0	9.500000+5	2.645000+0	9.750000+5	2.610800+0
1.000000+6	2.577400+0	1.025000+6	2.544600+0	1.050000+6	2.512500+0
1.075000+6	2.481100+0	1.100000+6	2.450300+0	1.125000+6	2.420100+0
1.150000+6	2.390500+0	1.175000+6	2.361500+0	1.200000+6	2.333100+0
1.225000+6	2.305200+0	1.250000+6	2.277900+0	1.275000+6	2.251100+0
1.300000+6	2.224900+0	1.325000+6	2.199100+0	1.350000+6	2.173900+0
1.375000+6	2.149200+0	1.400000+6	2.125000+0	1.425000+6	2.101200+0
1.450000+6	2.078000+0	1.475000+6	2.055200+0	1.500000+6	2.032800+0
1.525000+6	2.010500+0	1.550000+6	1.988800+0	1.575000+6	1.967400+0
1.600000+6	1.946500+0	1.625000+6	1.925900+0	1.650000+6	1.905900+0
1.675000+6	1.885800+0	1.680000+6	1.881900+0	1.700000+6	1.865500+0
1.710000+6	1.857400+0	1.715000+6	1.853700+0	1.720000+6	1.850700+0
1.725000+6	1.850100+0	1.730000+6	1.854700+0	1.732000+6	1.858300+0
1.734000+6	1.861600+0	1.736000+6	1.862500+0	1.738000+6	1.859800+0
1.740000+6	1.854400+0	1.745000+6	1.840800+0	1.750000+6	1.832700+0
1.755000+6	1.828000+0	1.760000+6	1.824400+0	1.770000+6	1.818000+0
1.775000+6	1.814700+0	1.780000+6	1.811500+0	1.790000+6	1.804800+0
1.800000+6	1.798000+0				

C(n,n) Total Elastic Scattering Cross Section Uncertainties
(at each point in the energy range)

Energy (keV)	Uncertainty (%)
1 - 500	0.46
500 - 1500	0.53
1500 - 1800	0.60

Table 5. C(n,n) Center of Mass Legendre Coefficients

$$DSIGMA = \frac{SIGMA}{4\pi} \sum_{\ell=0}^{N} (2\ell+1)\, A_\ell\, P_\ell \quad , \quad A_0 = 1$$

Linear-linear interpolation

Legendre Coefficients

E(ev)	A_1	A_2	A_3	A_4	A_5
1.000000-5	0.000000+0				
1.000000+3	1.401100-4				
5.000000+3	6.982000-4				
1.000000+4	1.372000-3				
5.000000+4	6.603000-3	7.423100-5			
1.000000+5	1.245700-2	2.801300-4			
1.100000+5	1.339600-2	3.524300-4			
1.200000+5	1.424700-2	4.297600-4			
1.300000+5	1.491100-2	5.240000-4			
1.400000+5	1.512000-2	7.038700-4			
1.450000+5	1.499300-2	9.579300-4			
1.475000+5	1.516000-2	1.225300-3			
1.500000+5	1.627200-2	1.635400-3			
1.529000+5	1.967700-2	1.983700-3			
1.550000+5	2.200800-2	1.845300-3			
1.575000+5	2.305600-2	1.505600-3			
1.600000+5	2.311400-2	1.250600-3			
1.650000+5	2.283700-2	1.013300-3			
1.700000+5	2.278700-2	9.371100-4			
1.750000+5	2.294100-2	9.177400-4			
1.800000+5	2.322000-2	9.221200-4			
1.900000+5	2.397600-2	9.601900-4			
2.000000+5	2.486800-2	1.014300-3			
3.000000+5	3.389700-2	1.946500-3	6.334400-5		
4.000000+5	4.148600-2	3.011600-3	1.281000-4		
5.000000+5	4.780200-2	4.132600-3	2.230800-4		
6.000000+5	5.314500-2	5.274000-3	3.476700-4		
7.000000+5	5.744800-2	6.394900-3	4.974000-4	-5.641100-5	
8.000000+5	6.078900-2	7.486100-3	6.650900-4	-1.013500-4	
9.000000+5	6.322600-2	8.553600-3	8.401900-4	-1.700600-4	
1.000000+6	6.479700-2	9.618100-3	1.008100-3	-2.704900-4	
1.100000+6	6.550000-2	1.070900-2	1.146800-3	-4.118800-4	
1.200000+6	6.536000-2	1.188100-2	1.234700-3	-6.050800-4	
1.300000+6	6.436300-2	1.319900-2	1.240500-3	-8.620300-4	
1.400000+6	6.247500-2	1.475200-2	1.122800-3	-1.195200-3	6.114500-5
1.500000+6	5.963500-2	1.664300-2	8.259800-4	-1.615700-3	8.828800-5
1.600000+6	5.578100-2	1.897000-2	2.492400-4	-2.126300-3	1.247900-4
1.650000+6	5.328500-2	2.039500-2	-2.552000-4	-2.416100-3	1.488000-4

Table 5 (Continued)

E(ev)	A_1	A_2	A_3	A_4	A_5
1.680000+6	5.180600-2	2.117000-2	-5.907000-4	-2.578500-3	1.632100-4
1.700000+6	5.076500-2	2.158000-2	-8.678800-4	-2.658500-3	1.728200-4
1.710000+6	4.995100-2	2.184900-2	-1.114800-3	-2.661400-3	1.789500-4
1.720000+6	4.878600-2	2.243800-2	-1.386900-3	-2.581800-3	1.850800-4
1.730000+6	4.760800-2	2.426300-2	-1.410200-3	-2.435300-3	1.912100-4
1.736000+6	4.763000-2	2.514000-2	-1.194900-3	-2.453600-3	1.948900-4
1.740000+6	4.770900-2	2.508700-2	-1.051500-3	-2.525400-3	1.973400-4
1.745000+6	4.747100-2	2.454800-2	-9.698700-4	-2.660800-3	2.004000-4
1.750000+6	4.693000-2	2.410800-2	-1.024200-3	-2.804400-3	2.034700-4
1.755000+6	4.639400-2	2.402300-2	-1.150300-3	-2.917200-3	2.065300-4
1.760000+6	4.596400-2	2.415400-2	-1.286800-3	-2.997300-3	2.096000-4
1.770000+6	4.529100-2	2.458900-2	-1.529300-3	-3.104400-3	2.157200-4
1.780000+6	4.468800-2	2.503500-2	-1.736800-3	-3.183100-3	2.218500-4
1.790000+6	4.408700-2	2.545600-2	-1.925600-3	-3.252000-3	2.279800-4
1.800000+6	4.347500-2	2.586000-2	-2.104400-3	-3.316800-3	2.341100-4

Table 6. Estimated (Expanded) Uncertainties Compared with those Obtained from the Evaluation Process

(Note the two types of uncertainties are defined differently)

$^{6}Li(n,t)$ Cross Section

Energy Range (keV)	Estimated Uncertainty (%)	Comb. Result (%)
(1.E-08) - 0.1	0.3	(0.14)
0.1 - 1	0.5	(0.14)
1 - 10	0.7	(0.14)
10 - 50	0.9	(0.16)
50 - 90	1.1	(0.25)
90 - 150	1.5	(0.33)
150 - 450	2.0	(0.29)
450 - 650	5.0	(0.32)
650 - 800	2.0	(0.36)
800 - 1000	5.0	(0.39)

$^{10}B(n,\alpha)$ Cross Section

Energy Range(keV)	Estimated Uncertainty (%)	Comb. Result (%)
(1.E-08) - 0.1	0.2	(0.16)
0.1 - 5	0.4	(0.17)
5 - 30	0.6	(0.20)
30 - 90	1.0	(0.34)
90 - 150	1.6	(0.46)
150 - 200	2.1	(0.57)
200 - 250	2.7	(0.60)

$^{10}B(n,\alpha_1)$ Cross Section

Energy Range(keV)	Estimated Uncertainty (%)	Comb. Result (%)
(1.E-08) - 0.1	0.2	(0.16)
0.1 - 5	0.4	(0.17)
5 - 30	0.6	(0.20)
30 - 90	1.0	(0.34)
90 - 150	1.5	(0.48)
150 - 200	2.0	(0.58)
200 - 250	2.5	(0.62)

Table 6 (Continued)

Au(n,γ) Cross Section

Energy (keV)	Estimated Uncertainty (%)	Comb. Result (%)
2.53E-05	0.14	(0.14)
200 - 500	3.0	(1.31)
500 - 1000	3.5	(2.1)
1000 - 2500	4.5	(2.0)

^{235}U(n,f) Cross Section

Energy (keV)	Estimated Uncertainty (%)	Comb. Result (%)
2.53E-05	0.2	(0.19)
150 - 600	1.5	(0.67)
600 - 1000	1.6	(0.60)
1000 - 3000	1.8	(0.55)
3000 - 6000	2.3	(0.69)
6000 - 10000	2.2	(0.94)
10000 - 12000	1.8	(1.14)
12000 - 14000	1.2	(0.88)
14000 - 14500	0.8	(0.55)
14500 - 15000	1.5	(0.68)
15000 - 16000	2.0	(0.97)
16000 - 17000	2.5	(1.18)
17000 - 19000	3.0	(1.26)
19000 - 20000	4.0	(1.39)

Table 7. $^{6}Li(n,t)$ Cross Section

ENDF/B-VI MAT 325

Recommended as a standard below 1 MeV
Log-log interpolation up to 500 keV
Linear-linear interpolation above 500 keV

Cross Section Values

E_n (MeV)	σ(b)	Uncertainty(%)	E_n (MeV)	σ(b)	Uncertainty(%)
0.2530E-07	940.9827	0.14	0.2360E+00	3.2416	0.24
0.9400E-05	48.7928	0.14	0.2370E+00	3.2495	0.24
0.1500E-03	12.1957	0.14	0.2380E+00	3.2546	0.24
0.2500E-03	9.4428	0.14	0.2390E+00	3.2571	0.24
0.3500E-03	7.9777	0.14	0.2400E+00	3.2568	0.23
0.4500E-03	7.0337	0.14	0.2410E+00	3.2539	0.23
0.5500E-03	6.3613	0.14	0.2420E+00	3.2485	0.23
0.6500E-03	5.8502	0.14	0.2430E+00	3.2403	0.23
0.7500E-03	5.4454	0.14	0.2440E+00	3.2297	0.23
0.8500E-03	5.1137	0.14	0.2450E+00	3.2164	0.23
0.9500E-03	4.8371	0.14	0.2500E+00	3.1145	0.24
0.1500E-02	3.8470	0.14	0.2600E+00	2.7896	0.26
0.2500E-02	2.9791	0.14	0.2700E+00	2.4026	0.28
0.3500E-02	2.5181	0.14	0.2800E+00	2.0366	0.29
0.4500E-02	2.2214	0.14	0.3000E+00	1.4743	0.31
0.5500E-02	2.0110	0.14	0.3100E+00	1.2746	0.32
0.6500E-02	1.8516	0.14	0.3250E+00	1.0498	0.32
0.7500E-02	1.7243	0.14	0.3350E+00	0.9365	0.32
0.8500E-02	1.6221	0.14	0.3500E+00	0.8056	0.32
0.9500E-02	1.5358	0.14	0.3600E+00	0.7376	0.32
0.1500E-01	1.2301	0.14	0.3750E+00	0.6565	0.31
0.2000E-01	1.0737	0.15	0.3850E+00	0.6128	0.31
0.2400E-01	0.9867	0.15	0.4000E+00	0.5591	0.31
0.3000E-01	0.8930	0.16	0.4100E+00	0.5294	0.31
0.3500E-01	0.8359	0.17	0.4250E+00	0.4919	0.31
0.4500E-01	0.7562	0.18	0.4350E+00	0.4706	0.31
0.5500E-01	0.7052	0.20	0.4500E+00	0.4431	0.31
0.6500E-01	0.6725	0.22	0.4600E+00	0.4273	0.31
0.7500E-01	0.6532	0.24	0.4750E+00	0.4065	0.31
0.8500E-01	0.6450	0.26	0.4850E+00	0.3944	0.31
0.9500E-01	0.6468	0.29	0.5000E+00	0.3782	0.31
0.1000E+00	0.6515	0.30	0.5200E+00	0.3597	0.31
0.1100E+00	0.6687	0.32	0.5400E+00	0.3441	0.32
0.1200E+00	0.6976	0.33	0.5700E+00	0.3249	0.32
0.1300E+00	0.7406	0.34	0.6000E+00	0.3093	0.33
0.1400E+00	0.8013	0.35	0.6500E+00	0.2891	0.34
0.1500E+00	0.8843	0.36	0.7000E+00	0.2740	0.35
0.1600E+00	0.9968	0.36	0.7500E+00	0.2623	0.36
0.1700E+00	1.1485	0.35	0.8000E+00	0.2529	0.37
0.1800E+00	1.3522	0.35	0.8500E+00	0.2454	0.38
0.1900E+00	1.6207	0.34	0.9000E+00	0.2391	0.39
0.2000E+00	1.9653	0.32	0.9400E+00	0.2349	0.39
0.2100E+00	2.3763	0.30	0.9600E+00	0.2331	0.40
0.2200E+00	2.8047	0.27	0.9800E+00	0.2313	0.40
0.2300E+00	3.1393	0.25	0.1000E+01	0.2297	0.41
0.2350E+00	3.2311	0.24			

Table 8. $^{10}B(n,\alpha)$ Cross Section

ENDF/B-VI MAT 525

This cross section is the sum of the $^{10}B(n,\alpha_0)$ and $^{10}B(n,\alpha_1)$ cross sections and is recommended as a standard below 250 keV.

Log-log interpolation

Cross Section Values

E_n (MeV)	σ(b)	Uncertainty(%)
0.2530E-07	3839.4960	0.16
0.9400E-05	198.9352	0.16
0.1500E-03	49.6172	0.16
0.2500E-03	38.3776	0.16
0.3500E-03	32.4006	0.16
0.4500E-03	28.5444	0.16
0.5500E-03	25.7955	0.16
0.6500E-03	23.7176	0.16
0.7500E-03	22.0661	0.16
0.8500E-03	20.7130	0.16
0.9500E-03	19.5736	0.16
0.1500E-02	15.5351	0.17
0.2500E-02	11.9871	0.17
0.3500E-02	10.1050	0.17
0.4500E-02	8.8924	0.17
0.5500E-02	8.0282	0.18
0.6500E-02	7.3740	0.18
0.7500E-02	6.8551	0.18
0.8500E-02	6.4321	0.18
0.9500E-02	6.0785	0.18
0.1500E-01	4.8211	0.20
0.2000E-01	4.1703	0.21
0.2400E-01	3.8072	0.23
0.3000E-01	3.4107	0.25
0.4500E-01	2.8081	0.30
0.5500E-01	2.5605	0.32
0.6500E-01	2.3775	0.34
0.7500E-01	2.2354	0.36
0.8500E-01	2.1212	0.39
0.9500E-01	2.0275	0.41
0.1000E+00	1.9851	0.43
0.1200E+00	1.8443	0.48
0.1500E+00	1.6747	0.53
0.1700E+00	1.5729	0.55
0.1800E+00	1.5248	0.56
0.1900E+00	1.4774	0.57
0.2000E+00	1.4314	0.58
0.2100E+00	1.3856	0.59
0.2200E+00	1.3411	0.59
0.2300E+00	1.2982	0.60
0.2350E+00	1.2776	0.60
0.2400E+00	1.2565	0.60
0.2450E+00	1.2365	0.60
0.2500E+00	1.2168	0.60

Table 9. $^{10}B(n,\alpha_1)$ Cross Section

ENDF/B-VI MAT 525

Recommended as a standard cross section below 250 keV

Log-log interpolation

Cross Section Values

E_n (MeV)	σ(b)	Uncertainty(%)
0.2530E-07	3598.2280	0.16
0.9400E-05	186.4350	0.16
0.1500E-03	46.5003	0.16
0.2500E-03	35.9671	0.16
0.3500E-03	30.3659	0.16
0.4500E-03	26.7516	0.16
0.5500E-03	24.1756	0.16
0.6500E-03	22.2287	0.16
0.7500E-03	20.6811	0.16
0.8500E-03	19.4130	0.17
0.9500E-03	18.3446	0.17
0.1500E-02	14.5603	0.17
0.2500E-02	11.2352	0.17
0.3500E-02	9.4717	0.17
0.4500E-02	8.3353	0.18
0.5500E-02	7.5254	0.18
0.6500E-02	6.9123	0.18
0.7500E-02	6.4260	0.18
0.8500E-02	6.0296	0.18
0.9500E-02	5.6981	0.18
0.1500E-01	4.5194	0.20
0.2000E-01	3.9090	0.21
0.2400E-01	3.5682	0.23
0.3000E-01	3.1959	0.25
0.4500E-01	2.6285	0.30
0.5500E-01	2.3943	0.33
0.6500E-01	2.2203	0.35
0.7500E-01	2.0844	0.38
0.8500E-01	1.9745	0.40
0.9500E-01	1.8835	0.43
0.1000E+00	1.8420	0.44
0.1200E+00	1.7031	0.49
0.1500E+00	1.5330	0.55
0.1700E+00	1.4303	0.57
0.1800E+00	1.3817	0.58
0.1900E+00	1.3340	0.59
0.2000E+00	1.2876	0.60
0.2100E+00	1.2417	0.61
0.2200E+00	1.1972	0.62
0.2300E+00	1.1543	0.62
0.2350E+00	1.1338	0.62
0.2400E+00	1.1127	0.62
0.2450E+00	1.0928	0.63
0.2500E+00	1.0732	0.63

Table 10. Au(n,γ) Cross Section

ENDF/B-VI MAT 7925

Recommended as a standard cross section from 200 keV to 2.5 MeV

Linear-linear interpolation

Cross Section Values

E_n (MeV)	σ(b)	Uncertainty(%)
0.2000E+00	0.2502	1.24
0.2100E+00	0.2469	1.43
0.2200E+00	0.2445	1.35
0.2300E+00	0.2415	1.35
0.2350E+00	0.2403	1.33
0.2400E+00	0.2388	1.67
0.2450E+00	0.2374	1.23
0.2500E+00	0.2360	1.36
0.2600E+00	0.2331	1.38
0.2700E+00	0.2299	1.49
0.2800E+00	0.2141	1.31
0.3000E+00	0.1999	1.30
0.3250E+00	0.1877	1.23
0.3500E+00	0.1778	1.25
0.3750E+00	0.1689	1.25
0.4000E+00	0.1614	1.16
0.4250E+00	0.1538	1.21
0.4500E+00	0.1462	1.17
0.4750E+00	0.1389	1.27
0.5000E+00	0.1324	1.15
0.5200E+00	0.1270	1.22
0.5400E+00	0.1236	1.33
0.5700E+00	0.1186	1.64
0.6000E+00	0.1084	1.37
0.6500E+00	0.1002	1.73
0.7000E+00	0.0964	1.42
0.7500E+00	0.0928	1.66
0.8000E+00	0.0897	1.57
0.8500E+00	0.0869	2.10
0.9000E+00	0.0843	3.10
0.9400E+00	0.0825	3.10
0.9600E+00	0.0818	3.70
0.9800E+00	0.0810	4.00
0.1000E+01	0.0803	2.50
0.1100E+01	0.0772	1.80
0.1250E+01	0.0729	1.48
0.1400E+01	0.0694	1.75
0.1600E+01	0.0665	1.70
0.1800E+01	0.0596	1.78
0.2000E+01	0.0534	2.05
0.2200E+01	0.0433	2.01
0.2400E+01	0.0360	3.02
0.2600E+01	0.0311	2.40

At thermal energy, E = 0.0253 eV, the ENDF/B-VI value is 98.71 b (the result of this evaluation process is 98.69 b with an uncertainty of 0.14%).

Table 11. $^{235}U(n,f)$ Cross Section

ENDF/B-VI MAT 9228

Recommended as a standard above 150 keV
Linear-linear interpolation

Cross Section Values

E_n (MeV)	σ(b)	Uncertainty(%)	E_n (MeV)	σ(b)	Uncertainty(%)
0.1500E+00	1.4203	0.58	0.1400E+01	1.2200	0.54
0.1700E+00	1.3967	0.72	0.1600E+01	1.2435	0.52
0.1800E+00	1.3800	0.70	0.1800E+01	1.2619	0.54
0.1900E+00	1.3647	0.82	0.2000E+01	1.2714	0.51
0.2000E+00	1.3510	0.79	0.2200E+01	1.2699	0.53
0.2100E+00	1.3370	0.71	0.2400E+01	1.2561	0.55
0.2200E+00	1.3265	0.71	0.2600E+01	1.2442	0.59
0.2300E+00	1.3130	0.63	0.2800E+01	1.2220	0.62
0.2350E+00	1.3100	0.67	0.3000E+01	1.2010	0.58
0.2400E+00	1.3070	0.68	0.3600E+01	1.1473	0.62
0.2450E+00	1.3030	0.64	0.4000E+01	1.1295	0.63
0.2500E+00	1.2930	0.58	0.4500E+01	1.1011	0.64
0.2600E+00	1.2690	0.63	0.4700E+01	1.0923	0.70
0.2700E+00	1.2500	0.62	0.5000E+01	1.0617	0.70
0.2800E+00	1.2350	0.65	0.5300E+01	1.0502	0.72
0.3000E+00	1.2300	0.60	0.5500E+01	1.0388	0.72
0.3250E+00	1.2300	0.70	0.5800E+01	1.0408	0.78
0.3500E+00	1.2230	0.64	0.6000E+01	1.0985	0.85
0.3750E+00	1.2130	0.70	0.6200E+01	1.1817	0.87
0.4000E+00	1.2020	0.66	0.6500E+01	1.3481	0.87
0.4250E+00	1.1900	0.74	0.7000E+01	1.5467	0.89
0.4500E+00	1.1662	0.70	0.7500E+01	1.6964	0.94
0.4750E+00	1.1510	0.73	0.7750E+01	1.7300	1.05
0.5000E+00	1.1410	0.59	0.8000E+01	1.7606	1.01
0.5200E+00	1.1365	0.72	0.8500E+01	1.7800	0.89
0.5400E+00	1.1300	0.62	0.9000E+01	1.7700	0.99
0.5700E+00	1.1220	0.67	0.1000E+02	1.7415	1.06
0.6000E+00	1.1185	0.62	0.1100E+02	1.7219	1.11
0.6500E+00	1.1182	0.58	0.1150E+02	1.7170	1.26
0.7000E+00	1.1135	0.59	0.1200E+02	1.7347	1.14
0.7500E+00	1.1120	0.58	0.1300E+02	1.9002	0.90
0.8000E+00	1.1100	0.56	0.1400E+02	2.0600	0.59
0.8500E+00	1.1135	0.59	0.1450E+02	2.0800	0.51
0.9000E+00	1.1372	0.57	0.1500E+02	2.0890	0.84
0.9400E+00	1.1691	0.60	0.1600E+02	2.0890	1.10
0.9600E+00	1.1876	0.64	0.1700E+02	2.0413	1.27
0.9800E+00	1.1992	0.72	0.1800E+02	1.9748	1.26
0.1000E+01	1.1969	0.52	0.1900E+02	1.9325	1.25
0.1100E+01	1.1938	0.54	0.2000E+02	1.9343	1.52
0.1250E+01	1.2020	0.51			

At thermal energy, E = 0.0253 eV, the ENDF/B-VI value [40] is 583.98 at 300 °K (the result of this evaluation process is 584.25 b with an uncertainty of 0.19%).

Table 12. Prompt Neutron Spectrum from the Spontaneous Fission of ^{252}Cf

Linear-linear interpolation

E (eV)	N(E) (1/eV)	E (eV)	N(E) (1/eV)	E (eV)	N(E) (1/eV)
1.00000-5	2.03300-12	2.00000-5	2.87500-12	5.00000-5	4.54600-12
1.00000-4	6.43000-12	2.00000-4	9.09300-12	5.00000-4	1.43800-11
1.00000-3	2.03300-11	2.00000-3	2.87500-11	5.00000-3	4.54600-11
1.00000-2	6.43000-11	2.00000-2	9.09300-11	5.00000-2	1.43800-10
1.00000-1	2.03300-10	2.00000-1	2.87500-10	5.00000-1	4.54600-10
1.00000+0	6.43000-10	2.00000+0	9.09300-10	5.00000+0	1.43800-09
1.00000+1	2.03300-09	2.00000+1	2.87500-09	5.00000+1	4.54600-09
1.00000+2	6.42900-09	2.00000+2	9.09200-09	5.00000+2	1.43700-08
1.00000+3	2.03200-08	2.00000+3	2.87100-08	5.00000+3	4.53000-08
1.00000+4	6.38500-08	2.50000+4	9.98900-08	3.00000+4	1.09000-07
3.50000+4	1.17400-07	4.50000+4	1.32200-07	5.50000+4	1.45200-07
7.00000+4	1.62200-07	8.50000+4	1.76900-07	1.00000+5	1.90000-07
1.30000+5	2.12300-07	1.60000+5	2.30800-07	2.00000+5	2.51200-07
2.50000+5	2.71600-07	3.00000+5	2.87700-07	3.70000+5	3.04900-07
4.60000+5	3.20100-07	5.00000+5	3.24800-07	6.00000+5	3.32900-07
7.00000+5	3.36300-07	8.50000+5	3.35200-07	1.00000+6	3.28900-07
1.20000+6	3.15200-07	1.50000+6	2.87500-07	2.00000+6	2.35200-07
2.40000+6	1.95000-07	2.70000+6	1.67700-07	3.00000+6	1.43100-07
3.30000+6	1.21300-07	3.50000+6	1.08200-07	3.70000+6	9.63600-08
3.90000+6	8.55900-08	4.10000+6	7.58800-08	4.30000+6	6.71600-08
4.50000+6	5.93700-08	4.70000+6	5.24200-08	4.90000+6	4.62500-08
5.10000+6	4.07800-08	5.30000+6	3.59200-08	5.50000+6	3.16300-08
5.70000+6	2.78200-08	5.90000+6	2.44600-08	6.10000+6	2.14900-08
6.30000+6	1.88700-08	6.50000+6	1.65500-08	6.70000+6	1.45100-08
6.90000+6	1.27200-08	7.10000+6	1.11400-08	7.30000+6	9.75500-09
7.50000+6	8.54000-09	7.70000+6	7.47500-09	7.90000+6	6.54100-09
8.10000+6	5.72500-09	8.30000+6	5.01100-09	8.50000+6	4.38500-09
8.70000+6	3.83800-09	8.90000+6	3.36000-09	9.10000+6	2.94000-09
9.30000+6	2.57300-09	9.50000+6	2.25200-09	9.70000+6	1.97000-09
9.90000+6	1.72300-09	1.01000+7	1.50600-09	1.03000+7	1.31700-09
1.05000+7	1.15100-09	1.07000+7	1.00700-09	1.09000+7	8.80200-10
1.11000+7	7.69700-10	1.13000+7	6.72900-10	1.15000+7	5.88300-10
1.17000+7	5.14200-10	1.19000+7	4.49400-10	1.21000+7	3.92700-10
1.23000+7	3.43000-10	1.25000+7	2.99600-10	1.27000+7	2.61700-10
1.29000+7	2.28400-10	1.31000+7	1.99400-10	1.32000+7	1.86200-10
1.34000+7	1.62500-10	1.35000+7	1.51700-10	1.37000+7	1.32300-10
1.39000+7	1.15400-10	1.41000+7	1.00700-10	1.42000+7	9.39900-11
1.44000+7	8.19500-11	1.46000+7	7.14500-11	1.53000+7	4.42000-11
1.60000+7	2.73300-11	1.67000+7	1.68800-11	1.74000+7	1.04200-11
1.81000+7	6.42200-12	1.88000+7	3.95000-12	1.95000+7	2.42700-12
2.00000+7	1.71300-12				

Table 13. Uncertainty in the Prompt Neutron Spectrum from the Spontaneous Fission of ^{252}Cf

Energy Range (eV)	Uncertainty (%)	Energy Range (eV)	Uncertainty (%)
0.000E+0 - 1.500E+4	30.00	2.150E+6 - 2.350E+6	1.14
1.500E+4 - 3.500E+4	10.35	2.350E+6 - 2.550E+6	1.14
3.500E+4 - 5.500E+4	4.68	2.550E+6 - 2.750E+6	1.22
5.500E+4 - 7.500E+4	4.28	2.750E+6 - 2.950E+6	1.19
7.500E+4 - 9.500E+4	4.78	2.950E+6 - 3.250E+6	1.17
9.500E+4 - 1.150E+5	3.41	3.250E+6 - 3.550E+6	1.19
1.150E+5 - 1.350E+5	3.34	3.550E+6 - 3.850E+6	1.18
1.350E+5 - 1.650E+5	2.65	3.850E+6 - 4.150E+6	1.19
1.650E+5 - 1.950E+5	2.24	4.150E+6 - 4.450E+6	1.32
1.950E+5 - 2.250E+5	2.25	4.450E+6 - 4.750E+6	1.37
2.250E+5 - 2.550E+5	1.85	4.750E+6 - 5.050E+6	1.35
2.550E+5 - 3.050E+5	1.84	5.050E+6 - 5.550E+6	1.50
3.050E+5 - 3.550E+5	1.69	5.550E+6 - 6.050E+6	1.47
3.550E+5 - 4.050E+5	1.73	6.050E+6 - 6.550E+6	1.58
4.050E+5 - 4.550E+5	1.66	6.550E+6 - 7.050E+6	1.65
4.550E+5 - 5.050E+5	1.65	7.050E+6 - 7.550E+6	1.79
5.050E+5 - 5.550E+5	1.80	7.550E+6 - 8.050E+6	1.86
5.550E+5 - 6.050E+5	1.75	8.050E+6 - 8.550E+6	2.07
6.050E+5 - 6.550E+5	1.62	8.550E+6 - 9.050E+6	2.16
6.550E+5 - 7.050E+5	1.82	9.050E+6 - 9.550E+6	2.25
7.050E+5 - 7.550E+5	1.87	9.550E+6 - 1.005E+7	2.47
7.550E+5 - 8.050E+5	1.83	1.005E+7 - 1.055E+7	2.69
8.050E+5 - 8.550E+5	1.75	1.055E+7 - 1.105E+7	2.90
8.550E+5 - 9.050E+5	1.93	1.105E+7 - 1.155E+7	2.93
9.050E+5 - 9.550E+5	1.74	1.155E+7 - 1.205E+7	3.44
9.550E+5 - 1.050E+6	1.56	1.205E+7 - 1.255E+7	3.59
1.050E+6 - 1.150E+6	1.22	1.255E+7 - 1.305E+7	5.04
1.150E+6 - 1.250E+6	1.21	1.305E+7 - 1.355E+7	4.47
1.250E+6 - 1.350E+6	1.24	1.355E+7 - 1.405E+7	6.27
1.350E+6 - 1.450E+6	1.24	1.405E+7 - 1.460E+7	9.61
1.450E+6 - 1.550E+6	1.23	1.460E+7 - 1.590E+7	12.41
1.550E+6 - 1.650E+6	1.23	1.590E+7 - 1.690E+7	14.70
1.650E+6 - 1.750E+6	1.25	1.690E+7 - 1.790E+7	19.44
1.750E+6 - 1.850E+6	1.20	1.790E+7 - 1.910E+7	32.31
1.850E+6 - 1.950E+6	1.23	1.910E+7 - 2.000E+7	76.95
1.950E+6 - 2.150E+6	1.15		

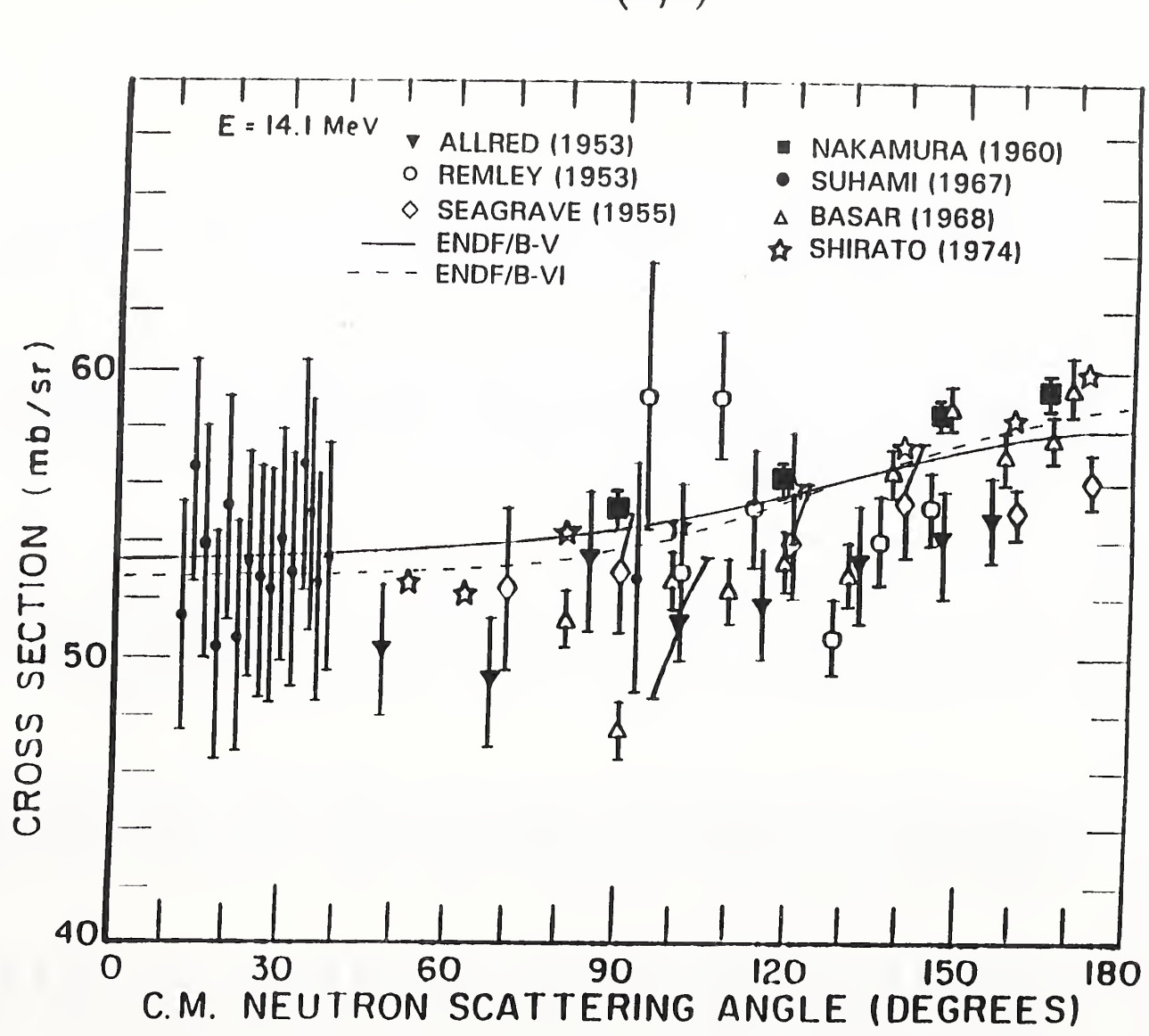

Fig. 1 Measurements of the hydrogen scattering cross section at 14.1 MeV compared with the ENDF/B-V and ENDF/B-VI evaluations. The references for the experimental data are given in reference [41].

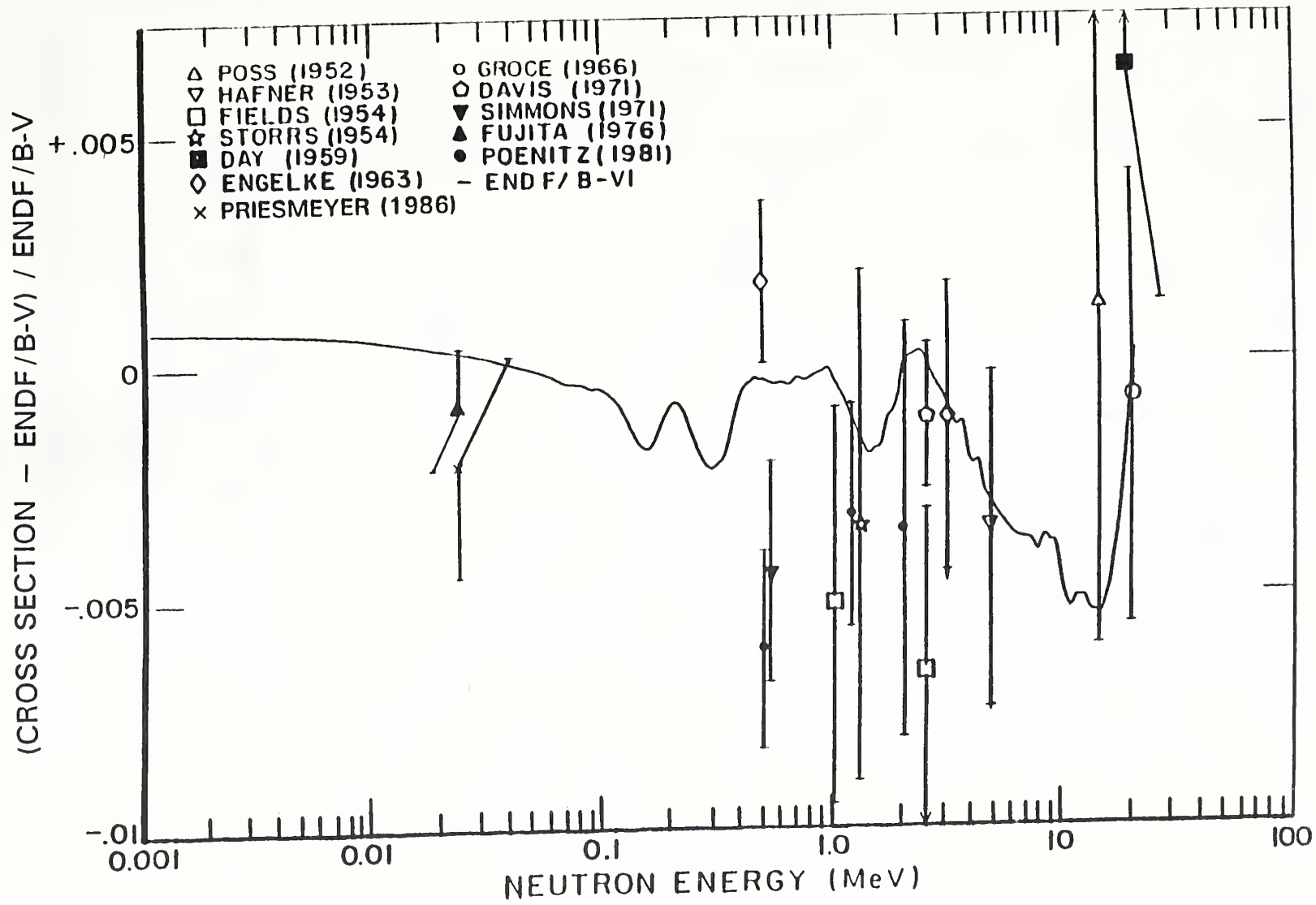

Fig. 2 Comparison of high accuracy measurements of the hydrogen total neutron cross section and the ENDF/B-V and ENDF/B-VI evaluations. The references for the experimental data except Priesmeyer, *et al.* [42] are given in reference [41].

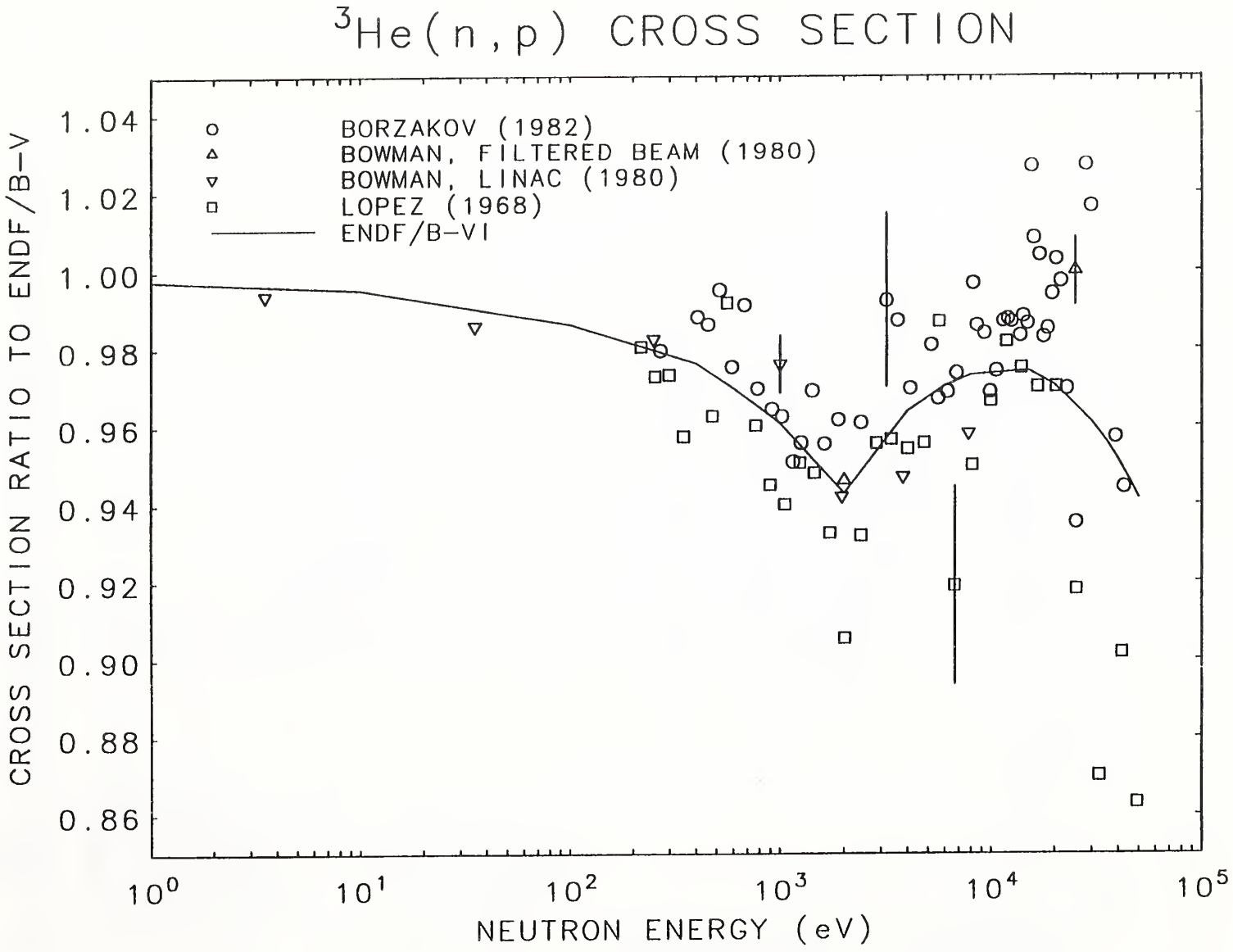

Fig. 3 Measurements of the ^{3}He(n,p) cross section compared with the ENDF/B-V and ENDF/B-VI evaluations. The references for the experimental data except Borzakov [43] are given in reference [41].

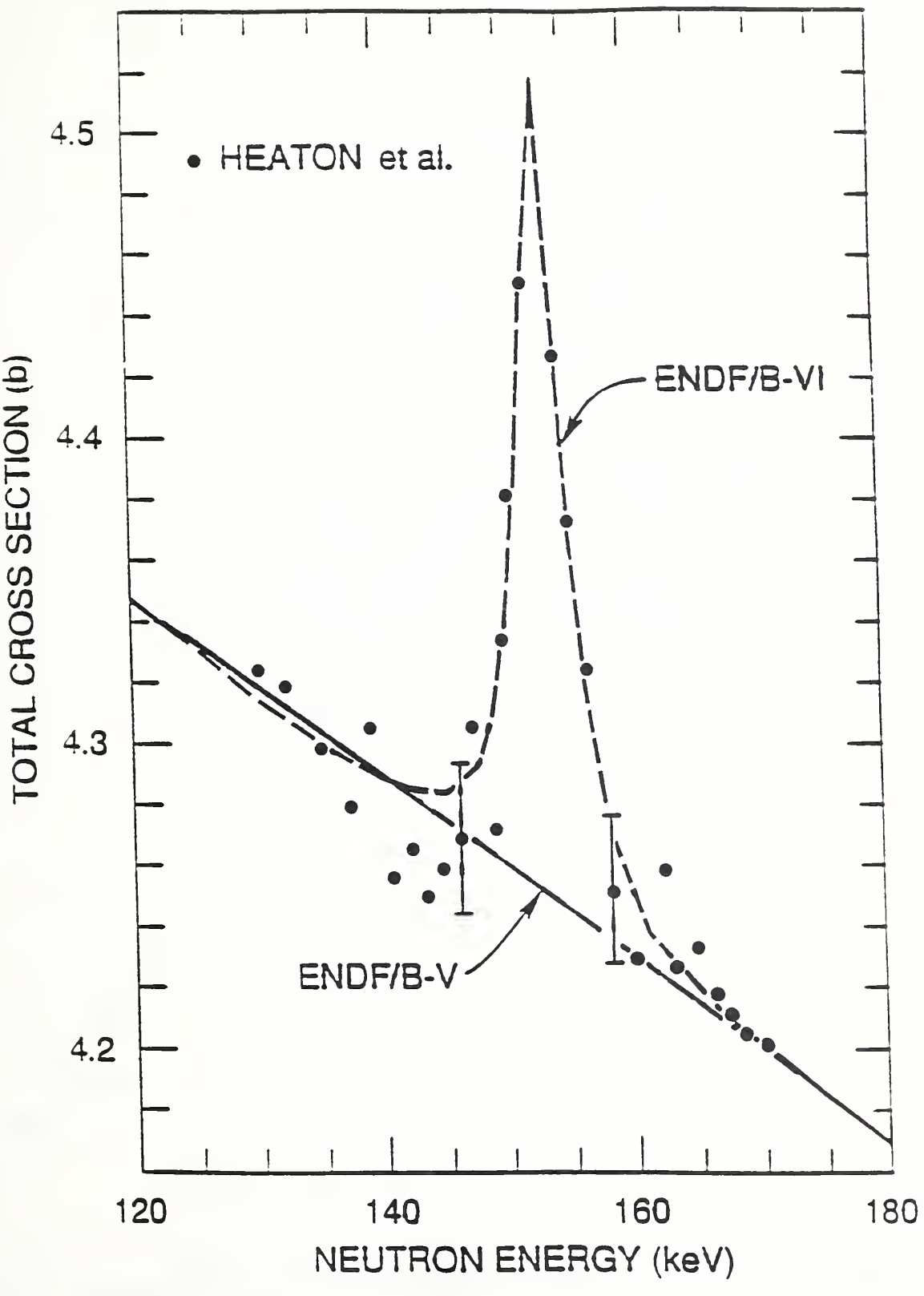

Fig. 4 Comparison of the measurements of Heaton *et al.* [32], of the carbon total cross section near the 152.9 keV resonance in ^{13}C with the ENDF/B-V and ENDF/B-VI evaluations.

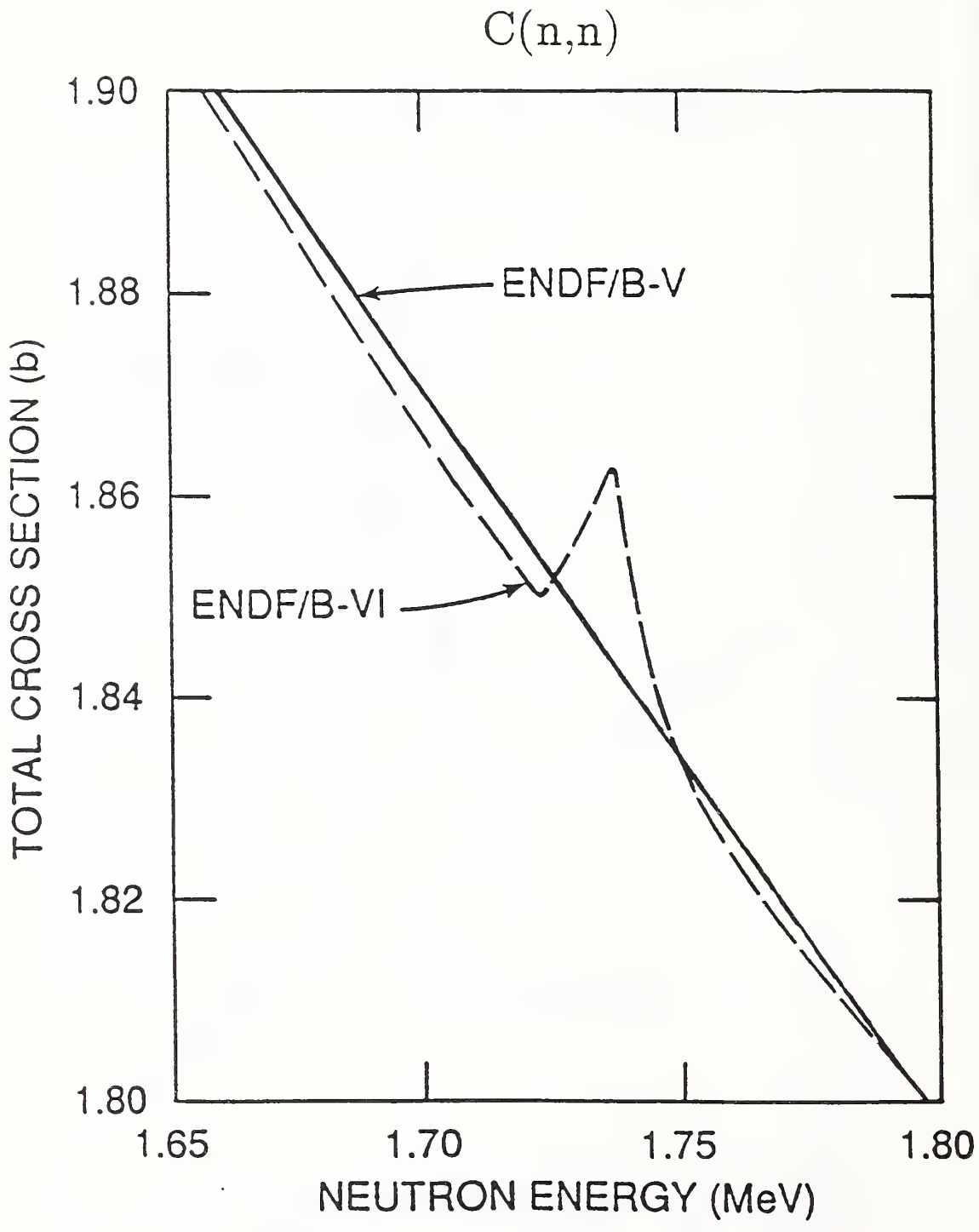

Fig. 5 Comparison of the ENDF/B-V and ENDF/B-VI carbon total cross sections near the 1.736 MeV resonance in ^{13}C.

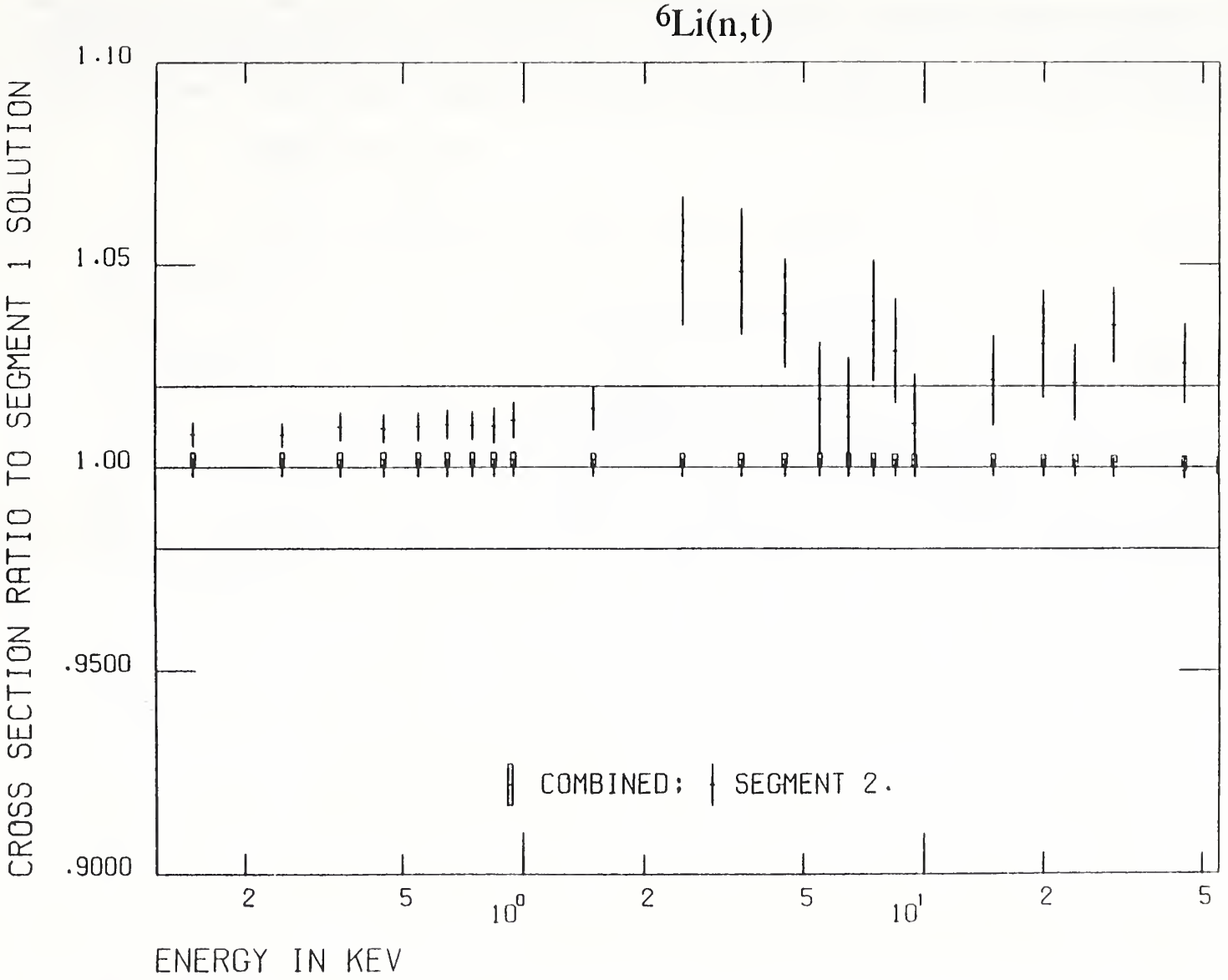

Fig. 6 Cross section ratios to the Segment 1 solution for the ^{6}Li(n,t) reaction from about 0.2 to 50 keV. The rectangles refer to the ratio of the combination output to the R-matrix fit of the Segment 1 data. The ┼'s refer to the ratio of the simultaneous evaluation of the segment 2 data to the R-matrix fit of the Segment 1 data. The error bars indicate the uncertainties for the fits. The error bars on the unit ratio line are the uncertainties in the R-matrix fit of the Segment 1 data. The lines at ratios of 0.98 and 1.02 are guides to the eye.

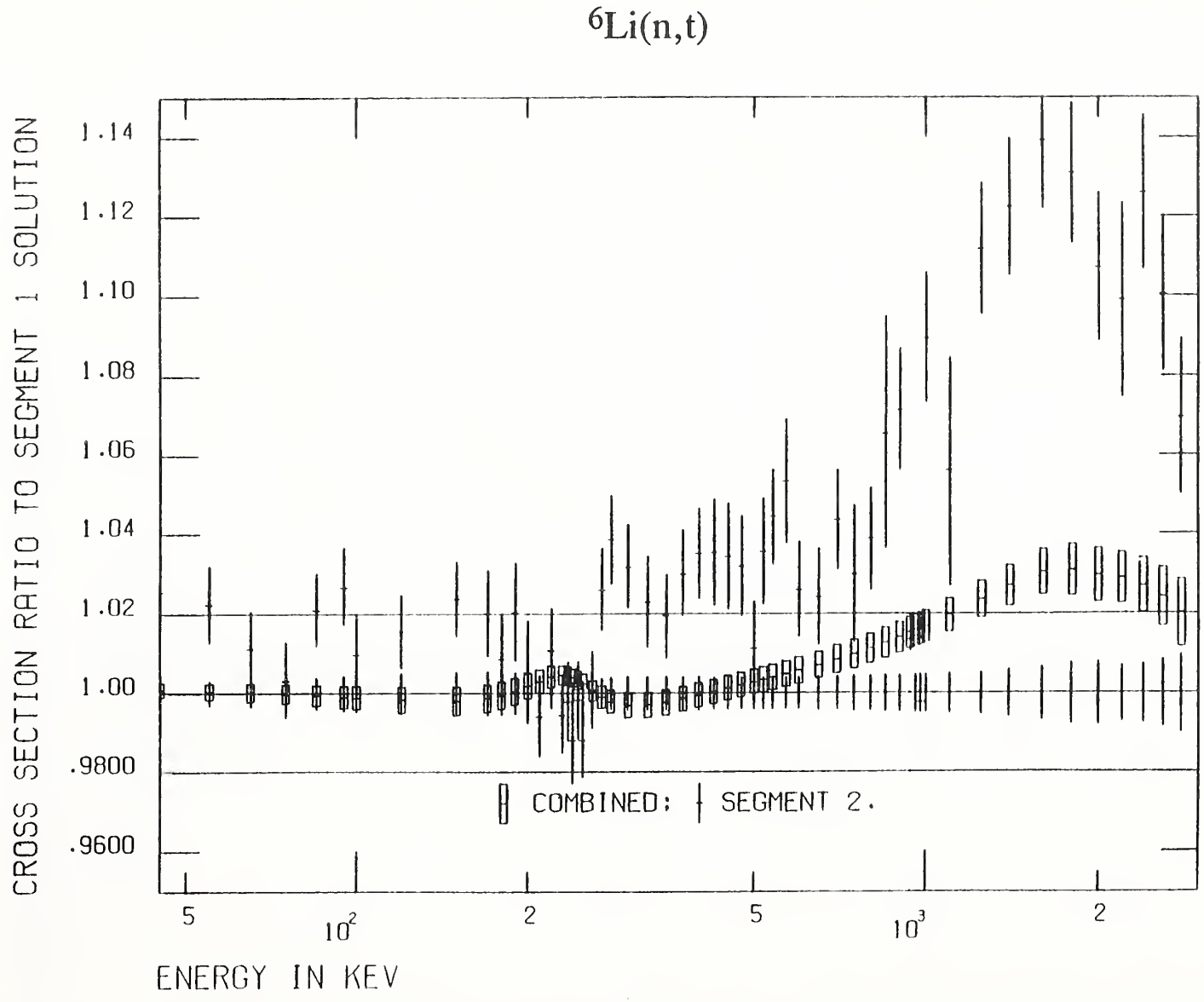

Fig. 7 Cross section ratios to the segment 1 solution for the ^{6}Li(n,t) reaction from about 50 keV to 2 MeV. The rectangles refer to the ratio of the combination output to the R-matrix fit of the segment 1 data. The ┼'s refer to the ratio of the simultaneous evaluation of the segment 2 data to the R-matrix fit of the segment 1 data. The error bars indicate the uncertainties for the fits. The error bars on the unit ratio line are the uncertainties in the R-matrix fit of the segment 1 data. The lines at ratios of 0.98 and 1.02 are guides to the eye.

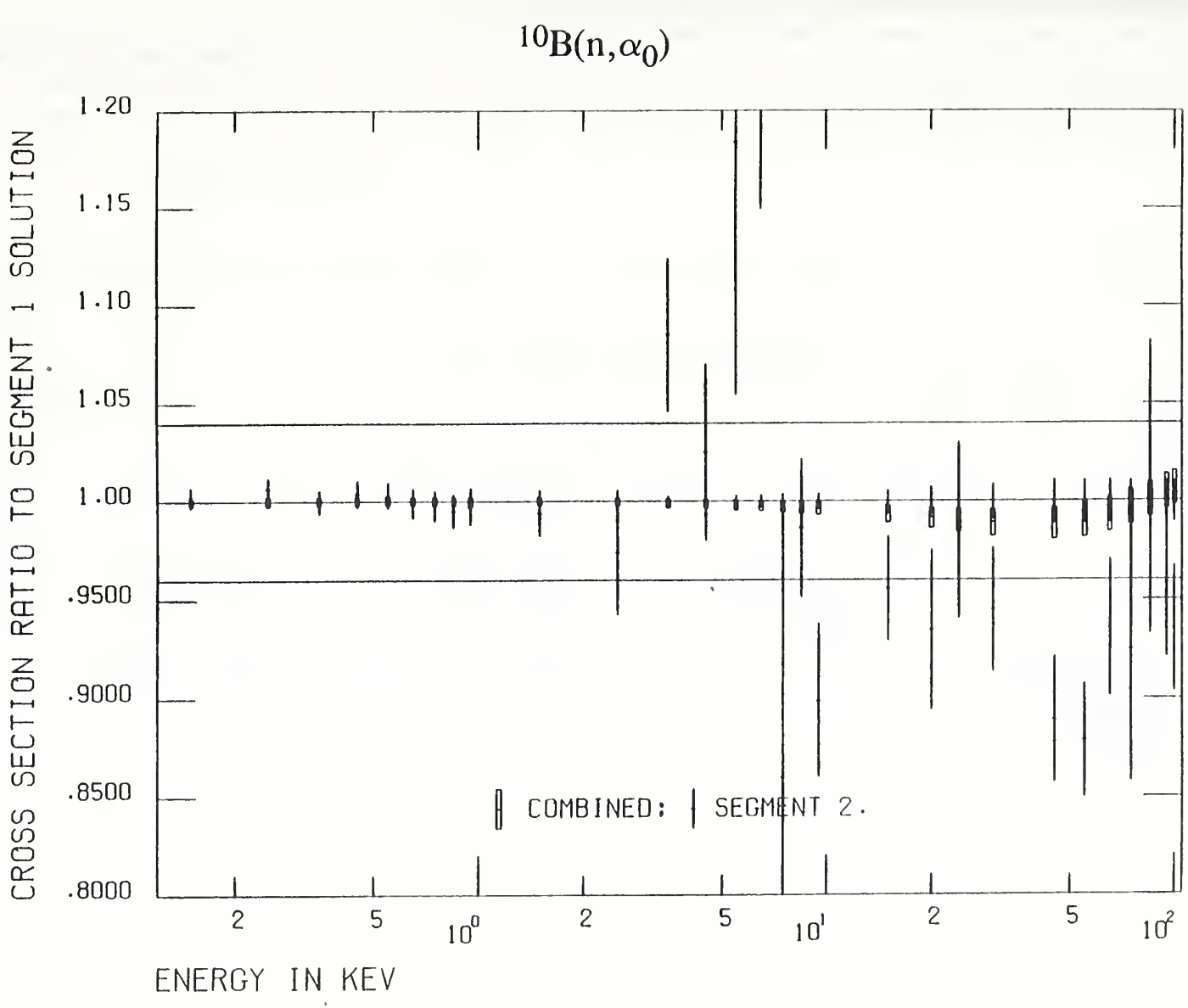

Fig. 8 Cross section ratios to the segment 1 solution for the $^{10}B(n,\alpha_0)$ reaction from about 0.2 to 100 keV. The rectangles refer to the ratio of the combination output to the R-matrix fit of the segment 1 data. The ┼'s refer to the ratio of the simultaneous evaluation of the segment 2 data to the R-matrix fit of the segment 1 data. The error bars indicate the uncertainties for the fits. The error bars on the unit ratio line are the uncertainties in the R-matrix fit of the segment 1 data. The lines at ratios of 0.96 and 1.04 are guides to the eye.

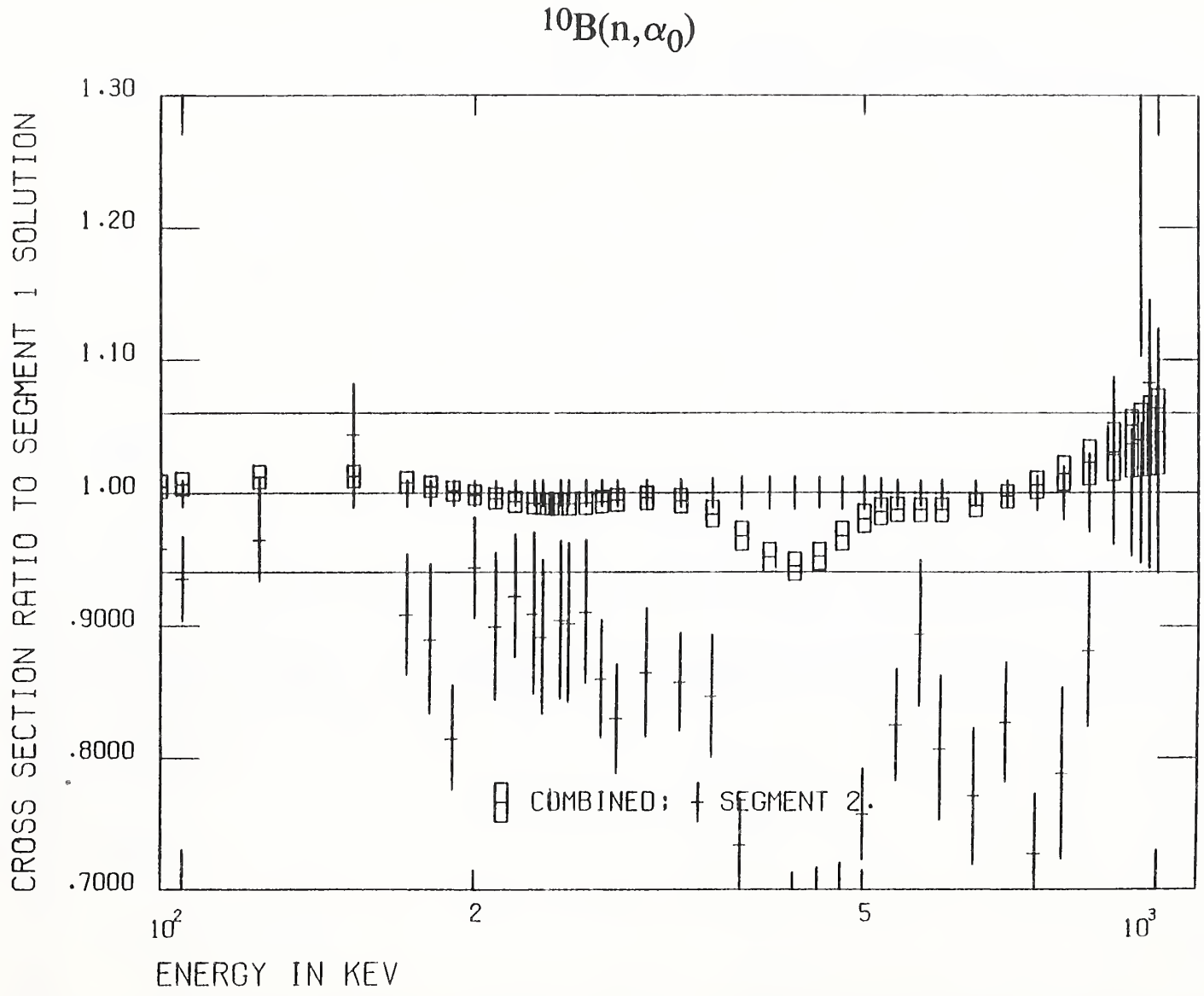

Fig. 9 Cross section ratios to the segment 1 solution for the $^{10}B(n,\alpha_0)$ reaction from about 100 keV to 1 MeV. The rectangles refer to the ratio of the combination output to the R-matrix fit of the segment 1 data. The +'s refer to the ratio of the simultaneous evaluation of the segment 2 data to the R-matrix fit of the segment 1 data. The error bars indicate the uncertainties for the fits. The error bars on the unit ratio line are the uncertainties in the R-matrix fit of the segment 1 data. The lines at ratios of 0.93 and 1.07 are guides to the eye.

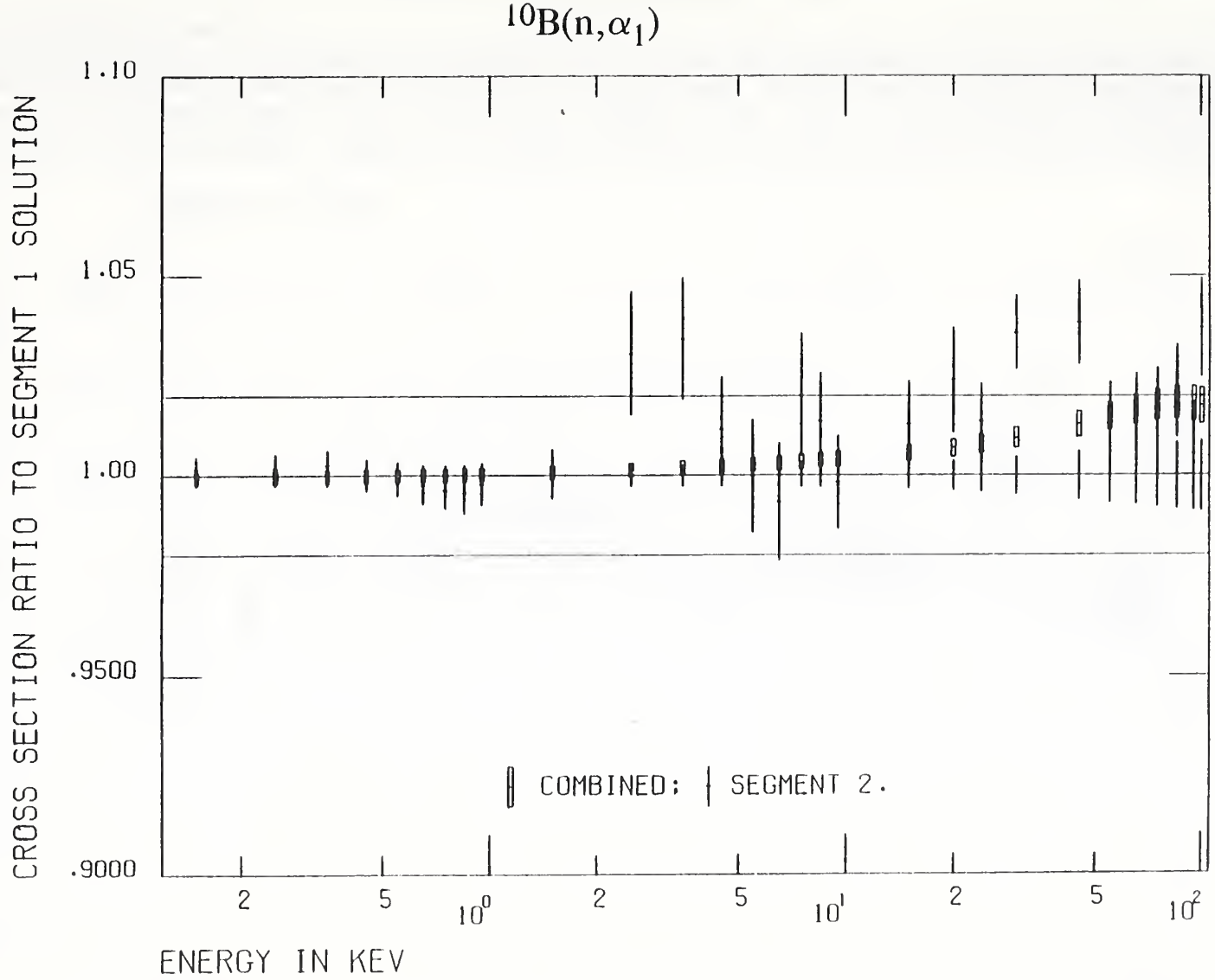

Fig. 10 Cross section ratios to the segment 1 solution for the $^{10}B(n,\alpha_1)$ reaction from about 0.2 keV to 100 keV. The rectangles refer to the ratio of the combination output to the R-matrix fit of the segment 1 data. The ┼'s refer to the ratio of the simultaneous evaluation of the segment 2 data to the R-matrix fit of the segment 1 data. The error bars indicate the uncertainties for the fits. The error bars on the unit ratio line are the uncertainties in the R-matrix fit of the segment 1 data. The lines at ratios of 0.98 and 1.02 are guides to the eye.

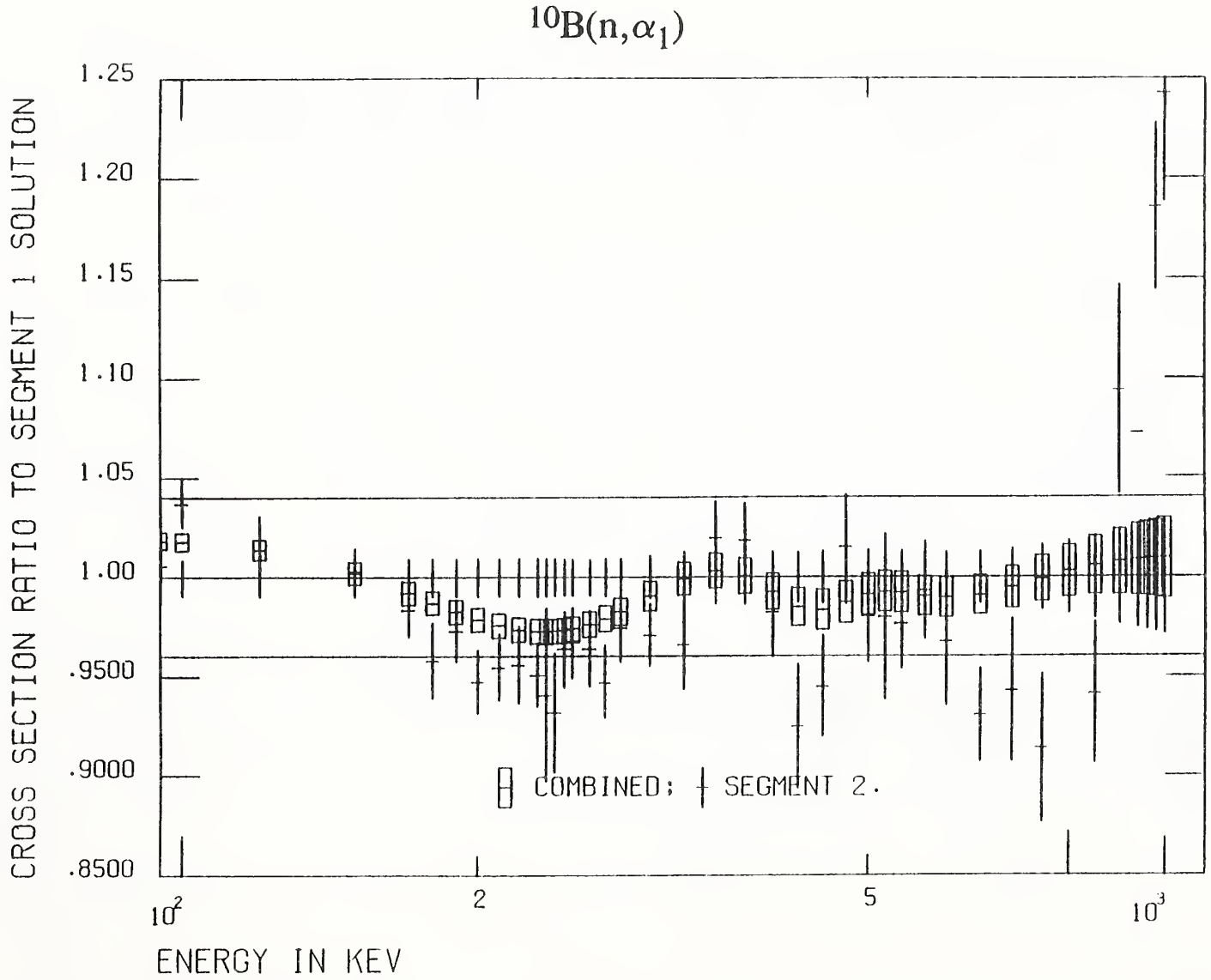

Fig. 11 Cross section ratios to the segment 1 solution for the $^{10}B(n,\alpha_1)$ reaction from about 100 keV to 1 MeV. The rectangles refer to the ratio of the combination output to the R-matrix fit of the segment 1 data. The +'s refer to the ratio of the simultaneous evaluation of the segment 2 data to the R-matrix fit of the segment 1 data. The error bars indicate the uncertainties for the fits. The error bars on the unit ratio line are the uncertainties in the R-matrix fit of the segment 1 data. The lines at ratios of 0.96 and 1.04 are guides to the eye.

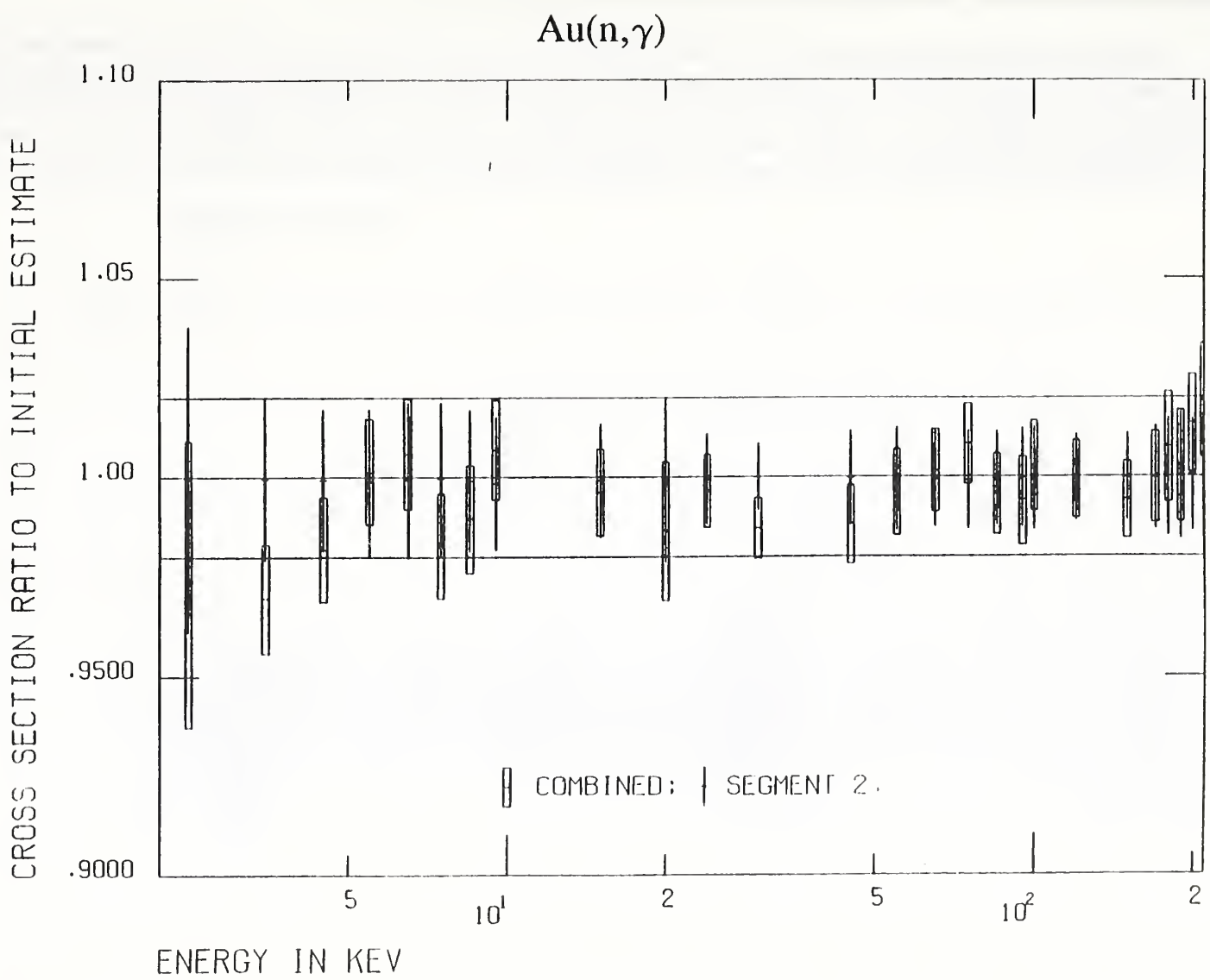

Fig. 12 Cross section ratios for the Au(n,γ) reaction from about 2 keV to 200 keV. Shown are the cross section ratios to the initial estimates for the final iteration of the simultaneous evaluation of the segment 2 data. The rectangles refer to the ratio of the combination output to the initial estimates. The ┼'s refer to the ratio of the simultaneous evaluation of the segment 2 data to the initial estimates. The error bars indicate the uncertainties for the fits. The error bars on the unit ratio line are the uncertainties in the simultaneous evaluation of the segment 2 data. The lines at ratios of 0.98 and 1.02 are guides to the eye.

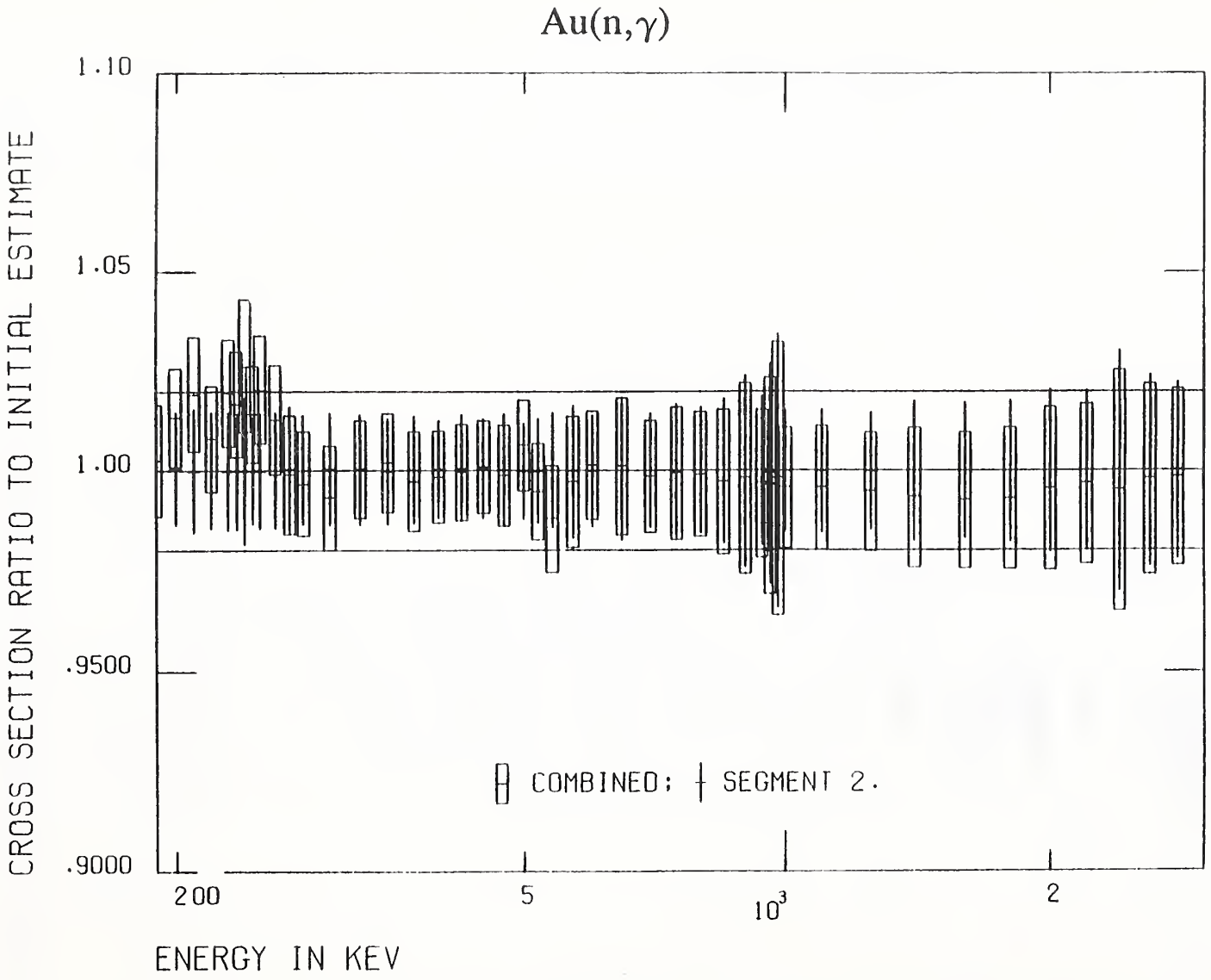

Fig. 13 Cross section ratios for the Au(n,γ) reaction from about 200 keV to 2.5 MeV. Shown are the cross section ratios to the initial estimates for the final iteration of the simultaneous evaluation of the segment 2 data. The rectangles refer to the ratio of the combination output to the initial estimates. The ┼'s refer to the ratio of the simultaneous evaluation of the segment 2 data to the initial estimates. The error bars indicate the uncertainties for the fits. The error bars on the unit ratio line are the uncertainties in the simultaneous evaluation of the segment 2 data. The lines at ratios of 0.98 and 1.02 are guides to the eye.

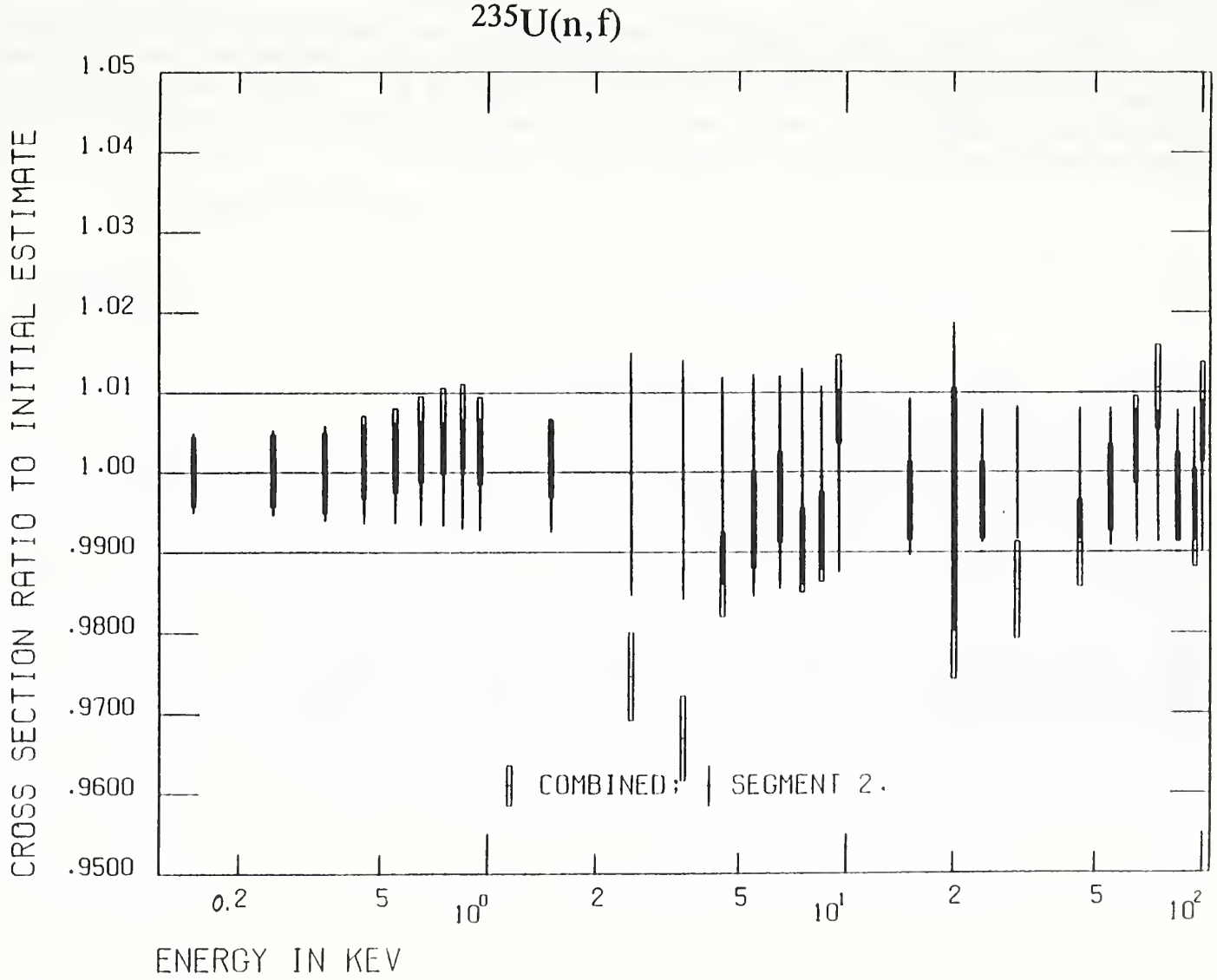

Fig. 14 Cross section ratios for the $^{235}U(n,f)$ reaction from about 0.2 keV to 100 keV. Shown are the cross section ratios to the initial estimates for the final iteration of the simultaneous evaluation of the segment 2 data. The rectangles refer to the ratio of the combination output to the initial estimates. The ┼'s refer to the ratio of the simultaneous evaluation of the segment 2 data to the initial estimates. The error bars indicate the uncertainties for the fits. The error bars on the unit ratio line are the uncertainties in the simultaneous evaluation of the segment 2 data. The lines at ratios of 0.99 and 1.01 are guides to the eye.

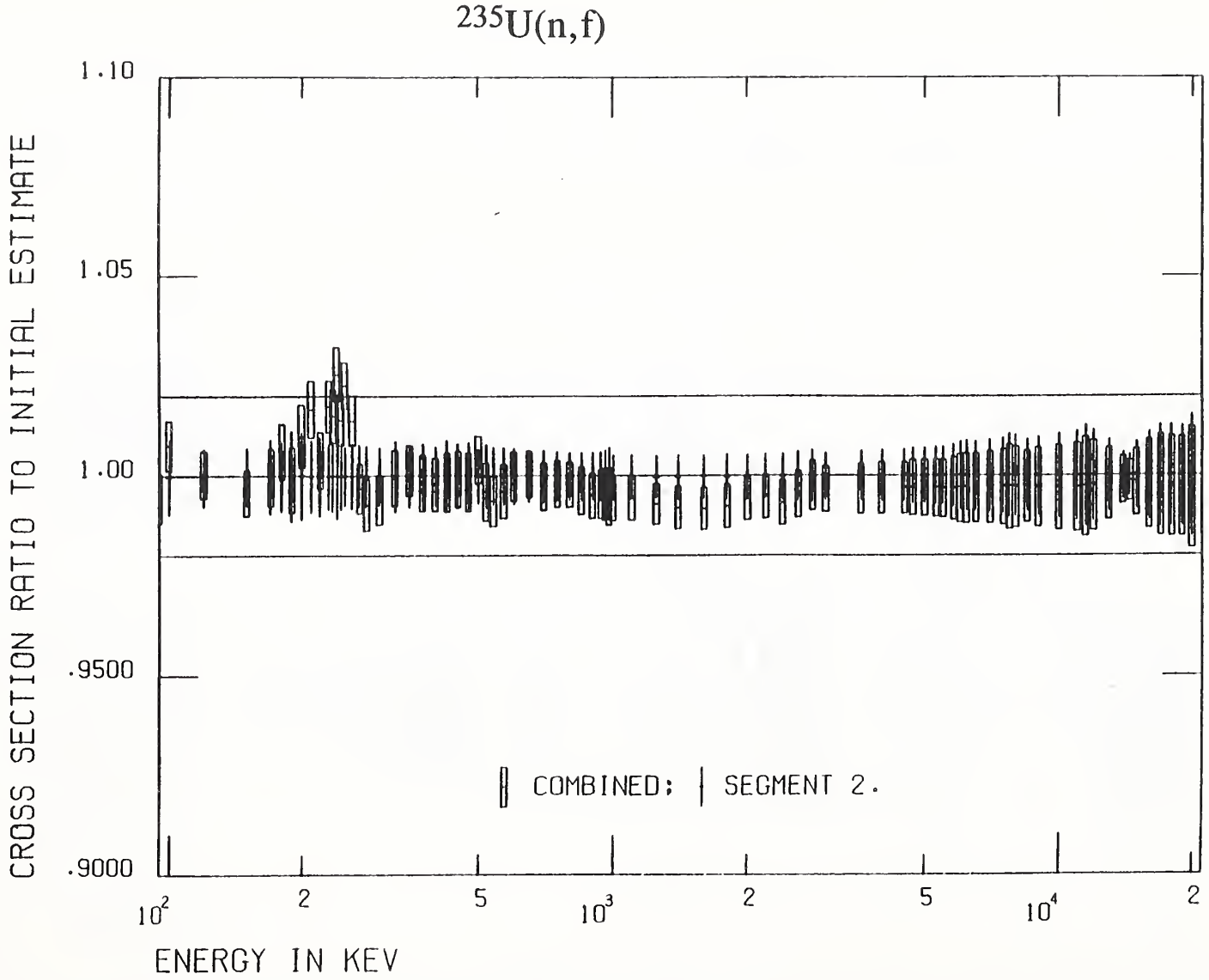

Fig. 15 Cross section ratios for the ^{235}U(n,f) reaction from about 0.1 MeV to 20 MeV. Shown are the cross section ratios to the initial estimates for the final iteration of the simultaneous evaluation of the segment 2 data. The rectangles refer to the ratio of the combination output to the initial estimates. The ┼'s refer to the ratio of the simultaneous evaluation of the segment 2 data to the initial estimates. The error bars indicate the uncertainties for the fits. The error bars on the unit ratio line are the uncertainties in the simultaneous evaluation of the segment 2 data. The lines at ratios of 0.98 and 1.02 are guides to the eye.

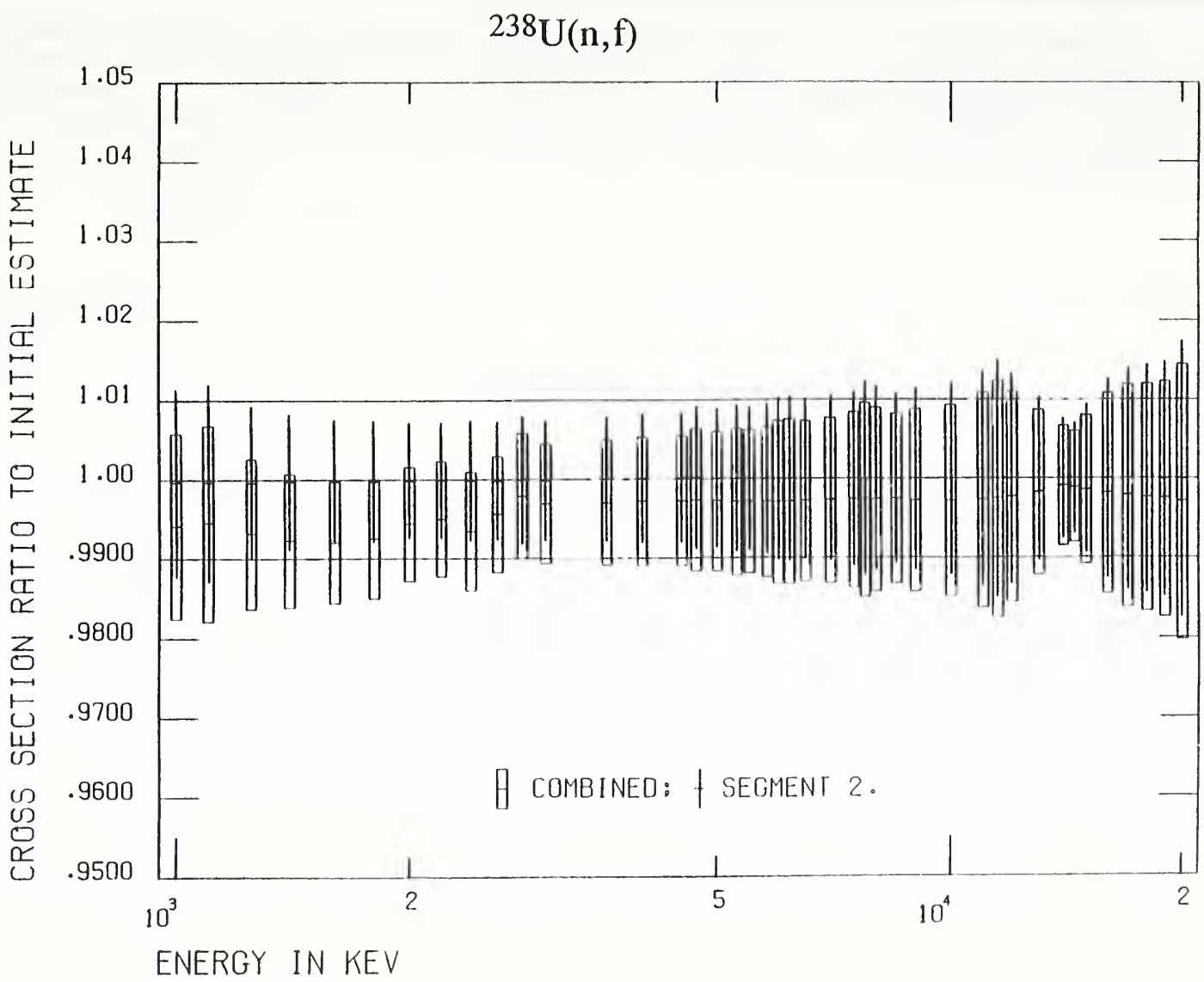

Fig. 16 Cross section ratios for the ^{238}U(n,f) reaction from about 1 MeV to 20 MeV. Shown are the cross section ratios to the initial estimates for the final iteration of the simultaneous evaluation of the segment 2 data. The rectangles refer to the ratio of the combination output to the initial estimates. The ┼'s refer to the ratio of the simultaneous evaluation of the segment 2 data to the initial estimates. The error bars indicate the uncertainties for the fits. The error bars on the unit ratio line are the uncertainties in the simultaneous evaluation of the segment 2 data. The lines at ratios of 0.99 and 1.01 are guides to the eye.

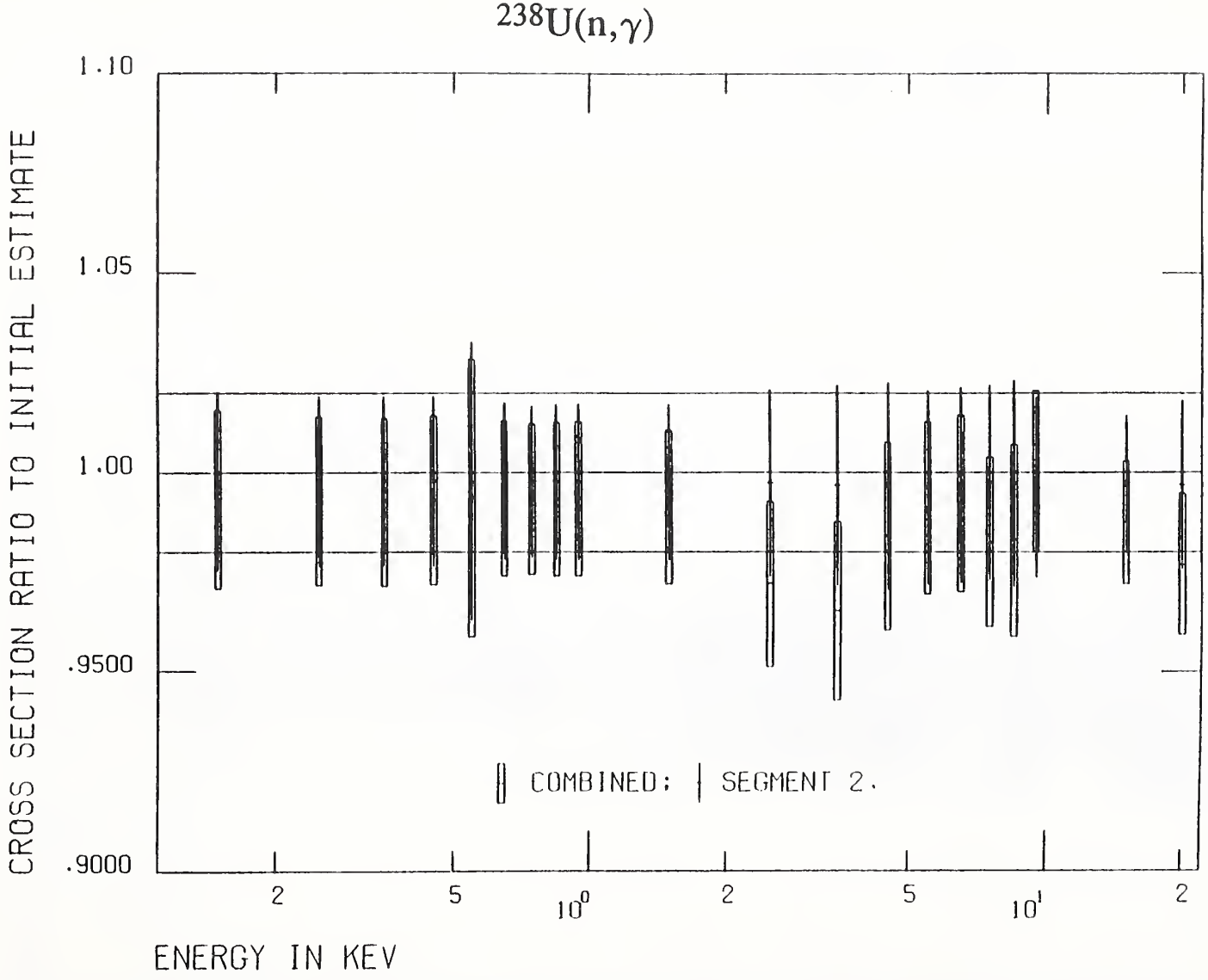

Fig. 17 Cross section ratios for the $^{238}U(n,\gamma)$ reaction from about 0.2 keV to 20 keV. Shown are the cross section ratios to the initial estimates for the final iteration of the simultaneous evaluation of the segment 2 data. The rectangles refer to the ratio of the combination output to the initial estimates. The ┼'s refer to the ratio of the simultaneous evaluation of the segment 2 data to the initial estimates. The error bars indicate the uncertainties for the fits. The error bars on the unit ratio line are the uncertainties in the simultaneous evaluation of the segment 2 data. The lines at ratios of 0.98 and 1.02 are guides to the eye.

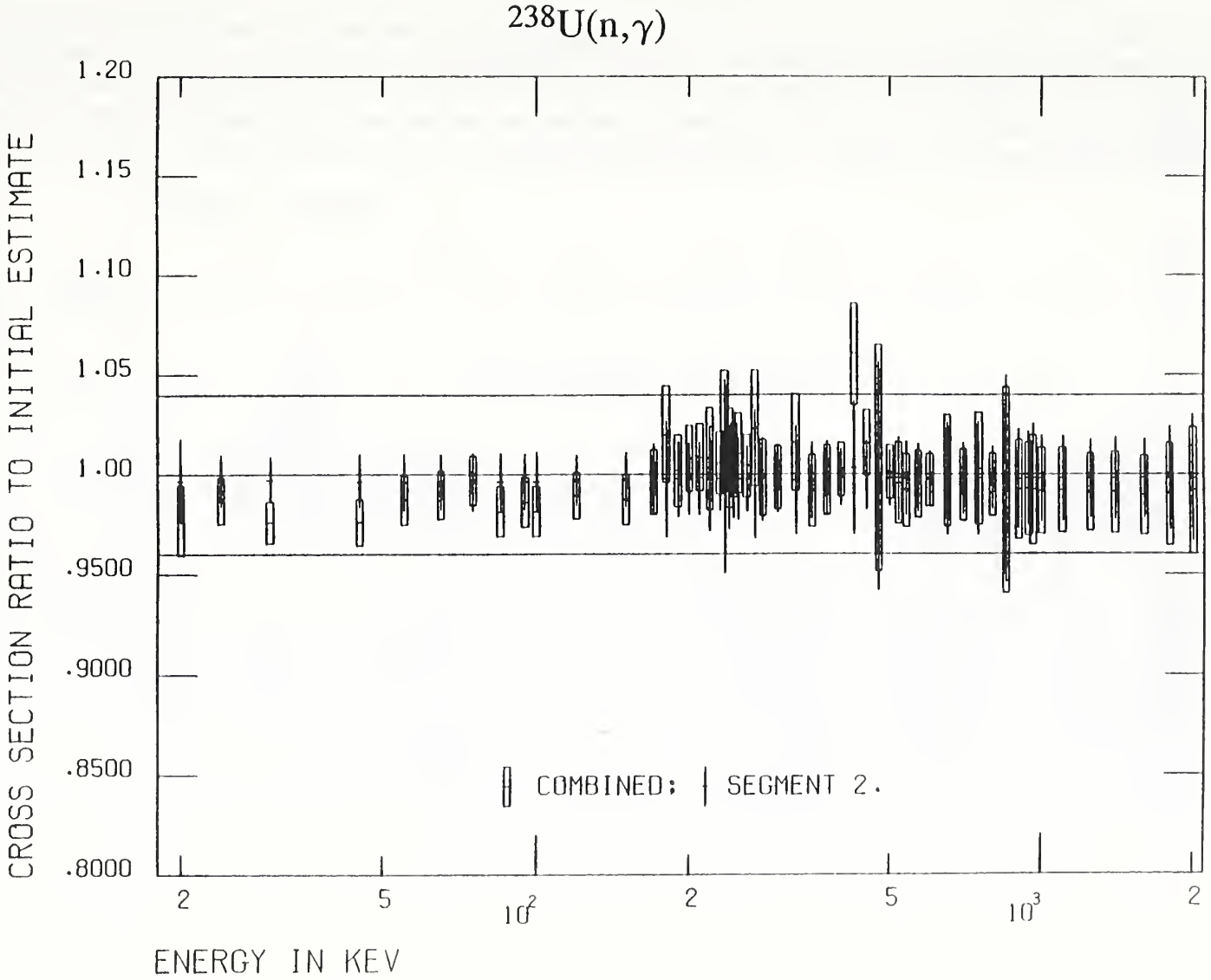

Fig. 18 Cross section ratios for the $^{238}U(n,\gamma)$ reaction from about 20 keV to 2 MeV. Shown are the cross section ratios to the initial estimates for the final iteration of the simultaneous evaluation of the segment 2 data. The rectangles refer to the ratio of the combination output to the initial estimates. The ┼'s refer to the ratio of the simultaneous evaluation of the segment 2 data to the initial estimates. The error bars indicate the uncertainties for the fits. The error bars on the unit ratio line are the uncertainties in the simultaneous evaluation of the segment 2 data. The lines at ratios of 0.96 and 1.04 are guides to the eye.

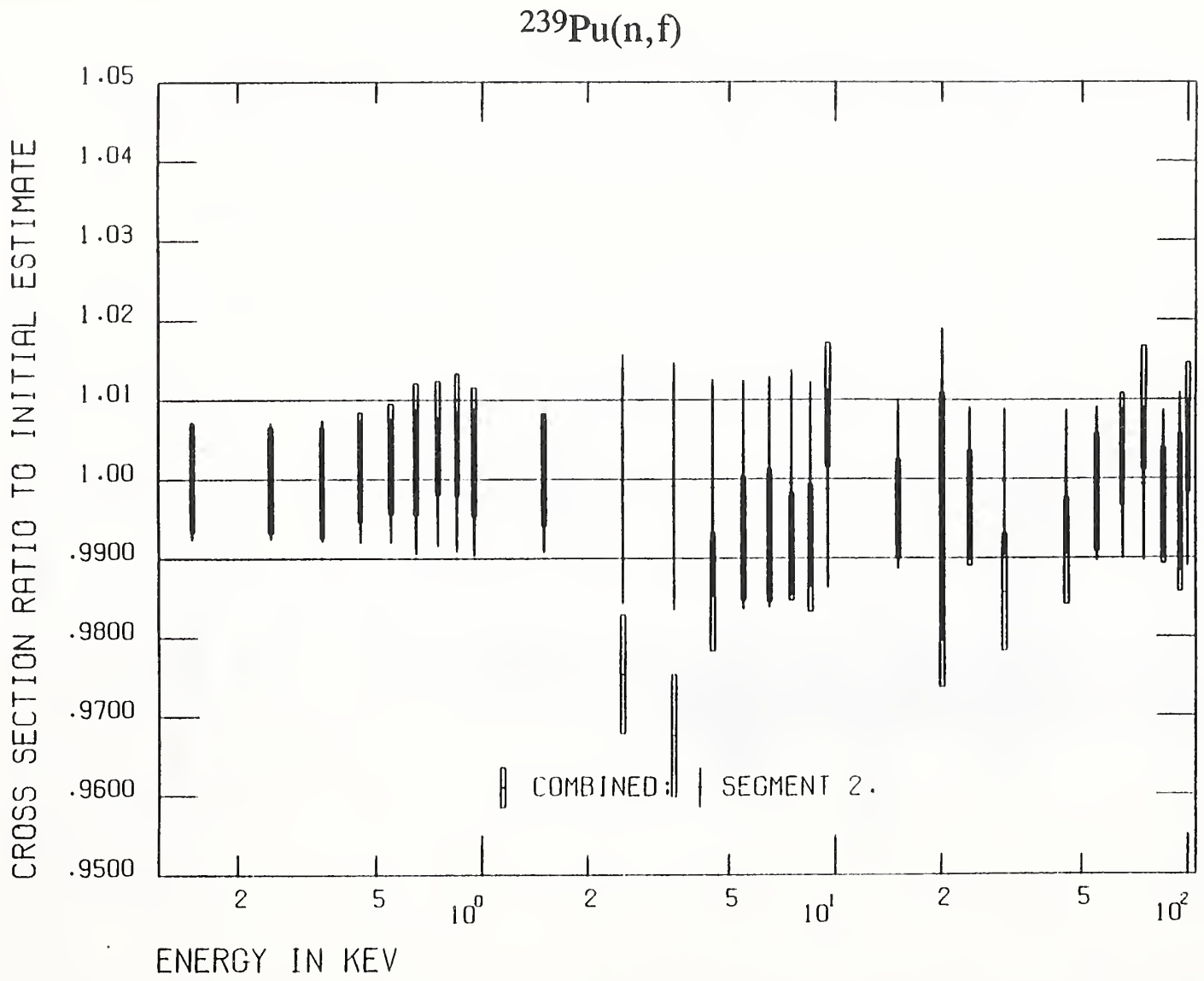

Fig. 19 Cross section ratios for the ^{239}Pu(n,f) reaction from about 0.2 keV to 100 keV. Shown are the cross section ratios to the initial estimates for the final iteration of the simultaneous evaluation of the segment 2 data. The rectangles refer to the ratio of the combination output to the initial estimates. The ┼'s refer to the ratio of the simultaneous evaluation of the segment 2 data to the initial estimates. The error bars indicate the uncertainties for the fits. The error bars on the unit ratio line are the uncertainties in the simultaneous evaluation of the segment 2 data. The lines at ratios of 0.99 and 1.01 are guides to the eye.

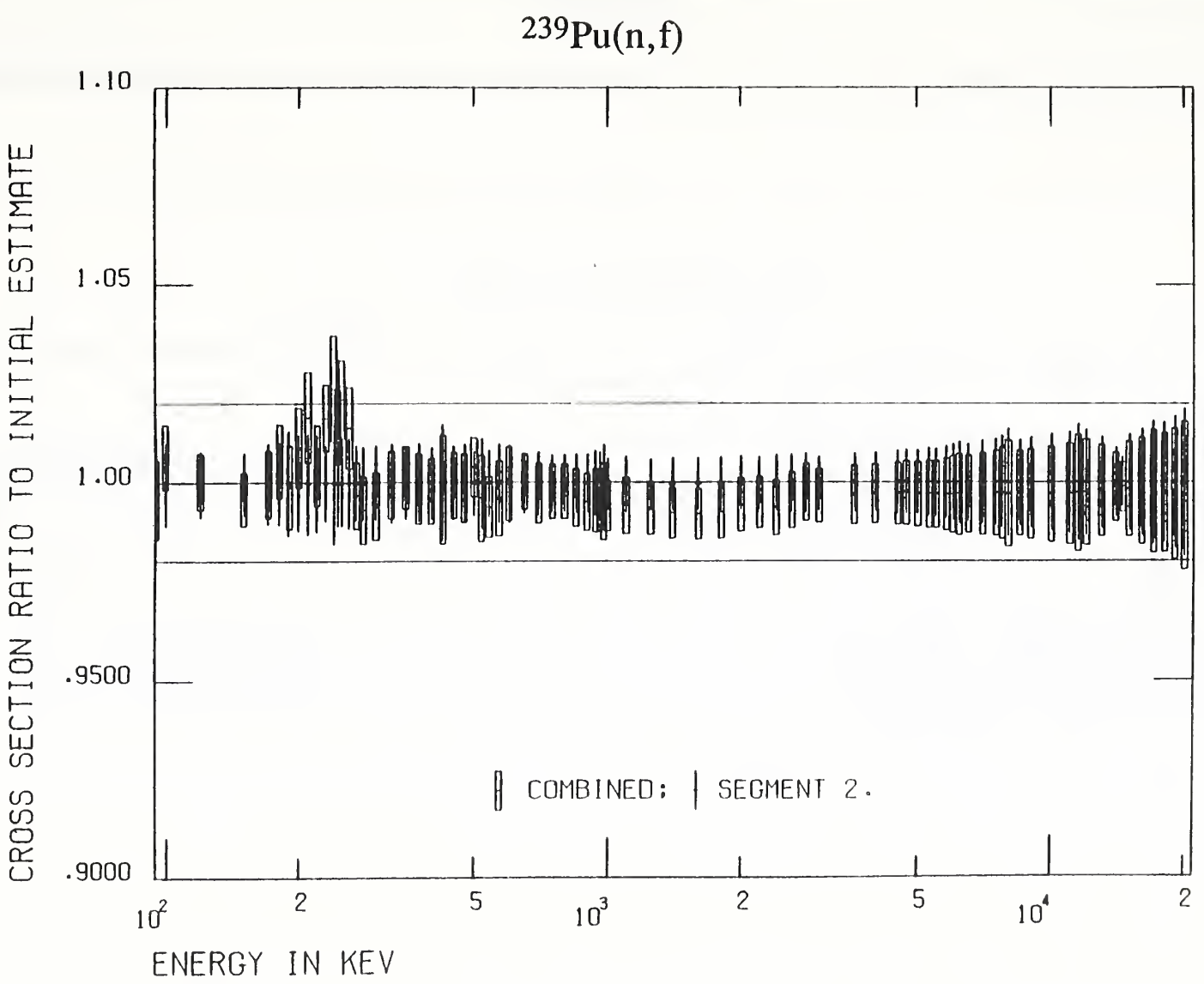

Fig. 20 Cross section ratios for the ^{239}Pu(n,f) reaction from about 100 keV to 20 MeV. Shown are the cross section ratios to the initial estimates for the final iteration of the simultaneous evaluation of the segment 2 data. The rectangles refer to the ratio of the combination output to the initial estimates. The ┼'s refer to the ratio of the simultaneous evaluation of the segment 2 data to the initial estimates. The error bars indicate the uncertainties for the fits. The error bars on the unit ratio line are the uncertainties in the simultaneous evaluation of the segment 2 data. The lines at ratios of 0.98 and 1.02 are guides to the eye.

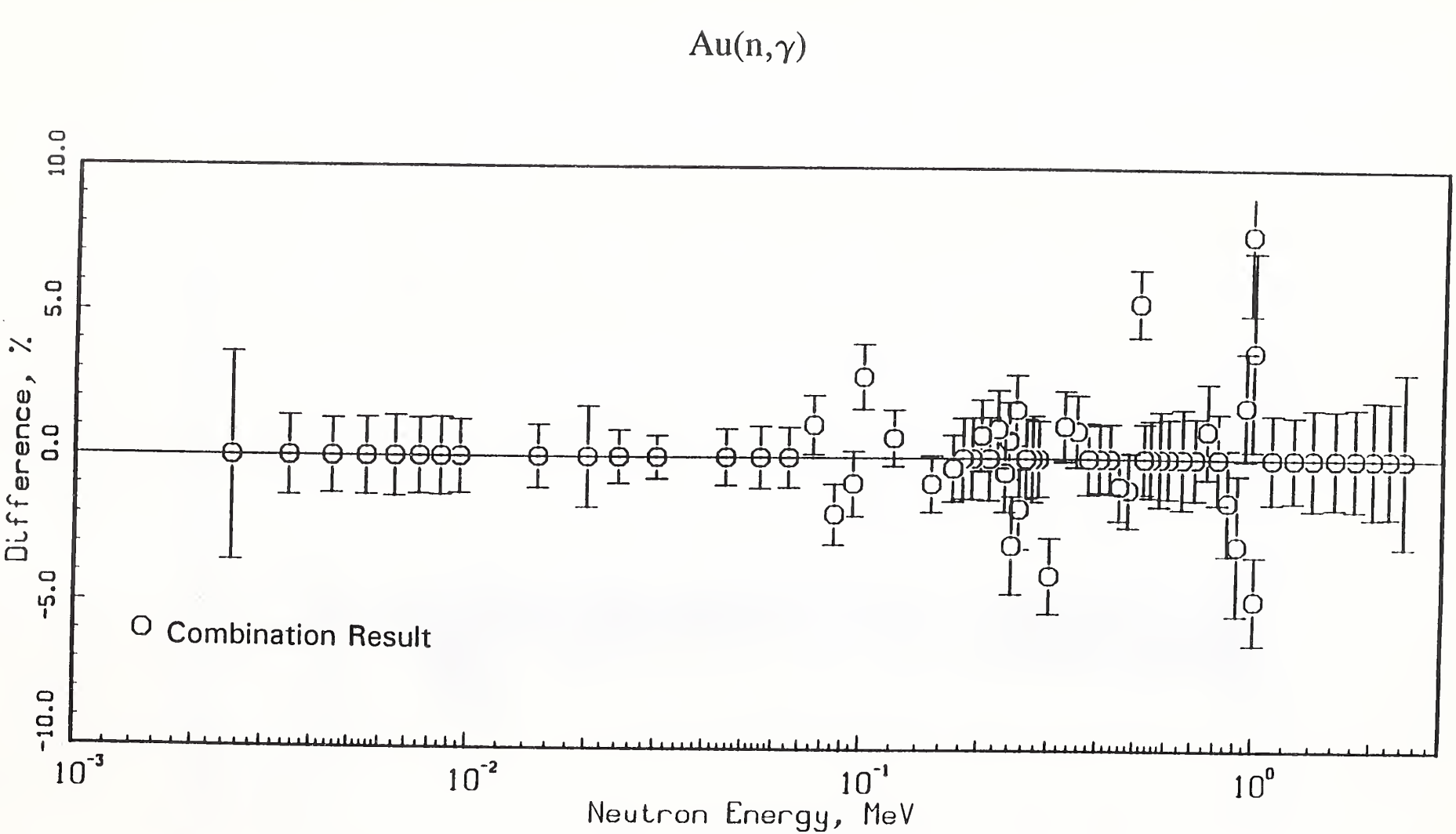

Fig. 21 Percentage difference between the combination result and the smoothed cross section for Au(n,γ) from about 1 keV to 3 MeV.

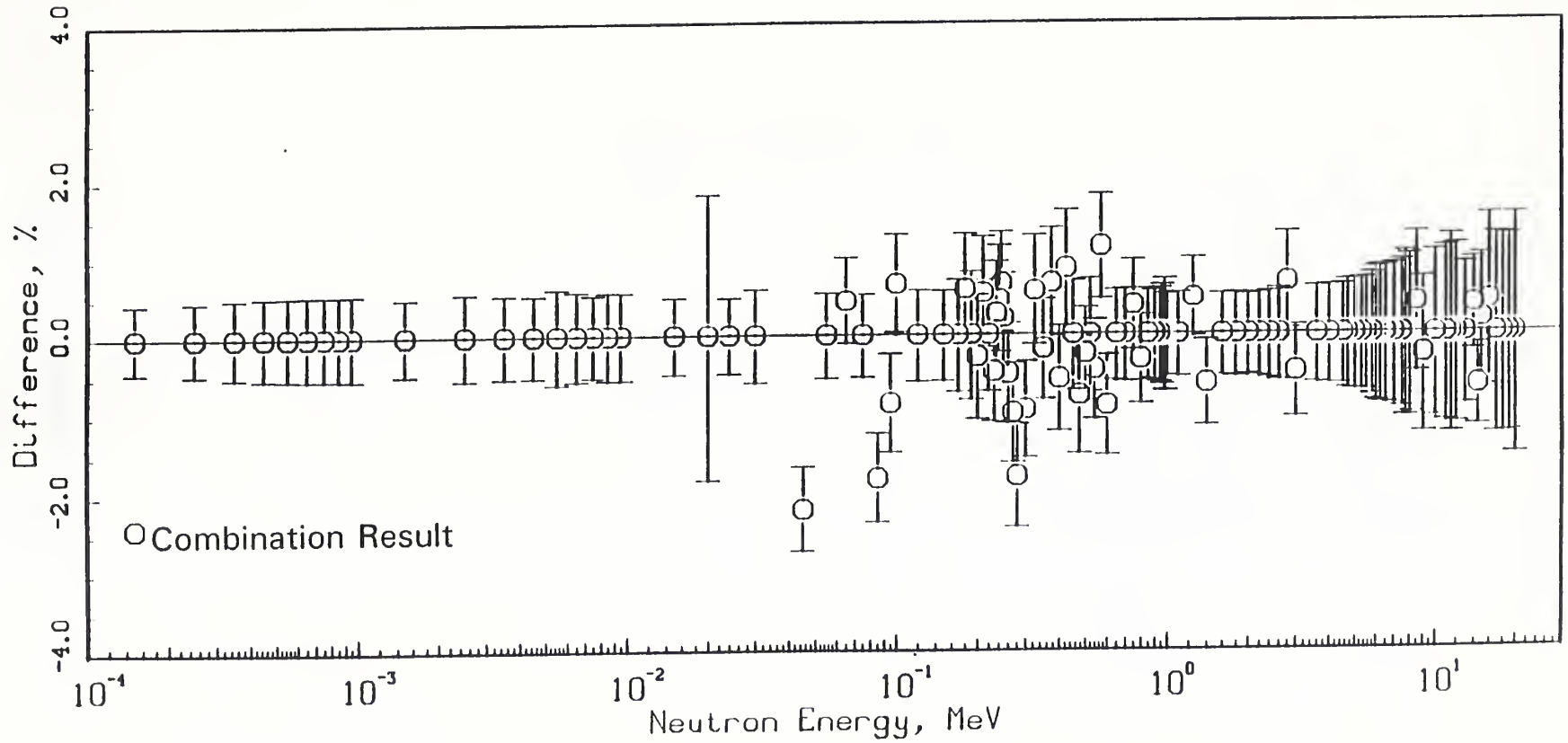

Fig. 22 Percentage difference between the combination result with reference to the smoothed cross section for $^{235}U(n,f)$ from about 0.1 keV to 20 MeV.

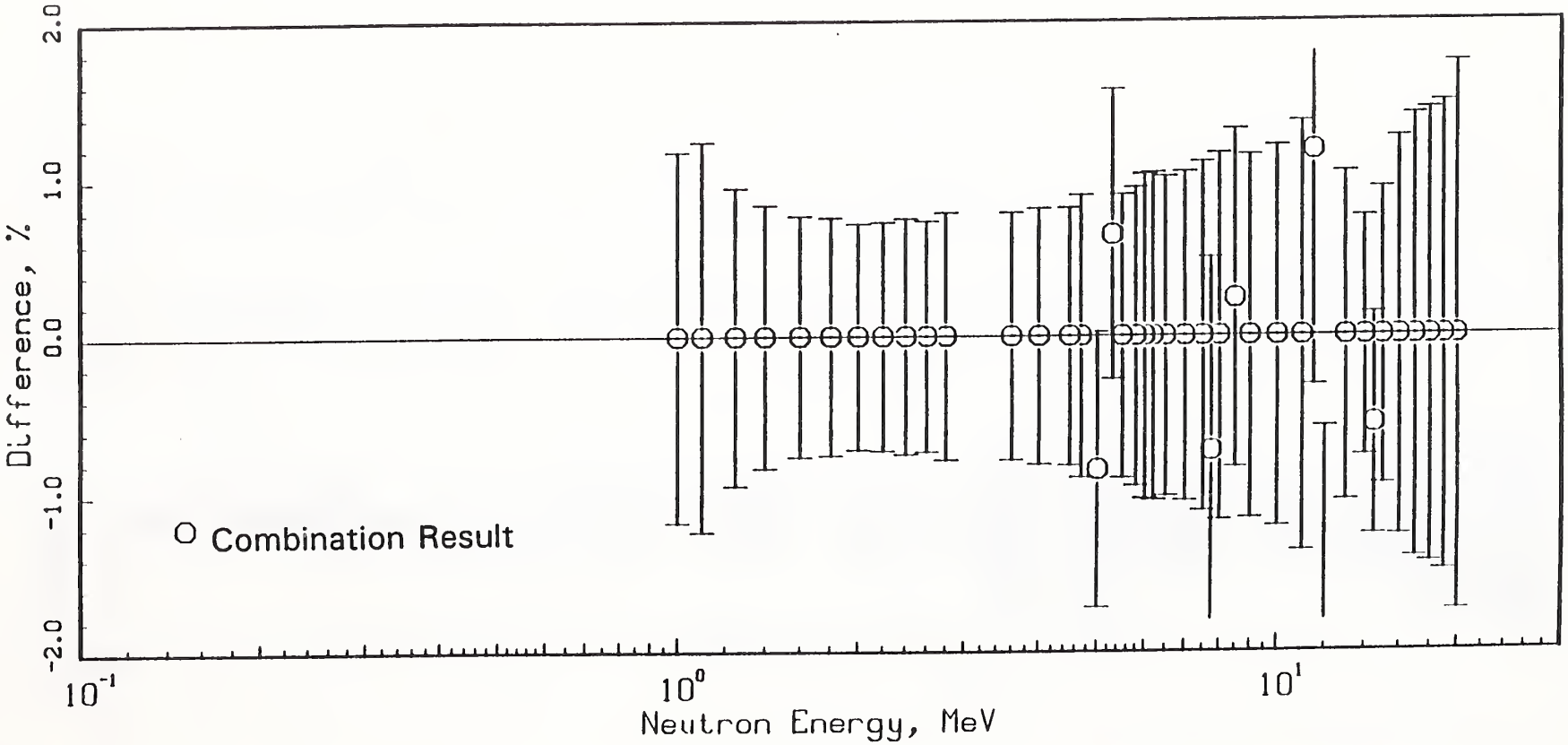

Fig. 23 Percentage difference between the combination result and the smoothed cross section for $^{238}U(n,f)$ from about 1 MeV to 20 MeV.

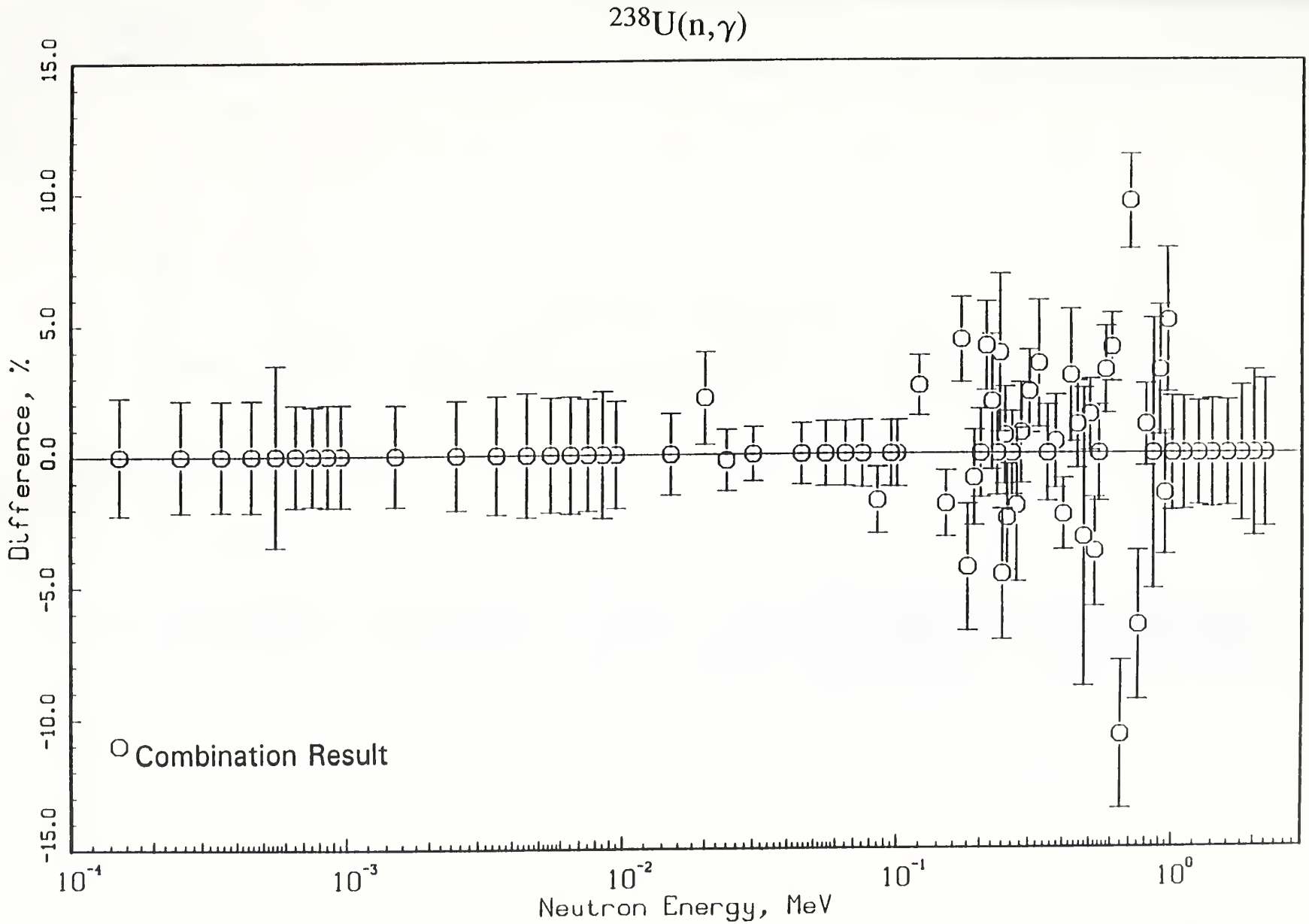

Fig. 24 Percentage difference between the combination result and the smoothed cross section for $^{238}U(n,\gamma)$ from about 0.1 keV to 3 MeV.

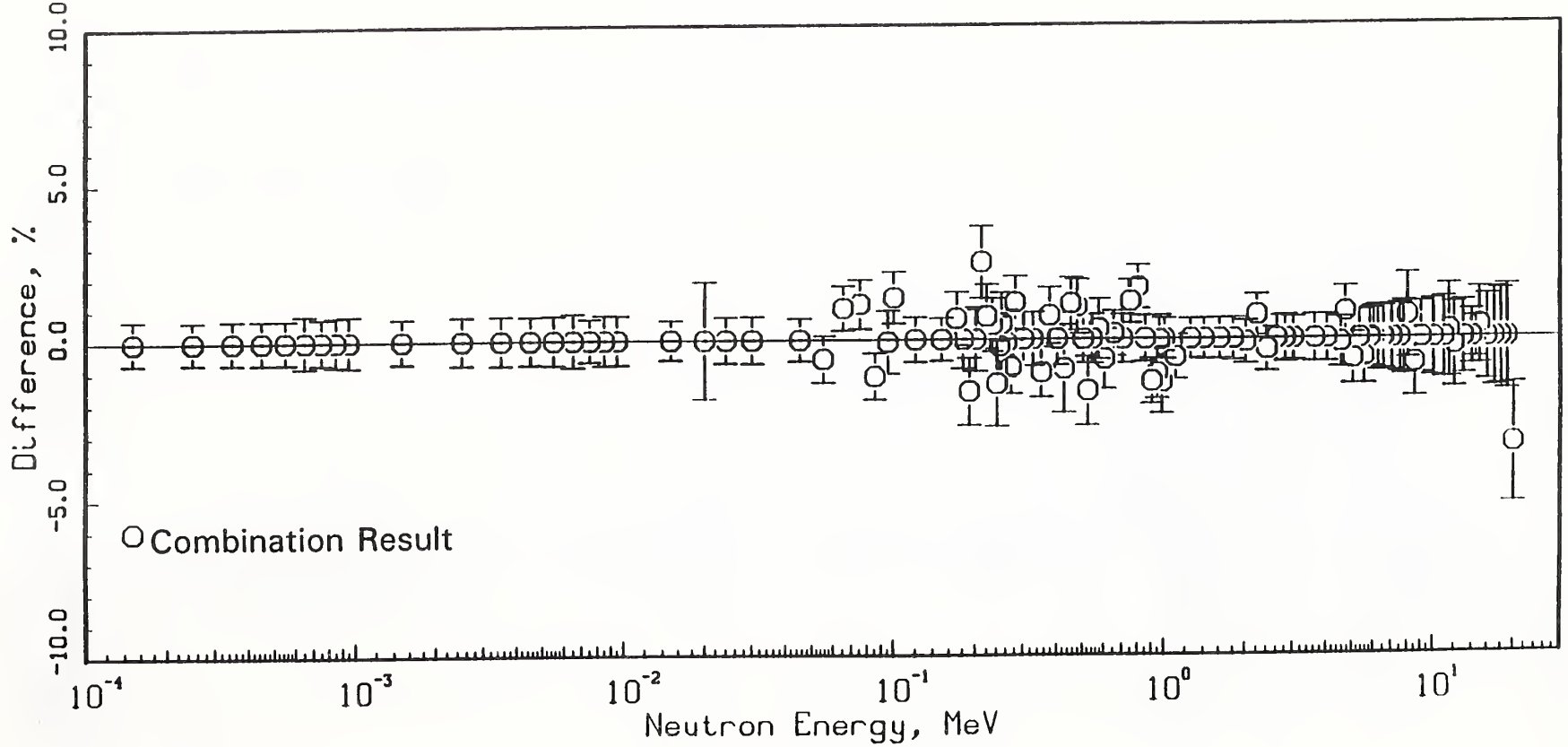

Fig. 25 Percentage difference between the combination result and the smoothed cross section for ^{239}Pu(n,f) from about 0.1 keV to 20 MeV.

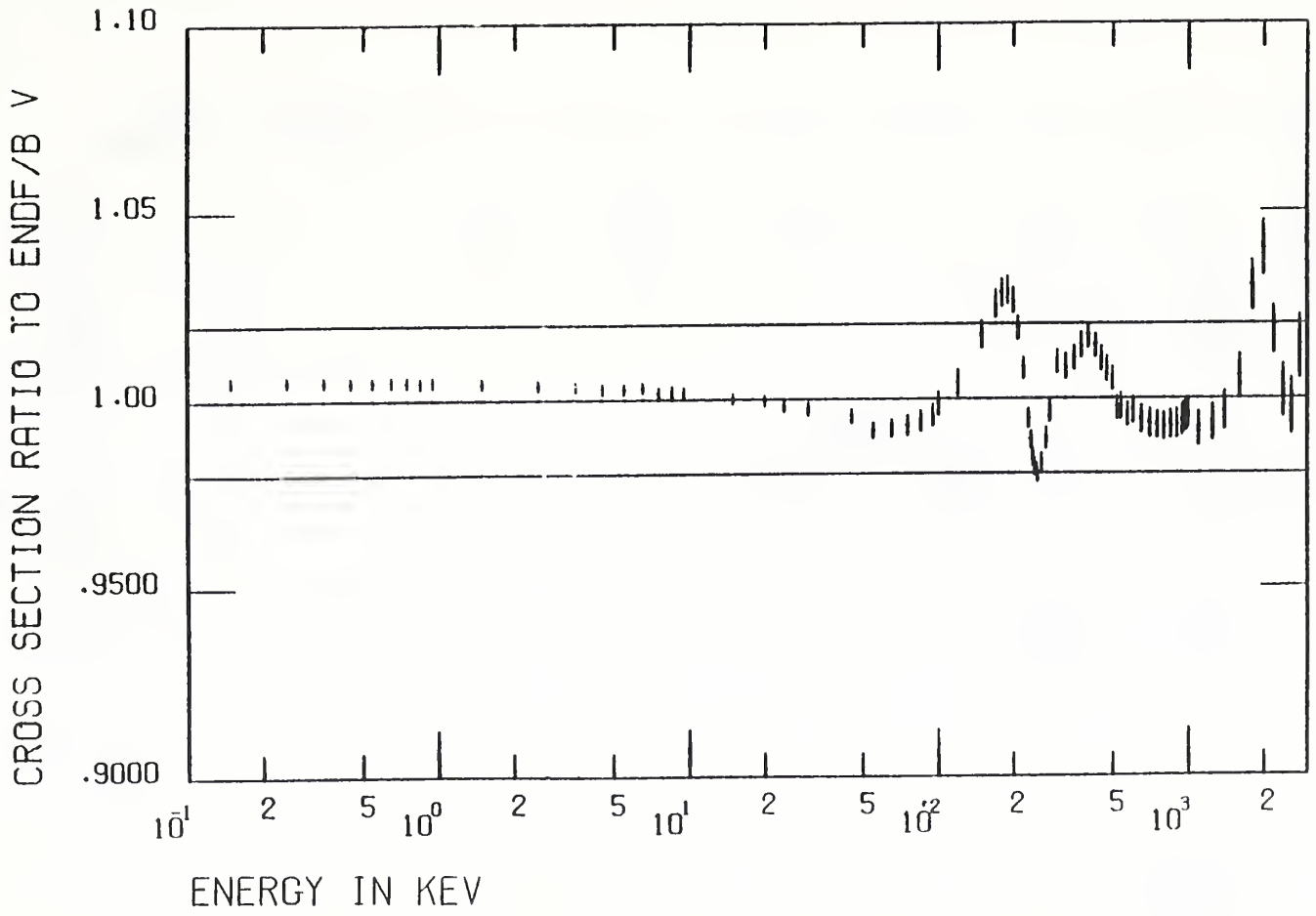

Fig. 26 Ratio of the result of this evaluation process to that of ENDF/B-V for ^{6}Li(n,t) from about 0.1 keV to 3 MeV. The uncertainties shown are those obtained from the combination output. The lines at ratios of 0.98 and 1.02 are guides to the eye.

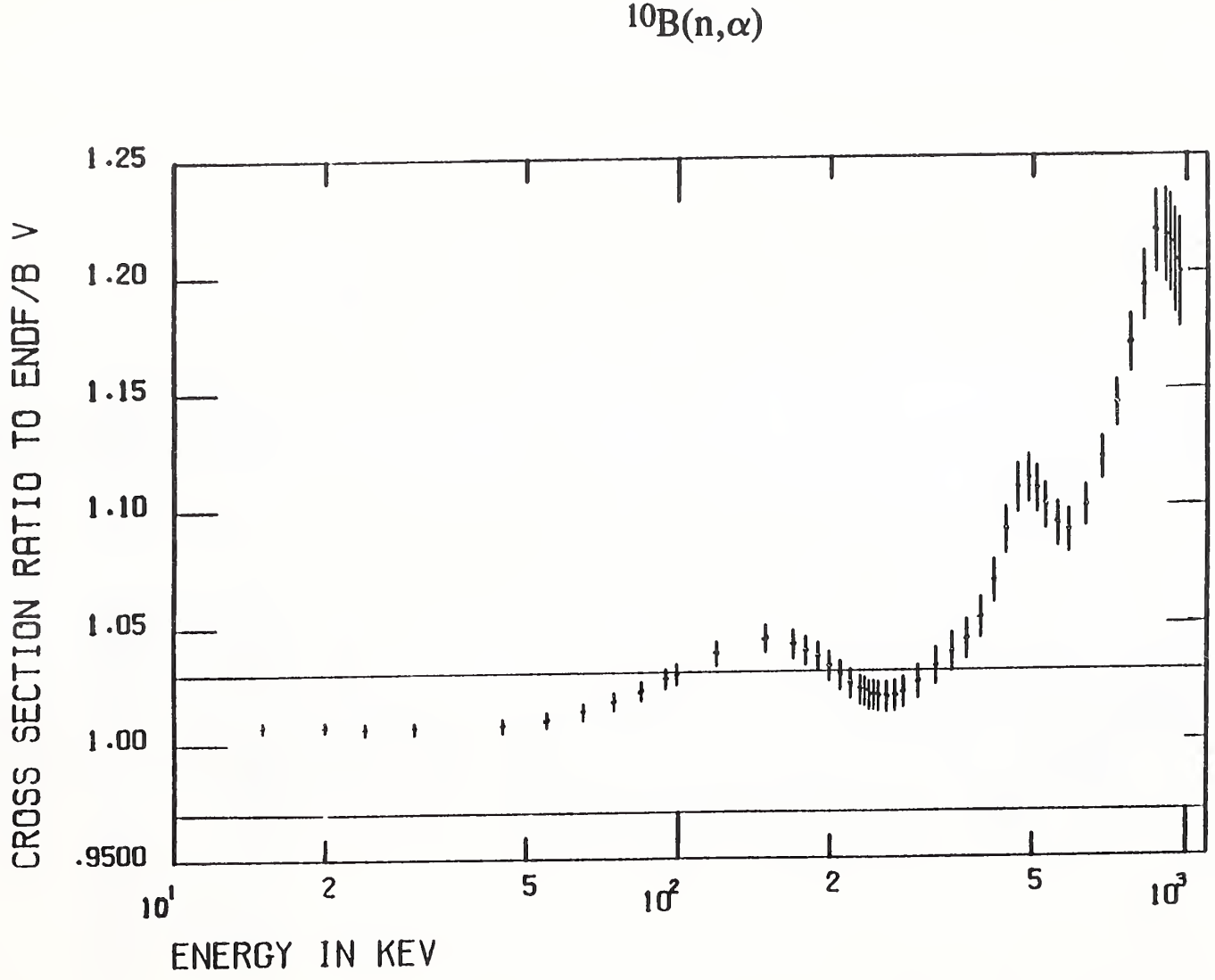

Fig. 27 Ratio of the result of this evaluation process to that of ENDF/B-V for the $^{10}B(n,\alpha)$ reaction from about 10 keV to 1 MeV. The lines at ratios of 0.97 and 1.03 are guides to the eye.

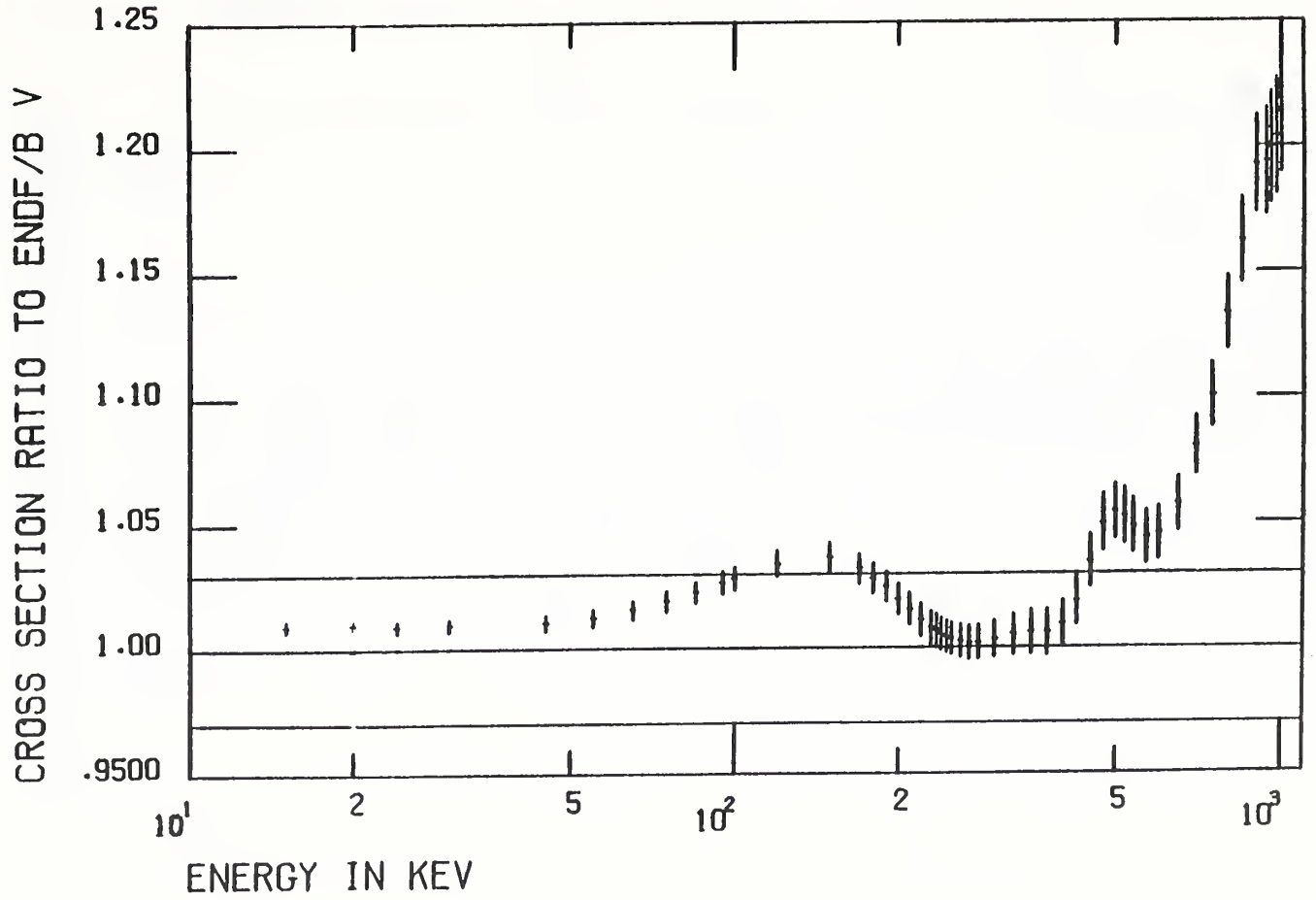

Fig. 28 Ratio of the result of this evaluation process to that of ENDF/B-V for the $^{10}B(n,\alpha_1)$ reaction from about 10 keV to 1 MeV. The lines at ratios of 0.97 and 1.03 are guides to the eye.

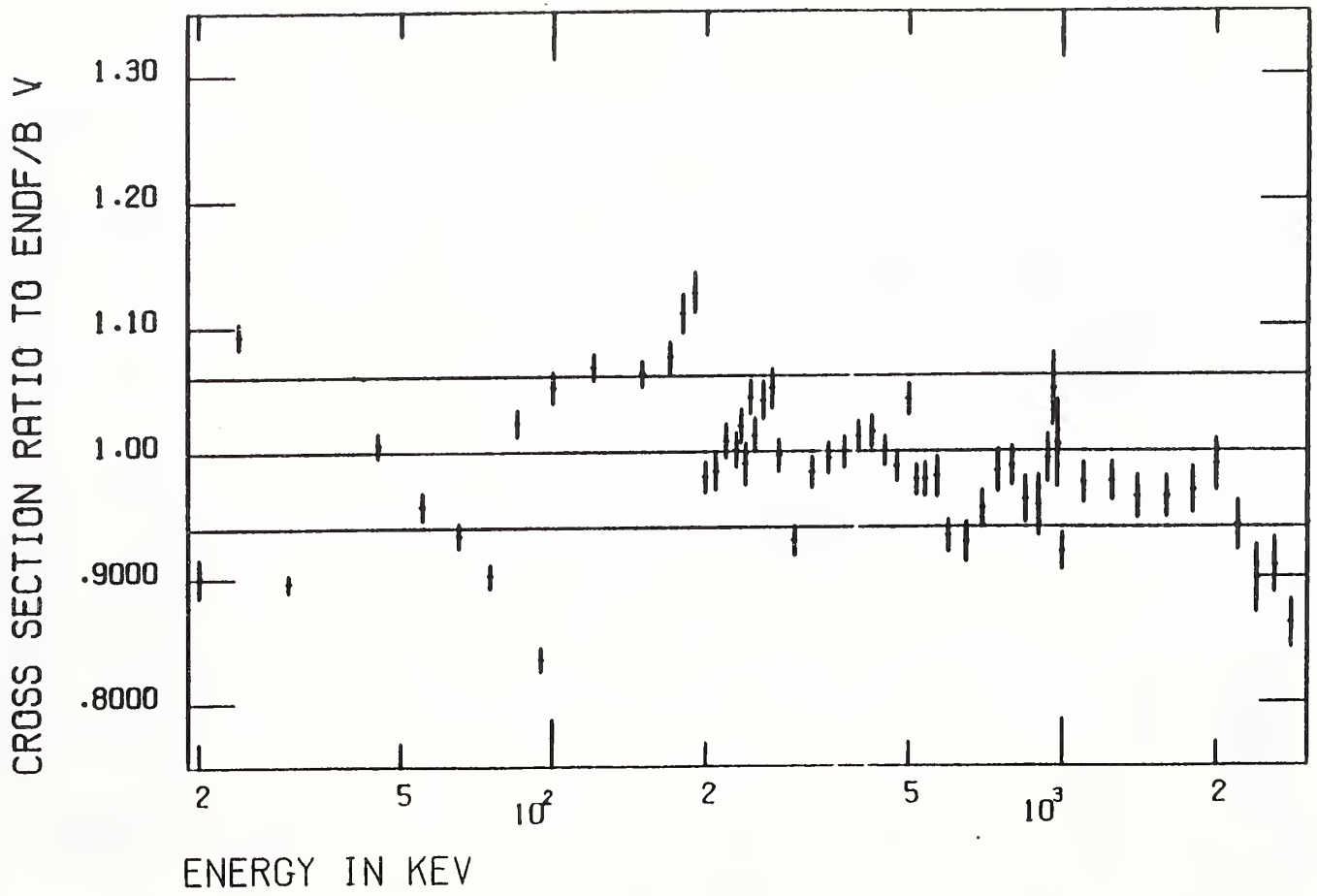

Fig. 29 Ratio of the unsmoothed result of this evaluation process to that of ENDF/B-V for the Au(n,γ) reaction from about 20 keV to 3 MeV. The lines at ratios of 0.94 and 1.06 are guides to the eye.

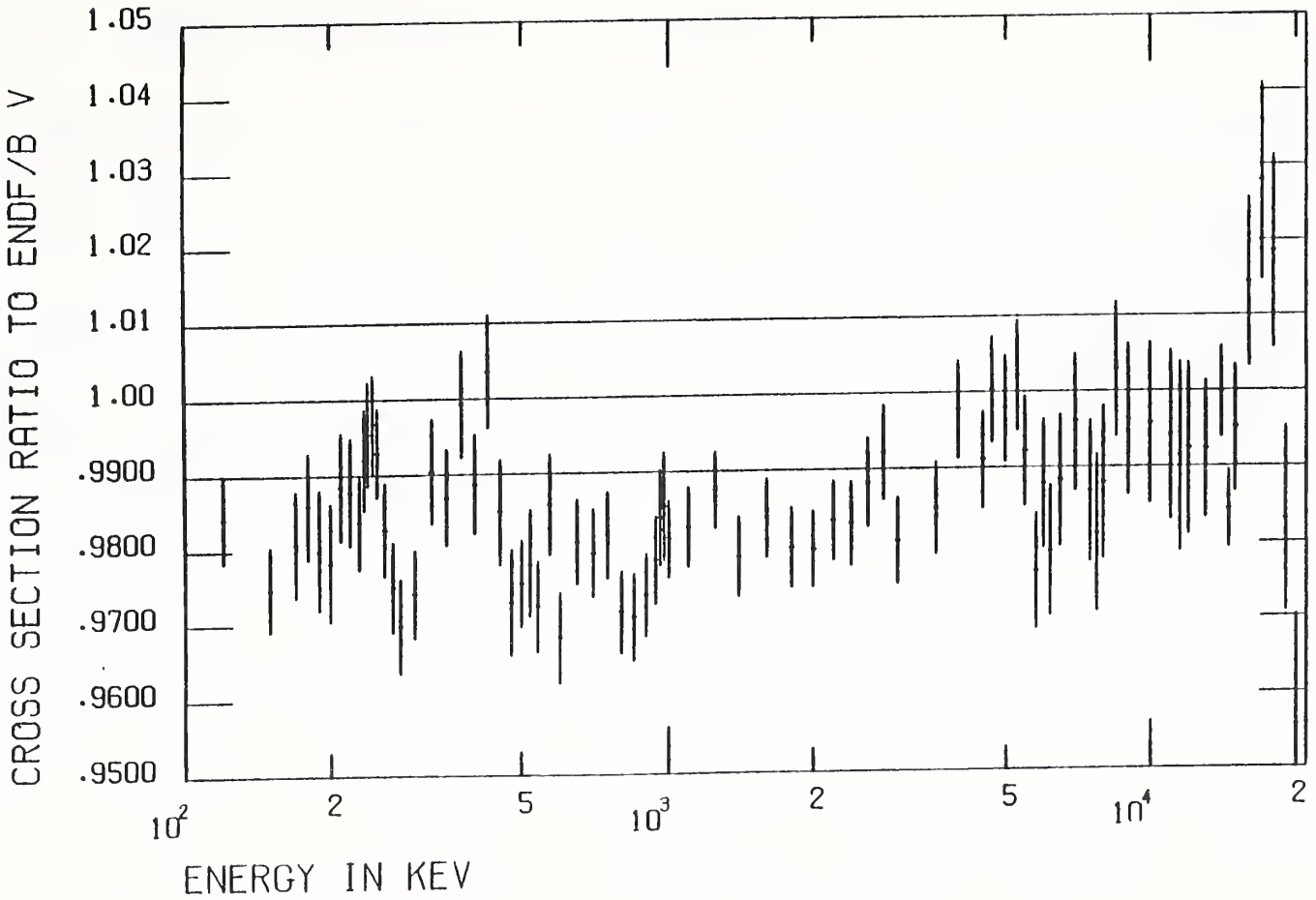

Fig. 30 Ratio of the unsmoothed result of this evaluation process to that of ENDF/B-V for the ^{235}U(n,f) reaction from about 100 keV to 20 MeV. The lines at ratios of 0.99 and 1.01 are guides to the eye.

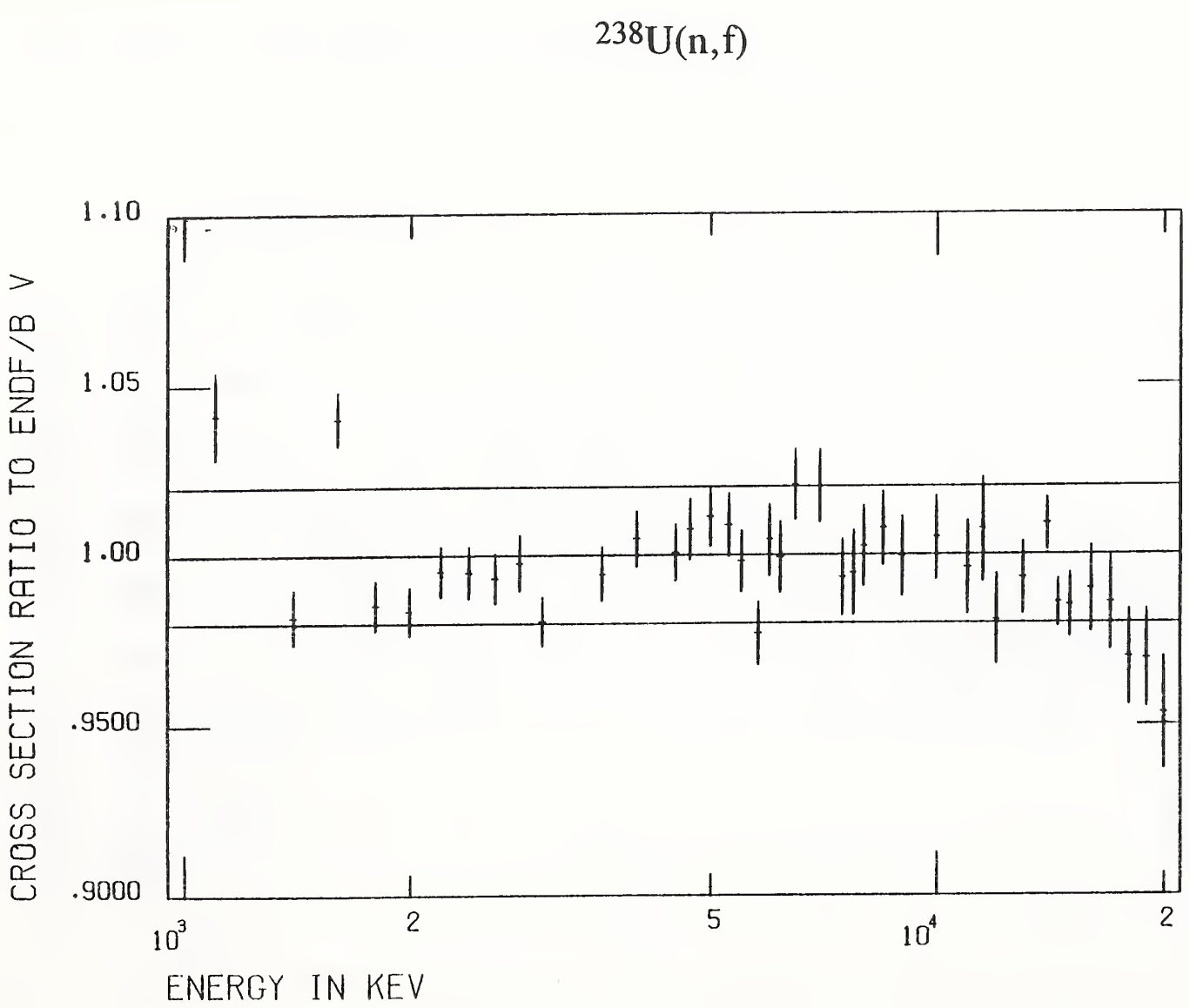

Fig. 31 Ratio of the unsmoothed result of this evaluation process to that of ENDF/B-V for the ^{238}U(n,f) reaction from about 1 MeV to 20 MeV. The lines at ratios of 0.98 and 1.02 are guides to the eye.

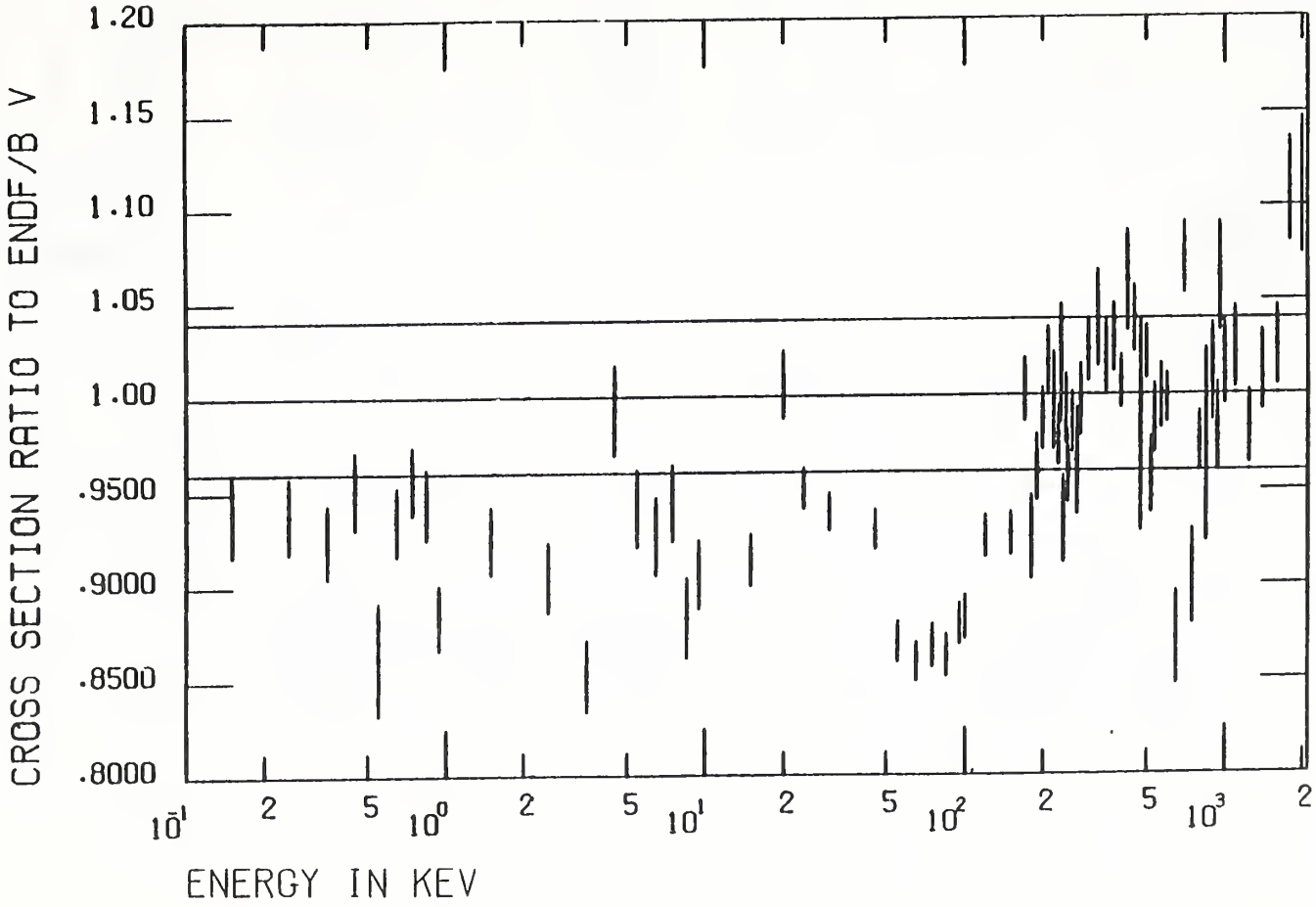

Fig. 32 Ratio of the unsmoothed result of this evaluation process to that of ENDF/B-V for the $^{238}U(n,\gamma)$ reaction from about 0.1 keV to 2 MeV. The lines at ratios of 0.96 and 1.04 are guides to the eye.

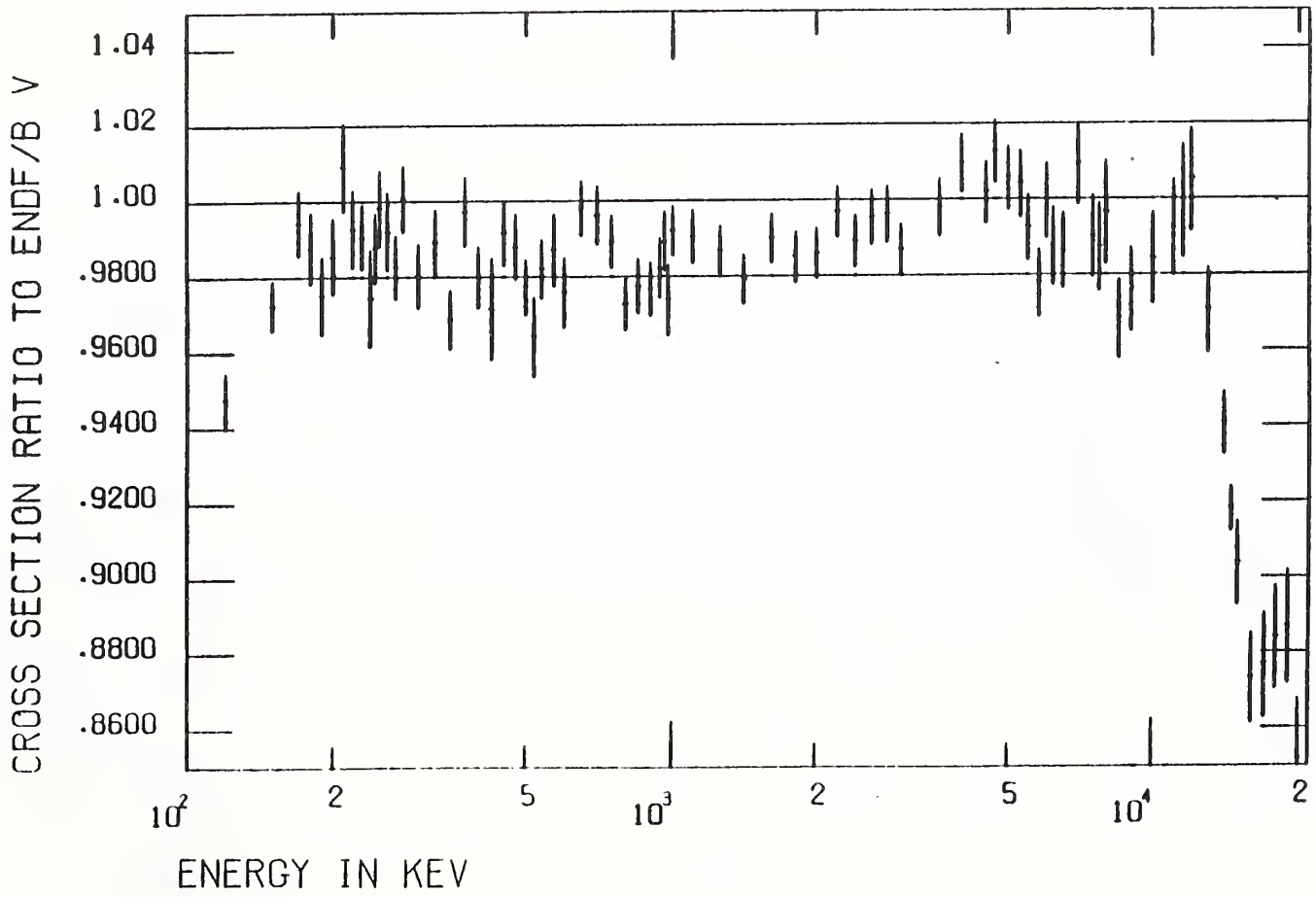

Fig. 33 Ratio of the unsmoothed result of this evaluation process to that of ENDF/B-V for the ^{239}Pu(n,f) reaction from about 100 keV to 20 MeV. The lines at ratios of 0.98 and 1.02 are guides to the eye.

APPENDIX A. References for the Data Base Used for the Simultaneous Evaluation

Adamchuk, Yu V., *et al.* (1977) Conf. on Neutron Physics, Kiev, **2**, 192; $^{238}U(n,\gamma)/^{10}B(n,\alpha_1)$ [445]

Adamov, V.M., *et al.* (1983) Int'l Nucl Data Comm. INDC(USSR)-180L; $^{235}U(n,f)$ Cf-AV [575]; also Adamov, V.M., *et al.* (1979) Radium Inst. Report RI-52; transl. in INDC(CCP)-180L; $^{235}U(n,f)$ Cf-AV [575]

Adams. B., *et al.* (1961) J. Nucl. Energy A/B **14**, 85; $^{235}U(n,f)/^{238}U(n,f)$, shape [836]; $^{238}U(n,f)$, shape [835]; $^{239}Pu(n,f)/^{238}U(n,f)$, shape [837]

Alfimenkov, V.P., *et al.* (1982) Nuclear Data for Science and Technology, Antwerp, 353; also Published in Yad. Fiz. **36**, 1089 (1982); transl: Sov. J. Nucl. Phys. **36**, 637; $^{6}Li(n,n)$ [210]

Allen, W.D. and Ferguson, A.T.G. (1957) Proc. Phys. Soc. **LXX**, 573; $^{239}Pu(n,f)$, shape [671]; $^{235}U(n,f)$ [735]; $^{235}U(n,f)$, shape [568]; $^{239}Pu(n,f)$ [672]

Andersson, P., *et al.* (1985) Nucl. Phys. **A443**, 404; $^{197}Au(n,\gamma)/^{235}U(n,f)$ [363]: {These measurements were relative to indium capture. They were converted using measurements made by D.L. Smith and J.W. Meadows ANL-NDM-14}.

Arlt, R., *et al.* (1984) Nuclear Standard Reference Data, Geel, IAEA-TECDOC-335; 174; $^{235}U(n,f)$ [590]

Asami, A. and Moxon, M.C. (1969) Harwell Report AERE-R-5980; also J. Nucl. Energy **24**, 85 (1970); $^{10}B(n,n)$ [178]

Asami, A. and Moxon, M.C. (1970) Nuclear Data for Reactors, Helsinki, STI/PUB/259, I, 153; $^{6}Li(n,n)$ [208]

Auchampaugh, G.F., *et al.* (1979) Nucl. Sci. Eng. **69**, 30; $^{10}B(tot)$ [180]

Axton, E.J. (1985) private communication; g_a ^{233}U [910]; g_f ^{233}U [911]; $^{233}U(n,n)$ [912]; $^{233}U(n,f)$ [913]; $^{233}U(n,\gamma)$ [914]; ν ^{233}U [915]; g_a ^{235}U [916]; g_f ^{235}U [917]; $^{235}U(n,n)$ [918]; $^{235}U(n,f)$ [919]; $^{235}U(n,\gamma)$ [920]; ν ^{235}U [921]; g_a ^{239}Pu [922]; g_f ^{239}Pu [923]; $^{239}Pu(n,n)$ [924]; $^{239}Pu(n,f)$ [925]; $^{239}Pu(n,\gamma)$ [926]; ν ^{239}Pu [927]; g_a ^{241}Pu [928]; g_f ^{241}Pu [929]; $^{241}Pu(n,n)$ [930]; $^{241}Pu(n,f)$ [931]; $^{241}Pu(n,\gamma)$ [932]; ν ^{241}Pu [933]; ν ^{252}Cf [934]

Barry, J.F., *et al.* (1964) J. Nucl. Energy A/B **18**, 481; $^{238}U(n,\gamma)/^{235}U(n,f)$ [415]

Barry, J.F. (1966) Neutron Cross Section Technology, Washington DC, AEC Report Conf-660303, **2**, 763; $^{6}Li(n,\alpha)/^{235}U(n,f)$, shape [288]

Bartle, C.M. (1979) Nucl. Phys. **A330**, 1; $^{6}Li(n,\alpha)$ [238]

Barton, D.M., *et al.* (1976) Nucl. Sci. Eng. **60**, 369; $^{235}U(n,f)$ [580]

Bastian, C. and Riemenschneider, H. (1984) Nuclear Standard Reference Data, Geel, IAEA-TECDOC-335, 118; $^{6}Li(n,\alpha)/^{10}B(n,\alpha)$, shape [297]

Becker, R.L. and Barschall, H.H. (1956) Phys. Rev. **102**, 1384; $^{10}B(tot)$ [185]

Beer, H. and Spencer, R.R. (1979) Nucl. Sci. Eng. **70**, 98; ^{10}B(tot) [192#,193#]

Behrens, J.W. and Carlson, G.W. (1977) Nucl. Sci. Eng. **63**, 250; ^{238}U(n,f)/^{235}U(n,f) [805]

Belanova, T.S., *et al.* (1966) J. Nucl. Energy A/B **20**, 411; ^{238}U(n,γ) [435]: {with reinterpretation by Miller, L.B. and Poenitz, W.P. (1969) Nucl. Sci. Eng. **35**, 295, and Dietze, K. (1977) in this Appendix}.

Bergman, A.A., *et al.* (1957) Zh. Eksp. Teor. Fiz. **33**, 9; transl. in Sov. Phys. JETP **6**, 6; ^{6}Li(n,α)/^{10}B(n,α), shape [160]

Bergman, A.A., *et al.* (1980) Conf. on Neutron Physics, Kiev, **3**, 49; ^{235}U(n,f)/^{10}B(n,α), shape [550,552]; ^{239}Pu(n,f)/^{10}B(n,α), shape [551]

Berezin, A.A., *et al.* (1958) At. Energ. **5**, 659; transl. in Sov. At. En. **5**, 1604; ^{235}U(n,f)/^{238}U(n,f) [870]

Bichsel, H. and Bonner, T.W. (1957) Phys. Rev. **108**, 1025; ^{10}B(n,$\alpha_0+\alpha_1$), shape [124]

Block, R.C., *et al.* (1972) New Developments in Reactor Physics and Shielding, Kiamesha Lake, New York, CONF-720901, **2**, 1107; ^{238}U(n,γ)/^{197}Au(n,γ) [470]

Blons, J. (1973) Nucl. Sci. Eng. **51**, 130; ^{235}U(n,f)/^{10}B(n,α), shape [718]; ^{239}Pu(n,f)/^{10}B(n,α), shape [719]

Blons, J., *et al.* (1977) Private Communication, ^{238}U(n,f)/^{235}U(n,f), shape [828]

Bockelman, C.K., *et al.* (1951) Phys. Rev. **84**, 69; ^{10}B(tot) [182]

Bogart, D. and Nichols, L.L. (1969) Nucl. Phys. **A125**, 463; ^{10}B(n,$\alpha_0+\alpha_1$), shape [130]

Bollinger, L., *et al.* (1958) Peaceful uses of Atomic Energy, Geneva, **15**, 127; ^{239}Pu(n,f)/^{10}B(n,α), shape [678]

Bowman, C.D., *et al.* (1963) Phys. Rev. **130**, 1482; ^{235}U(n,f)/^{10}B(n,α), shape [732]

Cancé, M. and Grenier, G. (1976) Fast Neutron Fission Cross Sections of ^{233}U, ^{235}U, ^{238}U, and ^{239}Pu, Argonne Nat'l Lab., ANL-76-90, 141; ^{238}U(n,f)/^{235}U(n,f) [832]

Cancé, M. and Grenier, G. (1978) Nucl. Sci. Eng. **68**, 197; ^{235}U(n,f) [596]; ^{239}Pu(n,f) [612]; ^{238}U(n,f) [812]

Cancé, M. and Grenier, G. (1981) Saclay Report CEA-N-2194; ^{235}U(n,f) [597]

Cancé, M. and Grenier, G. (1983) private communication; ^{235}U(n,f) [598]

Carlson, A.D. and Patrick, B.H. (1978) Neutron Physics and Nuclear Data for Reactors and other Applied Purposes, Harwell, 880; ^{235}U(n,f), shape [508-509]

Carlson, A.D., *et al.* (1984) Nuclear Standard Reference Data, Geel, IAEA-TECDOC-335, 162; ^{235}U(n,f) [523]

Carlson, G.W. and Behrens, J.W. (1978) Nucl. Sci. Eng. **66**, 205; ^{239}Pu(n,f)/^{235}U(n,f) [600]

Chen Ying, *et al.* (1982) Nuclear Data for Science and Technology, Antwerp, 462; also Chinese J. Nucl. Phys. **3**, 52 (1981); $^{197}Au(n,\gamma)$ [370]; $^{197}Au(n,\gamma)$, shape [371]

Cierjacks, S., *et al.* (1976) Fast Neutron Fission Cross Sections of ^{233}U, ^{235}U, ^{238}U, and ^{239}Pu,, ANL-76-90, 94; $^{238}U(n,f)/^{235}U(n,f)$, shape [824]

Clements, P.J. and Rickard, I.C. (1972) Harwell Report AERE-R7075; $^{6}Li(n,\alpha)$, shape [280,281]; $^{6}Li(n,\alpha)/^{238}U(n,f)$, shape [280,281]

Coates, M.S., *et al.* (1972) Neutron Standard Ref. Data, Vienna, STI/PUB/371, 129; $^{10}B(n,\alpha_1)$, shape [128]
Coates, M.S., *et al.* (1972) Neutron Standard Ref. Data, Vienna, STI/PUB/371, 105; $^{6}Li(n,\alpha)$, shape [205]
Coates, M.S., *et al.* (1975) Nuclear Cross Sections and Technology, Washington, DC, NBS Spec. Publ. 425, II, 568; also private communication; $^{238}U(n,f)/^{235}U(n,f)$, shape [826]

Condé, H., *et al.* (1964) Arkiv Fysik **29**, 45; $^{6}Li(n,\alpha)$ [198]
Condé, H., *et al.* (1982) Nuclear Data for Science and Technology, Antwerp, 447; $^{6}Li(n,\alpha)$, shape [226]

Coon, J.H., *et al.* (1952) Phys. Rev. **88**, 562; ^{10}B(tot) [183]

Corvi, F. (1983) Priv. Comm., $^{235}U(n,f)/^{6}Li(n,\alpha)$, shape [530,531]

Cox, S.A. and Pontet, F.R. (1966) J. Nucl. Energy **21**, 271; $^{10}B(n,\alpha_0+\alpha_1)$ [115]

Czirr, J.B. and Carlson, A.D. (1980) Nuclear Cross Sections for Technology, Knoxville, NBS Spec. Publ. 594, 84; $^{6}Li(n,\alpha)/^{10}B(n,\alpha)$, shape [120]
Czirr, J.B. and Carlson, G.W. (1977) Nucl. Sci. Eng. **64**, 892; $^{235}U(n,f)/^{6}Li(n,\alpha)$, shape [271,272]
Czirr, J.B. and Sidhu, G.S. (1975) Nucl. Sci. Eng. **57**, 18; $^{235}U(n,f)$, shape [510]
Czirr, J.B. and Sidhu, G.S. (1975) Nucl. Sci. Eng. **58**, 371; $^{235}U(n,f)$, shape [511]
Czirr, J.B. and Sidhu, G.S. (1976) Nucl. Sci. Eng. **60**, 383; $^{6}Li(n,\alpha)/^{235}U(n,f)$, shape [270]
Czirr, J.B. and Stelts, M.L. (1973) Nucl. Sci. Eng. **52**, 299; $^{197}Au(n,\gamma)/^{235}U(n,f)$, shape [378]

Davis, E.A., *et al.* (1961) Nucl. Phys. **27**, 448; $^{10}B(n,\alpha)$, abs [121]; $^{10}B(n,\alpha_0)/^{10}B(n,\alpha_1)$ [122]

Davis, M.C., *et al.* (1978) Annals Nucl. Energy **5**, 569; $^{235}U(n,f)$ [564]; $^{239}Pu(n,f)$ [640]
Davis, M.C. and Knoll, G.F. (1978) Annals Nucl. Energy **5**, 583; $^{235}U(n,f)$ Cf-AV [565]; $^{239}Pu(n,f)$ Cf-AV [641]

Davletshin, A.N., *et al.* (1980) At. Energ. **48**, 87; transl. in Sov. J. At. En. **48**, 97; $^{197}Au(n,\gamma)$ [350]; $^{238}U(n,\gamma)$ [436]

Debus, G.H. and De Bievre, P.J. (1967) J. Nucl. Energy **21** 373; $^{10}B(n,\alpha)$ [708#]

Deruytter, A.J. and Wagemans, C. (1971) J. Nucl. Energy **25**, 263; $^{235}U(n,f)/^{10}B(n,\alpha)$, shape [731]

De Saussure, G. and Weston, L.W. (1963) Oak Ridge Report ORNL-3360, 51; $^{238}U(n,\gamma)/^{235}U(n,f)$ [478]

De Saussure, G., *et al.* (1966) Nuclear Data for Reactors, Paris, **II**, 233; $^{235}U(n,f)/^{10}B(n,\alpha)$, shape [578,730]
De Saussure, G., *et al.* (1973) Nucl. Sci. Eng., **51**, 385; $^{238}U(n,\gamma)/^{10}B(n,\alpha)$ [408]
De Saussure, G., *et al.* (1978) Oak Ridge National Lab, ORNL/TM-6152; $^{238}U(n,\gamma)$ evaluation [480]

Dietze, K. (1977) Zentralinst. f. Kernforsch., Rossendorf, Report ZFK-341; $^{238}U(n,\gamma)$ [432]

Difilippo, F.C., *et al.* (1978) Nucl. Sci. Eng. **68**, 43; $^{238}U(n,f)/^{235}U(n,f)$ [808]

Diment, K.M. (1967) Harwell Report AERE-R-5224; $^{10}B(tot)$ [194#,195#,196#]

Diven, B.C. (1957) Phys. Rev. **105**, 1350; $^{235}U(n,f)$, shape [572]; $^{235}U(n,f)$ [573]

Dushin, V.N., *et al.* (1983) Proc. IAEA Consultants' Meeting, The ^{235}U Fast-Neutron Fission Cross Section, and the ^{252}Cf Fission Neutron Spectrum, Smolenice, July 1983, INDC(NDS)-146 53; $^{235}U(n,f)$ [591-595]; $^{238}U(n,f)$ [811]; $^{239}Pu(n,f)$ [611]

Ferguson, A.T.G. and Paul, E.B. (1959) J. Nucl. Eng. A **10**, 19; $^{197}Au(n,\gamma)$ [355]

Flerov, N.N., *et al.* (1958) At. Energ. **5**, 657; transl. in Sov. J. At. En. **5**, 1600; $^{238}U(n,f)$ [860]

Fort, E. (1970) Nuclear Data for Reactors, Helsinki, STI/PUB/259; $^{6}Li(n,\alpha)$ [294]
Fort, E. and Marquette, J.P. (1972) European-American Nucl. Data Committee Doc. EANDC(E) 148"U"; $^{6}Li(n,\alpha)$ [290-292]
Fort, E. and Rigoleur, C.Le (1975) Nuclear Cross Sections and Technology, Washington, DC, NBS Spec. Publ. 425, 957; $^{197}Au(n,\gamma)$ [345]

Fricke, M.P., *et al.* (1970) Nuclear Data for Reactors, Helsinki June 1970, STI/PUB/259, **2**, 265; $^{197}Au(n,\gamma)/^{10}B(n,\alpha)$ [300]; $^{197}Au(n,\gamma)$, shape [301]
Fricke, M.P., *et al.* (1971) Neutron Cross Section and Technology, Knoxville, CONF-710301, **1**, 252; $^{238}U(n,\gamma)/^{10}B(n,\alpha)$ [400]; $^{238}U(n,\gamma)$, shape [401]

Friesenhahn, S.J., *et al.* (1974) Intelcom Radiation Technology Report INTEL-RT 7011-001; $^{10}B(n,\alpha_0+\alpha_1)$, shape [100]; $^{10}B(n,\alpha_1)$, shape [103]; $^{6}Li(n,\alpha)$, shape [246]

Fursov, B.I., *et al.* (1977) At. Energ. **43**, 261; transl. in Sov. J. At. En. **43**, 891; $^{239}Pu(n,f)/^{235}U(n,f)$ [653]; $^{239}Pu(n,f)/^{235}U(n,f)$ shape [654]
Fursov, B.I., *et al.* (1977) At. Energ. **43**, 181; transl. in Sov. J. At. En. **43**, 808; $^{238}U(n,f)/^{235}U(n,f)$ [844]; $^{238}U(n,f)/^{235}U(n,f)$ shape [845]

Garlea, I., *et al.* (1983) Int'l Nucl. Data Comm. Rep. INDC(ROM)-15, Rev. Roumaine Phys. **26**, 643; $^{239}Pu(n,f)/^{235}U(n,f)$ [633]; $^{238}U(n,f)/^{235}U(n,f)$ [863]

Gayther, D.B. (1975) Neutron Cross Sections and Technology, Washington, DC, NBS Spec. Publ. 425, 2, 564; $^{235}U(n,f)$, shape [588]; $^{239}Pu(n,f)$, shape [589]
Gayther, D.B. (1977) Annals Nucl. Energy **4**, 515; $^{6}Li(n,\alpha)/^{235}U$, shape [261]

Gibbons, J.G. and Macklin, R.L. (1959) Phys. Rev. **114**, 571; $^{10}B(n,\alpha_0)$ [114]

Goulding, C., *et al.* (1972) US Nucl. Data Committee Report USNDC-3, 161; $^{6}Li(tot)$ [257]

Goverdovskii, A.A., *et al.* (1983) Conf. on Neutron Physics, Kiev, **2**, 159; $^{238}U(n,f)/^{235}U(n,f)$ [853]
Goverdovskii, A.A., *et al.* (1984) At. Energ. **56**, 162; transl. in Sov. J. At. En. **56**, 173; $^{238}U(n,f)/^{235}U(n,f)$ [854]

Grench, H.A., *et al.* (1965) European-American Nucl. Data Committee Doc. EANDC-79, 72, also private communication; $^{197}Au(n,\gamma)/^{235}U(n,f)$ [331]

Guenther, P., *et al.* (1982) Nucl. Phys. A **373, 305**; $^{6}Li(tot)$ [220-222]

Gwin, R., *et al.* (1976) Nucl. Sci. Eng. **59**, 79; $^{197}Au(n,\gamma)/^{10}B(n,\alpha)$ [304]; $^{197}Au(n,\gamma)/^{10}B(n,\gamma)$ [305]
Gwin, R., *et al.* (1976) Nucl. Sci. Eng. **45**, 25; $^{239}Pu(n,f)/^{10}B(n,\alpha)$, shape [681,682]
Gwin, R., *et al.* (1976) Nucl. Sci. Eng. **61**, 116; $^{239}Pu(n,f)/^{10}B(n,\alpha)$, shape [676]
Gwin, R. (1984) Nucl. Sci. Eng. **88**, 37; $^{235}U(n,f)/^{10}B(n,\alpha)$, shape [710-714]

Harris, K.K., *et al.* (1965) Nucl. Phys. **69**, 37; $^{197}Au(n,\gamma)$ [332]

Harvey, J. and Hill, N. (1975) Nuclear Cross Sections and Technology, Washington, DC, NBS Spec. Publ. 425, 244; also private communications 1976 and 1981; $^{6}Li(tot)$ [$274^{\#}$,$275^{\#}$,$276^{\#}$,$277^{\#}$]

Heaton, H.T., *et al.* (1975) Proc. Conf. Nuclear Cross Sections and Technology, Washington, DC, NBS Spec. Publ. 425: also, Heaton, H.T., *et al.* (1982) Memo to J. Grundl; $^{235}U(n,f)$ Cf-AV [576]: also Grundl, J.A. and Gilliam, D.M. (1983) Trans. Amer. Nucl. Soc. **44**, 533; $^{239}Pu(n,f)$ Cf-AV [674]

Herbach, C.M., *et al.* (1983) Int'l Nucl. Data Comm. INDC(GDR)-35; $^{239}Pu(n,f)$ [615-617]: also ZFK-592, 152 (1986)
Herbach, C.M., *et al.* (1985) Int'l Nucl. Data Comm. INDC(GDR)-37; $^{235}U(n,f)$ [587]: also ZFK-592, 152 (1986)

Holden, N.E. (1981) Brookhaven National Lab. BNL-NCS-51388; $^{197}Au(n,\gamma)$ [704]

Hughes, D.J., *et al.* (1958) Report WASH-745, 9; $^{10}B(tot)$ [190]

Hussain, H.A. and Hunt, S.E. (1983) Int. J. Appl. Radiat. Isot. **34**, 731; $^{197}Au(n,\gamma)$ [315]

Iyer, R.H. and Sampathkumar, R. (1969) Nuclear Phys. and Solid State Phys., Roorkee, **2**, 289; $^{239}Pu(n,f)/^{238}U(n,f)$ [668]; $^{235}U(n,f)/^{238}U(n,f)$ [871]

James, G.D. (1970) Nuclear Data for Reactors, Helsinki, STI/PUB/259, **I**, 267; $^{239}Pu(n,f)/^{10}B(n,\alpha)$, shape [679]

Jarvis, G.A., *et al.* (1953) Los Alamos Report LA-1571; $^{238}U(n,f)/^{235}U(n,f)$ [855]

Johnsrud, A.E., *et al.* (1959) Phys. Rev. **116**, 927; $^{197}Au(n,\gamma)/^{235}U(n,f)$, shape [235]

Joly, S., *et al.* (1979) Nucl. Sci. Eng. **70**, 53; $^{197}Au(n,\gamma)$ [344]

Käppeler, F. (1973) Karlsruhe Report KFK-1772; $^{235}U(n,f)$ [581]; $^{235}U(n,f)$, shape [582]

Kalinin, P. and Pankratov, V.M., (1962) Peaceful Uses of Atomic Energy, Geneva, **16**, 136; $^{238}U(n,f)$, shape [875]

Kari, K. (1978) Karlsruhe, Report KFK-2673; $^{235}U(n,f)$ [520]; $^{239}Pu(n,f)$ [521]

Kazakov, L.E., *et al.* 3(1986) Yadern. Konst. **3**, 37; $^{238}U(n,\gamma)/^{6}Li(n,\alpha)$ [482,483]; $^{238}U(n,\gamma)/^{10}B(n,\alpha)$ [484,485]

Knitter, H.-H. and Coppola, M. (1967) Euratom Report EUR-3454E; $^{6}Li(n,n\alpha)$ [212]
Knitter, H.-H., *et al.* (1977) Euratom Report EUR-5726E; $^{6}Li(tot)$ [214]; $^{6}Li(n,n)$ [215]

Knoll, G.F. and Poenitz, W.P. (1967) J. Nucl. Eng. **21**, 643; $^{235}U(n,f)$ [518]; $^{235}U(n,\gamma)/^{197}Au(n,\gamma)$ [519]

Konks, V.A., *et al.* (1964) Zh. Eksp. Teor. Fiz. **46**, 80; transl. in Sov. Phys. JETP **19**, 59; $^{197}Au(n,\gamma)/^{10}B(n,\alpha)$ [265]

Kononov, V.N., *et al.* (1977) Yad. Fiz. **26**, 947; transl. in Sov. Nucl. Phys. **26**, 500; $^{197}Au(n,\gamma)/^{10}B(n,\alpha_1)$, shape [352]

Koroleva, V.P. and Stavisskii, Yu.Ya. (1966) At. Energ. **20**, 431; transl. in Sov. J. At. En. **20**, 493; $^{238}U(n,\gamma)$ [438]

Kuks, I.M., *et al.* (1971) At. Energ. **30**, 55; $^{238}U(n,f)$ [877]
Kuks, I.M., *et al.* (1971) Conf. on Neutron Physics, Kiev, **4**, 18; $^{235}U(n,f)$ [878]

Lamaze, G.P., *et al.* (1975) Nucl. Sci. Eng. **56**, 94; $^{10}B(n,\alpha_0)/^{10}B(n,\alpha_1)$, [145]
Lamaze, G.P., *et al.* (1978) Nucl. Sci. Eng. **68**, 183; $^{6}Li(n,\alpha)$, shape [232]

Lampere, R.W. (1956) Phys. Rev. **104**, 1654; $^{238}U(n,f)/^{235}U(n,f)$ [821]

Lane, R.O., *et al.* (1961) Ann. Phys. **12**, 135; $^{6}Li(n,n)$ [253-255]
Lane, R.O., *et al.* (1971) Phys. Rev. **C4**, 380; $^{10}B(n,n)$ [170#]

Lemley, J.R., *et al.* (1971) Nucl. Sci. Eng. **43**, 281; $^{235}U(n,f)/^{6}Li(n,\alpha)$, shape [244]

Lehto, W.K. (1970) Nucl. Sci. Eng. **39**, 361; $^{239}Pu(n,f)/^{235}U(n,f)$, shape [635]

Le Rigoleur, C., *et al.* (1975) Nuclear Cross Sections and Technology, Washington, DC, NBS Spec. Publ. 425, **II**, 953; $^{238}U(n,\gamma)$ [428]
Le Rigoleur, C., *et al.* (1976) Saclay Report CEA-R-4788; $^{197}Au(n,\gamma)$ [342-343]

Li Jingwen, *et al.* (1982) Nuclear Data for Science and Technology, Antwerp, 55; ^{235}U(n,f) [643]; ^{239}Pu(n,f) [644]
Li Jingwen, *et al.* (1986) Int. Nucl. Data Comm. Doc. INDC(CPR)-009; ^{235}U(n,f) [645]; ^{238}U(n,f)/^{235}U(n,f) [646]

Lindner, M., *et al.* (1976) Nucl. Sci. Eng. **59**, 381; ^{197}Au(n,γ)/^{235}U(n,f) [302]; ^{238}U(n,γ)/^{235}U(n,f) [410]

Linenberger, G.A., *et al.* (1944) Los Alamos Report LA-179; ^{238}U(n,γ)/^{235}U(n,f), shape [425]

Macklin, R.L. (1981) Nucl. Sci. Eng. **79**, 265; ^{197}Au(n,γ)/^{235}U(n,f) [314]; ^{197}Au(n,γ)/^{6}Li(n,α) [313]
Macklin, R.L. and Gibbons, J.H. (1965) Phys. Rev. **140**, B324; ^{10}B(n,α_0)/^{10}B(n,α_1) [149]
Macklin, R.L. and Gibbons, J.H. (1968) Phys. Rev. **165**, 1147; ^{10}B(n,α_0)/^{10}B(n,α_1) [125#]; ^{10}B(n,α_0) [126#]
Macklin, R.L., *et al.* (1975) Phys. Rev. **C11**, 1270; ^{197}Au(n,γ)/^{6}Li(n,α) [312]
Macklin, R.L., *et al.* (1979) Nucl. Sci. Eng. **71**, 205; ^{6}Li(n,α)/^{235}U(n,f), shape [200]

Mahdavi, M., *et al.* (1982) Nuclear Data for Science and Technology, Antwerp, 58; ^{239}Pu(n,f)/^{235}U(n,f) [637]

Manabe, M., *et al.* (1986) Tohoku Univ. Report NETU-47, 61; ^{238}U(n,f)/^{235}U(n,f) [856]

Mangialajo, M., *et al.* (1963) Nucl. Phys. **43**, 124; ^{238}U(n,f), shape [881]

Meadows, J.W. (1970) Neutron Standards and Flux Normalization, Argonne Nat'l Lab., 129; ^{6}Li(n,α) [707#]; ^{10}B(n,α) [703]
Meadows, J.W. (1983) Argonne Report ANL-NDM-83; ^{238}U(n,f)/^{235}U(n,f) [803]; ^{239}Pu(n,f)/^{235}U(n,f) [602]
Meadows, J.W. (1988) Ann. Nucl. Energy **15**, 421; ^{238}U(n,f)/^{235}U(n,f) [865]; ^{239}Pu(n,f)/^{235}U(n,f) [685]
Meadows, J.W. and Whalen, J.F. (1972) Nucl. Sci. Eng. **48**, 221; ^{6}Li(tot) [229]

Menlove, H.O. and Poenitz, W.P. (1968) Nucl. Sci. Eng. **33**, 24; ^{238}U(n,γ)/^{197}Au(n,γ) [419]; ^{238}U(n,γ) [420]; ^{238}U(n,γ), shape [421]

Michaudon, A., *et al.* (1960) J. Phys. Radium **21**, 429; ^{235}U(n,f)/^{10}B(n,α), shape [728]

Moat, A. (1958) private communication to J. Nucl. Energy A/B **14**, 85; ^{238}U(n,f) [861]; ^{235}U(n,f) [584]; ^{239}Pu(n,f) [657]

Mooring, F.P., *et al.* (1966) Nucl. Phys. **82**, 16; ^{10}B(tot) [187]; ^{10}B(n,n) [187]

Mostovaya, T.A., *et al.* (1980) Conf. on Neutron Physics, Kiev, **3**, 30; ^{235}U(n,f)/^{10}B(n,α), shape [530]

Moxon, M.C. (1969) Harwell Report AERE-R6074; ^{238}U(n,γ)/^{10}B(n,α_1) [450]

Muradyan, H.W., *et al.* (1977) Conf. on Neutron Physics, Kiev, **3**, 119; ^{235}U(n,f)/^{10}B(n,α_1), shape [538]

Murzin, A.V., *et al.* (1980) Conf. on Neutron Physics, Kiev, **2**, 257; $^{235}U(n,f)/^{10}B(n,\alpha_1)$ [540]

Nellis, D.O., *et al.* (1970) Phys. Rev. **C1**, 847; $^{10}B(n,\alpha_1)$ [107]

Nereson, N.G. (1954) Los Alamos Report LA-1655; ^{10}B(tot) [181]

Nordborg, C., *et al.* (1976) Fast Neutron Fission Cross Sections of ^{233}U, ^{235}U, ^{238}U, and ^{239}Pu, Argonne Nat'l Lab., ANL-76-90, 128; $^{238}U(n,f)/^{235}U(n,f)$ [830]

Olson, M.D. and Kavanagh, R.W. (1984) Phys. Rev. C **30**, 1375; $^{10}B(n,\alpha_0)$ [118#]

Overley, J.C., *et al.* (1974) Nucl. Phys. **A221**, 573; $^{6}Li(n,\alpha)$ [285]

Panitkin, Yu G., *et al.* (1971) Nuclear Data for Reactors, Helsinki, STI/PUB/259 **2**, 57; also Conf. on Neutron Phys., Kiev, **1**, 321; $^{238}U(n,\gamma)/^{235}U(n,f)$, shape [466]
Panitkin, Yu G. and Tolstikov, V.A. (1972) At. Energ. **33**, 782; transl. in Sov. J. At. En. **33**, 893; $^{238}U(n,\gamma)/^{235}U(n,f)$, shape [465]
Panitkin, Yu G. and Sherman, L.E. (1975) At. Energ. **39**, 17; transl. in Sov. J. At. En. **39**, 591; $^{238}U(n,\gamma)$ [464]

Paulsen, A., *et al.* (1975) Atomkern **26**, 80; $^{197}Au(n,\gamma)$ [337,338]

Perez, R.B., *et al.* (1973) Nucl. Sci. Eng. **52**, 46; $^{235}U(n,f)/^{10}B(n,\alpha)$, shape [514]
Perez, R.B., *et al.* (1974) Nucl. Sci. Eng. **55**, 203; $^{235}U(n,f)/^{10}B(n,\alpha)$, shape [513]

Perkin, J.L., *et al.* (1965) J. Nucl. Eng. A/B **19**, 423; $^{235}U(n,f)$ [725]; $^{239}Pu(n,f)$ [619]

Petree, B., *et al.* (1951) Phys. Rev. **83**, 1148; $^{10}B(n,\alpha_0)/^{10}B(n,\alpha_1)$ [162,163]

Pfletschinger, E. and Käppeler, F. (1970) Nucl. Sci. Eng. **40**, 375; $^{239}Pu(n,f)/^{235}U(n,f)$ [605]

Poenitz, W.P. (1970) Nucl. Sci. Eng. **40**, 383; $^{238}U(n,\gamma)/^{235}U(n,f)$, shape [405]; $^{238}U(n,\gamma)/^{235}U(n,f)$ [406]; $^{238}U(n,\gamma)/^{239}Pu(n,f)$ [407]; $^{239}Pu(n,f)/^{235}U(n,f)$ [626]
Poenitz, W.P. (1974) Nucl. Sci. Eng. **53**, 370; $^{235}U(n,f)$, shape [556,559]; $^{235}U(n,f)$ [557,558,560,561]; $^{235}U(n,f)/^{6}Li(n,\alpha)$, shape [562]
Poenitz, W.P. (1975) Nucl. Sci. Eng. **57**, 300; $^{197}Au(n,\gamma)$, shape [310]; $^{197}Au(n,\gamma)$ [311]; $^{238}U(n,\gamma)/^{197}Au(n,\gamma)$ [412]
Poenitz, W.P. (1977) Nucl. Sci. Eng. **64**, 894; $^{235}U(n,f)$, shape [553]; $^{235}U(n,f)$ [554,555]
Poenitz, W.P. (1984) pre-evaluation at thermal; $^{10}B(n,\alpha_0)/^{10}B(n,\alpha_1)$ [706]; $^{238}U(n,\gamma)$ [705]
Poenitz, W.P. and Armani, R.J. (1972) J. Nucl. Eng. **26**, 483; $^{238}U(n,f)/^{235}U(n,f)$ [816-818]; $^{238}U(n,f)/^{235}U(n,f)$, shape [819]
Poenitz, W.P. (1985) $^{6}Li(n,\alpha)$ [702]: {additional data was added to the evaluation at thermal of Holden, N.E. (1981) Brookhaven National Lab. BNL-NCS-51388}
Poenitz, W.P. and Meadows, J.W. (1974) Neutron Standard Ref. Data, Vienna, STI/PUB/371, 95; $^{6}Li(n,\alpha)$ [241]
Poenitz, W.P. and Meadows, J.W. (1976) Unpublished, $^{6}Li(n,\alpha)/^{235}U(n,f)$, shape [250]

Poenitz, W.P., *et al.* (1966) J. Nucl. Energy A/B **20**, 825; $^{197}Au(n,\gamma)$ [358-359]
Poenitz, W.P., *et al.* (1968) J. Nucl. Energy **22**, 505; $^{197}Au(n,\gamma)$, shape [360]
Poenitz, W.P., *et al.* (1981) Nucl. Sci. Eng. **78**, 239; $^{238}U(n,\gamma)/^{235}U(n,f)$ [460]; $^{238}U(n,\gamma)/^{197}Au(n,\gamma)$ [461]

Pankratov, V.M., *et al.* (1960) At. Energ. **9**, 399; transl. in Sov. J. At. En. **9**, 939 (1961): also J. Nucl. Energy A/B **16**, 494 (1962); $^{235}U(n,f)$, shape [721]; $^{238}U(n,f)$, shape [873]
Pankratov, V.M., *et al.* (1964) At. Energ. **14**, 177; transl. in Sov. J. At. En. **14**, 167; $^{235}U(n,f)$, shape [722]; $^{238}U(n,f)$, shape [874]

Quan, B.L. and Block, R.C. (1976) Chicago Operations Office, AEC Report COO-2479-14 $^{238}U(n,\gamma)/^{10}B(n,\alpha_1)$ [471]

Renner, C. (1978) University Sao Paulo, Brazil, Thesis; $^{6}Li(n,\alpha)$, shape [202#]

Rimawi, K. and Chrien, R.E. (1975) Neutron Cross Sections and Technology, Washington DC, NBS Spec. Publ. 425, **II**, 920; $^{196}Au(n,\gamma)/^{10}B(n,\alpha_1)$ [380]; $^{238}U(n,\gamma)/^{10}B(n,\alpha_1)$ [440]; $^{238}U(n,\gamma)/^{197}Au(n,\gamma)$ [441]

Robertson, J.C., *et al.* (1971) J. Nucl. Energy **23**, 205; $^{197}Au(n,\gamma)$ [367]

Rohrer, W. (1960) private comm. to authors, Ann. Phys. **10**, 455; $^{10}B(tot)$ [186]

Ryabov, Yu.V. (1971) At. Energ. **46**, 154; transl. in Sov. J. At. En. **46**, 178; $^{239}Pu(n,f)/^{10}B(n,\alpha)$, shape [660-663]

Ryves, T.B., *et al.* (1969) J. Nucl. Energy **23**, 205; Ryves, T.B. and Robertson, J.C. (1971) J. Nucl. Energy **25**, 557; $^{197}Au(n,\gamma)$ [367]
Ryves, T.B., *et al.* (1973) J. Nucl. Energy **27**, 519; $^{238}U(n,\gamma)$, shape [455]

Safford, G.J., *et al.* (1960) Phys. Rev. **119**, 1291; $^{10}B(tot)$ [188]

Sato, O., *et al.* (1983) Tohoku Univ. NETU-41, 33 [859]

Schomberg, M., *et al.* (1970) Nuclear Data for Reactors, Helsinki, STI/PUB/259, **I**, 315; $^{239}Pu(n,f)/^{10}B(n,\alpha)$, shape [680]

Schrack, R.A., *et al.* (1978) Nucl. Sci. Eng. **68**, 189; $^{10}B(n,\alpha_1)$, shape [105]

Schmitt, H.W., *et al.* (1960) Nucl. Phys. **17**, 109; $^{10}B(tot)$ [189]
Schmitt, H.W. and Cook, C.W. (1960) Nucl. Phys. **20**, 202; $^{197}Au(n,\gamma)$ [330]

Schroeder, I.G., *et al.* (1984) private communication; also Nuclear Standard Reference Data, Geel, IAEA-TECDOC-335, 320, $^{235}U(n,f)$, Cf-AV [517]; $^{239}Pu(n,f)$, Cf-AV [614]

Sealock, R.M. and Overlay, J.C. (1976) Phys. Rev. C **13**, 2149; $^{10}B(n,\alpha_0)$ [110]; $^{10}B(n,\alpha_1)$ [111]
Sealock, R.M., *et al.* (1981) Nucl. Phys. A **357**, 279; $^{10}B(n,\alpha_0)$ inverse reaction [112]

Shengyun, *et al.* (1984) Chinese J. Nucl. Phys. **6**, 1; $^{197}Au(n,\gamma)$ [372]

Smith, A.B., *et al.* (1977) Argonne Nat'l Lab. Report ANL/NDM-29; $^{6}Li(tot)$ [218,219]
Smith, A.B., *et al.* (1982) Nucl. Phys. **A373**, 305; $^{6}Li(n,n)$ [223]

Smith, R.K., *et al.* (1975) Private Communication, G. Hanson; $^{235}U(n,f)$ [567]; $^{238}U(n,f)$ [648]

Sowerby, M.G. (1966) J. Nucl. Energy A/B **20**, 135; $^{10}B(n,\alpha_0)/^{10}B(n,\alpha_1)$, [140]; $^{10}B(n,\alpha_0)/^{10}B(n,\alpha_1)$, shape [141]
Sowerby, M.G., *et al.* (1970) J. Nucl. Energy **24**, 323; $^{6}Li(n,\alpha)/^{10}B(n,\alpha)$, [131]; $^{6}Li(n,\alpha)/^{10}B(n,\alpha_1)$, shape [132]

Spencer, R.R. and Käppeler, F. (1975) Nuclear Cross Sections and Technology, Washington DC, NBS Spec. Publ. 425 **II**, 620; $^{238}U(n,\gamma)/^{197}Au(n,\gamma)$, shape [457]; $^{238}U(n,\gamma)/^{235}U(n,f)$, shape [458]

Stavisskii, Yu.Ya., *et al.* (1966) At. Energ. **20**, 431; $^{238}U(n,\gamma)$ [438]
Stavisskii, Yu.Ya., *et al.* (1971) Nucl. Constants, Issue 7, 218; transl. in INDC(CCP)-43/L, 225; $^{238}U(n,\gamma)/^{10}B(n,\alpha)$ [475]

Stein, W.E., *et al.* (1968) Nuclear Cross-Sections and Technology, Washington DC, NBS Spec. Publ. 299, **1**, 627; $^{238}U(n,f)/^{235}U(n,f)$ [822]

Stelts, M.L., *et al.* (1979) Phys. Rev. **C19**, 1159; $^{10}B(n,\alpha_0)/^{10}B(n,\alpha_1)$ [142#]

Szabo, I., *et al.* (1970) Neutron Standards and Flux Normalization, Argonne Nat'l Lab. 257, 208; revised in Fast Neutron Fission Cross Sections of ^{233}U, ^{235}U, ^{238}U, and ^{239}Pu, Argonne Nat'l Lab., ANL-76-90, 208; $^{235}U(n,f)$ [503]; $^{239}Pu(n,f)$ [620];
Szabo, I., *et al.* (1971) Neutron Cross-Sections and Technology, Univ. Tennessee, Knoxville, CONF-710301, 573; revised in Fast Neutron Fission Cross Sections of ^{233}U, ^{235}U, ^{238}U, and ^{239}Pu, Argonne Nat'l Lab., ANL-76-90, 208; $^{235}U(n,f)$ [504]; $^{239}Pu(n,f)$ [621]
Szabo, I., *et al.* (1973) Conf. on Neutron Physics, Kiev, **3**, 27; revised in Fast Neutron Fission Cross Sections of ^{233}U, ^{235}U, ^{238}U, and ^{239}Pu, Argonne Nat'l Lab., ANL-76-90, 208; $^{235}U(n,f)$ [505]; $^{239}Pu(n,f)$ [622]
Szabo, I., *et al.* (1976) Fast Neutron Fission Cross Sections of ^{233}U, ^{235}U, ^{238}U, and ^{239}Pu, Argonne Nat'l Lab., ANL-76-90, 208; $^{235}U(n,f)$ [506]; $^{239}Pu(n,f)$ [623]

Tsukada, K. and Tanaka, O. (1963) unpublished; $^{10}B(tot)$ [191]

Uttley, C.A. and Phillips, J.A. (1956) Harwell Report AERE NP/R1996; $^{238}U(n,f)$ [869]; $^{235}U(n,f)$ [526]; $^{239}Pu(n,f)$ [628]
Uttley, C.A., *et al.* (1970) Neutron Standards and Flux Normalization, Argonne Nat'l Lab., 80; $^{6}Li(tot)$ [235]

Van Shi-Di, *et al.* (1965) Physics and Chemistry of Fission, Salzburg, **I**, 287; $^{235}U(n,f)/^{10}B(n,\alpha)$, shape [727]

Varnagy, M. and Csikai, J. (1982) Nucl. Instr. Meth. **196**, 465; $^{238}U(n,f)/^{235}U(n,f)$ [848]; $^{239}Pu(n,f)/^{235}U(n,f)$ [666]

Viesti, G. and Liskien, H. (1979) Annals Nucl. Energy **6**, 13; $^{10}B(n,\alpha_1)$, shape [135#,136#,137#]

Vorotnikov, P.E., *et al.* (1975) Yad. Fiz. Issled. CCCP, Issue 20, 9; transl. in INDC(CCP)-66, 6; $^{238}U(n,f)$, shape [839]

Wagemans, C. and Deruytter, A.J. (1976) Annals Nucl. Eng. **3**, 437; $^{235}U(n,f)/^{10}B(n,\alpha)$, shape [544]
Wagemans, C. and Deruytter, A.J. (1984) Nuclear Standard Reference Data, Geel, IAEA-TECDOC-335, 156; $^{235}U(n,f)/^{10}B(n,\alpha)$, shape [545-546]
Wagemans, C., *et al.* (1980) Nuclear Cross Sections for Technology, Knoxville, Oct. 1979, NBS Spec. Publ. 594, 961; $^{235}U(n,f)/^{10}B(n,\alpha)$, shape [541-543]; $^{235}U(n,f)/^{6}Li(n,\alpha)$, shape [542]
Wagemans, C., *et al.* (1980) Annals Nucl. Eng. **7**, 495; $^{239}Pu(n,f)/^{6}Li(n,\alpha)$, shape [547]; $^{239}Pu(n,f)/^{10}B(n,\alpha)$, shape [548]; $^{239}Pu(n,f)/^{235}U(n,f)$, shape [549]

Wasson, O.A., *et al.* (1982) Nucl. Sci. Eng. **80**, 282; $^{235}U(n,f)$ [599]
Wasson, O.A., *et al.* (1982) Nucl. Sci. Eng. **81**, 196; $^{235}U(n,f)/^{6}Li(n,\alpha)$, shape [585]; $^{235}U(n,f)$, shape [586]; $^{235}U(n,f)$ [570]

Weston, L.W. and Lyon, W.S. (1961) Phys. Rev. **123**, 948; $^{197}Au(n,\gamma)$ [335]
Weston, L.W. and Todd, J.H. (1972) private comm. to R. Chrien; $^{239}Pu(n,f)/^{10}B(n,\alpha)$, shape [672]
Weston, L.W. and Todd, J.H. (1983) Nucl. Sci. Eng. **84**, 248; $^{239}Pu(n,f)/^{235}U(n,f)$, shape [536]
Weston, L.W. and Todd, J.H. (1984) Nucl. Sci. Eng. **88**, 567; $^{235}U(n,f)/^{10}B(n,\alpha)$, shape [532]; $^{235}U(n,f)/^{6}Li(n,\alpha)$, shape [533]; $^{239}Pu(n,f)/^{10}B(n,\alpha)$, shape [534]; $^{239}Pu(n,f)/^{6}Li(n,\alpha)$, shape [535]

White, P.H. (1965) J. Nucl. Energy A/B **19**, 325; $^{235}U(n,f)$ [499-502]
White, P.H., *et al.* (1965) Physics and Chemistry of Fission, Salzburg, **I**, 219; $^{239}Pu(n,f)/^{235}U(n,f)$ [608]
White, P.H. and Warner, G.P. (1967) J. Nucl. Energy **21**, 671; $^{239}Pu(n,f)/^{235}U(n,f)$ [609]; $^{238}U(n,f)/^{235}U(n,f)$ [815]

Willard, H.B., *et al.* (1955) Phys. Rev. **98**, 669; $^{10}B(n,n)$ [175]

Wisshak, K. and Käppeler, F. (1978) Nucl. Sci. Eng. **66**, 363; $^{238}U(n,\gamma)/^{197}Au(n,\gamma)$ [430,431]

Wu Jingxia, *et al.* (1983) Chinese J. Nucl. Phys. **5**, 158; $^{238}U(n,f)$ [850]

Yamamuro, N., *et al.* (1978) J. Nucl. Sci. Tech. (Japan) **15**, 637; $^{238}U(n,\gamma)/^{10}B(n,\alpha)$ [423]
Yamamuro, N., *et al.* (1980) J. Nucl. Sci. Tech. (Japan) **17**, 582; $^{238}U(n,\gamma)/^{10}B(n,\alpha_1)$, shape [422]
Yamamuro, N., *et al.* (1983) J. Nucl. Sci. Tech. (Japan) **20**, 797; $^{197}Au(n,\gamma)/^{10}B(n,\alpha_1)$ [340]; $^{197}Au(n,\gamma)/^{10}B(n,\alpha_1)$, shape [341]

Yan Wuguang, *et al.* (1975) At. Energ. Sci. Tech. (1975)#2, 1; $^{235}U(n,f)$ [738]

Yoshida, K., *et al.* (1983) NETU-44 (Tohoku), 30; ^{235}U(n,f) [528]; ^{238}U(n,f) [528]

Zhagrov, E.A., *et al.* (1980) Conf. on Neutron Physics, Kiev, **3**, 45; ^{235}U(n,f) [525]

Zhuravlev, K.D., *et al.* (1977) At. Energ. **42**, 56; transl. in Sov. J. At. En. **42**, 62; ^{235}U(n,f)/^{10}B(n,α), shape [515]; ^{239}Pu(n,f)/^{10}B(n,α), shape [630]; ^{239}Pu(n,f)/^{10}B(n,α) [631]

[#] These data sets were excluded from the simultaneous evaluation so they would be available for use in the R-matrix analyses.

APPENDIX B. References for the Data Base Used for the R-matrix Evaluations

^{7}Li System Data

Bartle, C. M. (1980) Nucl. Instr. Meth. **176**, 503; ^{6}Li(n,t)^{4}He, $\sigma(\theta)$, E_n=2.2-3.9 MeV.

Brown, R. E., *et al.* (1977) Phys. Rev. C **16**, 513; ^{6}Li(n,t)^{4}He, $\sigma(\theta)$, E_n=87-398 keV.

Condé, H., *et al.* (1982) Proc. Antwerp Conf. on Nuclear Data for Science and Technology, p. 447; ^{6}Li(n,t)^{4}He, $\sigma(\theta)$, E_n=1.3-3.5 MeV.

Drigo, L. and Tornielli, G. (1982) Nuovo Cimento **70A**, 402; ^{6}Li(n,n)^{6}Li, $A_y(\theta)$, E_n=1.5-4.0 MeV.

Drosg, M., *et al*, (1982) Los Alamos report LA-9129-MS; ^{4}He(t,n)^{6}Li, $\sigma(\theta)$, E_t=8.5-12.9 MeV.

Drosg, M., *et al*, (1982) Los Alamos report LA-9129-MS; ^{4}He(t,n$_1$)^{6}Li*, $\sigma(\theta)$, E_t=12.9 MeV.

Hardekopf, R. A., *et al.* (1977) Los Alamos Report LA-6188; ^{4}He(t,t)^{4}He, $\sigma(\theta)$, $A_y(\theta)$, E_t=7-14 MeV.

Harvey, J. A. and Hill, N. W. (1975) Proc. Conf. on Nuclear Cross Sections & Technology, NBS Spec. Pub. **425**, 244, and private communication from J. Harvey; ^{6}Li(n,n)^{6}Li, σ_T(E), E_n=10 eV-4 MeV.

Ivanovich, M., Young, P. G., and Ohlsen, G. G. (1968) Nucl. Phys. **A110**, 441; ^{4}He(t,t)^{4}He, $\sigma(\theta)$, E_t=1-7 MeV.

Jarmie, N., *et al.* (Nov. 1980) Los Alamos Report LA-8492; ^{4}He(t,t)^{4}He, $\sigma(\theta)$, $A_y(\theta)$, E_t=6-17 MeV.

Knitter, H. H., *et al.* (1983) Nucl. Sci. Eng. **83**, 229; ^{6}Li(n,t)^{4}He, $\sigma(\theta)$, E_n=0.035-325 keV (relative data).

Knox, H. D., *et al.* (1982) Bull. Am. Phys. Soc. **27**, 723, and private communication from H. Knox (1985); ^{6}Li(n,t)^{4}He, $\sigma(\theta)$, E_n=2-3.5 MeV.

Lane, R. O. (1961) Ann. Phys. **12**, 135; ^{6}Li(n,n)^{6}Li, $\sigma(\theta)$, E_n=0.05-1.44 MeV.

Lane, R. O. (1964) Phys. Rev. **136**, B1710; ^{6}Li(n,n)^{6}Li, $A_y(\theta)$, E_n=0.2-1.7 MeV.

Meadows, J. W. (1971) *Neutron Standards and Flux Normalizations* (AEC **23**), 129; ^{6}Li(n,t)^{4}He, $\sigma(E_{therm})$.

Overley, J. C., *et al.* (1974) Nucl. Phys. **A221**, 573; ^{6}Li(n,t)^{4}He, $\sigma(\theta)$, E_n=0.1-1.9 MeV.

Renner, C., *et al.* (1978) Bull. Am. Phys. Soc. **23**, 526, and private communication from J. Harvey; ^{6}Li(n,t)^{4}He, σ(E), E_n=82-467 keV (renormalized -5%).

Smith, A. B., *et al.* (1982) Nucl. Phys. **A373**, 305; ^{6}Li(n,n)^{6}Li, $\sigma(\theta)$, E_n=1.5-3.7 MeV.

Spiger, R. J. and Tombrello, T. A. (1967) Phys. Rev. **163**, 964; ^{4}He(t,t)^{4}He, σ_T(E), E_α=12-18 MeV.

Stelts, M. L., *et al.* (1979) Phys. Rev. **C19**, 1159; ^{6}Li(n,t)^{4}He relative $\sigma(\theta)$, E_n=2, 24 keV.

^{11}B System Data

Bockelman, C. K., *et al.* (1951) Phys. Rev. **84**, 69; $^{10}B(n,n)^{10}B$, $\sigma_T(E)$, E_n=0.02-1.01 MeV.

Cusson, R. Y. (1966) Nucl. Phys. **86**, 481; also Thesis, Cal. Tech. (1965); $^{7}Li(\alpha,\alpha)^{7}Li$, $\sigma(\theta)$, E_α=3-6 MeV.

Cusson, R. Y. (1966) Nucl. Phys. **86**, 481; also Thesis, Cal. Tech. (1965); $^{7}Li(\alpha,\alpha_1)^{7}Li^*$, $\sigma(\theta)$ $\sigma(E)$, E_α=3-6 MeV.

Diment, K. M. (1967) Harwell Report AERE-R-5224; $\sigma_T(E)$, E_n=0.076 keV−1 MeV.

Kavanagh, R. W. and Marcley, R. G. (1987) Phys. Rev. C **36**, 1194; $^{10}B(n,t)2\alpha$, $\sigma(E_{therm})$.

Lane, R. O., *et al.* (1971) Phys. Rev. C **4**, 380; $^{10}B(n,n)^{10}B$, $\sigma(\theta)$, $A_y(\theta)$, E_n=0.1-1.0 MeV.

Olson, M. D. and Kavanagh, R. W. (1984) Phys. Rev. C **30**, 1375; $^{7}Li(\alpha,n)^{10}B$, $\sigma(E)$ E_α=4.4-5.5 MeV.

Sealock, R.M. and Overley, J. C. (1976) Phys. Rev. C **13**, 2149; $^{10}B(n,\alpha_1)^{7}Li^*$, $\sigma(\theta)$ E_n=0.2-1.0 MeV.

Spencer, R. R., *et al.* (1973) Report EANDC(E) **147**, A1; $^{10}B(n,n)^{10}B$, $\sigma_T(E)$, E_n=94-411 keV.

Van der Zwaan, L. and Geiger, K. W. (1972) Nucl. Phys. **A180**, 615; $^{10}B(n,\alpha)^{7}Li$, $\sigma(\theta)$ E_n=0.28-0.77 MeV.

Viesti, G. and Liskien, H. (1979) Annals Nucl. Energy **6**, 13; $^{10}B(n,\alpha_1)$, shape, E_n=0.1-2.2 MeV.

APPENDIX C. Memorandum to the Cross Section Evaluation Working Group

May 19, 1986

A TECHNIQUE FOR OBTAINING A GLOBAL FIT COMBINING ADVANTAGEOUS CHARACTERISTIC OF GMA AND EDA

R. W. PEELLE

SUMMARY

Equations are developed that are planned to be used in the combination of the outputs of the EDA analysis of the ^{7}Li and ^{11}B composite nucleus reaction systems at LANL and the GMA simultaneous evaluation at ANL of $^{6}Li(n,\alpha)$, $^{6}Li(n,n)$, $^{10}B(n,\alpha_0)$, $^{10}B(n,\alpha_1)$, $^{10}B(n,n)$, $^{197}Au(n,\gamma)$, $^{238}U(n,\gamma)$, $^{235}U(n,f)$, $^{239}Pu(n,f)$, and $^{238}U(n,f)$ pointwise cross sections.

1. INTRODUCTION

In an earlier letter to CSEWG[1] and in papers by Carlson *et al.*, at Geel and Santa Fe Conferences,[2] a plan was described to combine results from LANL EDA R-matrix analyses[3] and ANL GMA simultaneous evaluations.[4] Since the earlier letter is somewhat vague on details and since the general concept has now been well documented in Refs. 2 and 3, the present note attempts primarily to clarify the development of the equation to be used.

In addition, there are some preliminary comments on the proper inclusion of (a) shape information for the fission cross sections in the thermal energy range, and (b) the thermal fissile constants.

2. THE PROBLEM AND ITS "IDEAL" SOLUTION

Our problem is to employ properly the upgraded data and evaluation techniques now available to produce an excellent evaluation of neutron standard and other important cross sections that we can fully defend. This goal implies the need to (1) evaluate in a consistent way all the standards and other cross sections for which absolute cross sections have been well measured, (2) retain the advantages of use of the R-matrix evaluation tool for the light elements, and (3) obtain the output covariance information corresponding to the data combination method employed.

The problem statement presumes the conclusions that through ratio measurements (1) knowledge of the ^{6}Li cross section affects the $^{235}U(n,f)$ standard, (2) vice versa, (3) absolute measurements on non-standards such as $^{239}Pu(n,f)$ are sufficiently precise to affect the standards to some degree. The Standards Evaluation Subcommittee of CSEWG has sought an evaluation strategy that treats these possibilities in a consistent way.

Neglect "practicality" for the moment and consider an ideal solution scheme for the problem posed. Since we do not know all the uses of the evaluated data well enough to know if loss to the sponsors would be more severe for cross section values too high or too low, it is reasonable to seek a solution vector e such that $z^t e$ has minimum variance for any vector z. Subject to general conditions, a least-squares solution meets this criterion provided the input data are weighted with their inverse variance-covariance matrix.[5] Here, the evaluation is parameterized in the vector (e_α) by whatever means are best; R-matrix parameters are components of e along with whatever parameters represent the $^{235}U(n,f)$ and other cross sections as a function of energy. Some parameters may represent the normalizing constants for cross section "shape" measurements. The parameter vector change in one iteration toward this solution is given by the solution of the least-squares matrix equation.

$$G^t V^{-1} G \, \delta e = G^t V^{-1} \, \delta \bar{y} \tag{1}$$

or equivalent forms, where the $(\bar{y}_i)$ vector stacks up all the significant absolute and ratio data and $\delta \bar{y}$ represents differences between $\bar{y}_i$ and $y_i^0(e^0)$, the calculated value at the same point based on the current best-estimate parameters e_α^0. (V_{ij}) is the variance-covariance matrix of these experimental data including effects of energy uncertainty, and the

$$G_{i\alpha} = \frac{dy_i}{de_\alpha}\bigg|_{e=e^0}$$

are the derivatives with respect to the evaluation parameters of the interpolated values for the cross sections at the energies for which these are input data elements. The derivatives are evaluated at the best known parameter set e_α^0. For the approach to be valid, we must demand (1) that the equations relating y to e can be linearized near the solution point, and (2) that any formula from which the derivatives are obtained does represent the observed physical phenomena.

Since the problem is nonlinear, the convenient variables are the indicated relative or absolute differences in e and y from sequential estimates refined in the course of iteration. The corresponding covariance matrix of the output parameters is $C = (G^t V^{-1} G)^{-1}$, a choice that can be defended when the input data scatter is consistent with the data covariance matrix V. The point is that the needed evaluation outputs would be available from such a global least-squares effort if (1) input data covariance matrices are available and sufficiently well-drawn that they can be inverted, (2) the

derivatives $G_{i\alpha}$ are available both for R-matrix parameters and pointwise cross section parameters such as are used in the ANL code GMA, (3) the evaluators could devise means to deal with any discrepancies in the data base, and (4) the numerical problem could be put on a machine and solved.

Condition (1) requires considerable evaluator effort and codification of the results if the consequent evaluated cross sections are to be fully credible. W. Poenitz has completed much or all of this effort.[6] Derivatives $G_{i\alpha}$ are now largely available, but not all in the same computer program. Handling discrepancies in the data base must occur in any case; global evaluation may point up discrepancies more sharply. Getting the global least-squares problem on one machine is not incredible for the future; however, as seen in the next section, a global fitting program should not be needed.

Fortunately, many of the measured data sets required for input to the hypothetical least-squares problem are not intercorrelated. This fact greatly increases the tractability of the data variance-covariance matrix and its inverse, and leads to consequent simplification of the numerical problem.[4] The first step of the analysis can proceed separately for each subset or "segment" of the overall data for which the experimental results are not correlated with the data in the other subsets. The complexity of the resulting formulae depends on the degree to which the fitting parameters in this first step can be the same as those for the final evaluation.

The idea of the present approach is to obtain the numerical values of the sums on the right side and the term $G^t\ V^{-1}\ G$ on the left of the global least-squares Eq. (1) above by combining values from the existing separate fitting programs set up at LANL and ANL, using "segment 1" and "segment 2" data sets, respectively. It is assumed that we will know at the outset how to estimate an overall parameter vector (e_α^0) very close to the final global solution, so that the ψ^2 minimization can be linearized.

3. SEPARATION OF THE DATA AND PARAMETER VECTORS

First one separates the overall relevant data base into segments not correlated with each other. For our example, segment 1 consists of all the charged-particle data in the ^{7}Li and ^{11}B reaction systems, plus a portion of the neutron cross section data on ^{6}Li and ^{10}B strictly uncorrelated with the second segment. The segment 1 of the data base is further separated into subsegments 1L for the ^{7}Li system and 1B for the ^{11}B system. It is assumed that no experimental value in segment 1A is correlated with any value in segment 1B. The segment 2 data base consists of all the neutron cross section and ratio data for ^{235,238}U(n,f), ^{239}Pu(n,f), ^{6}Li(n,α), etc., from measurements uncorrelated with those in segment 1. Suitable divisions of the global data base have been shown to be possible in practice.[6]

The trial parameter vector for the global fit can be separated into a stack of subvectors as follows:

$$e^0 = \begin{pmatrix} e^0_{LR} \\ e^0_{BR} \\ e^0_P \end{pmatrix} , \tag{2}$$

where e^0_{LR} and e^0_{BR} are respectively the best estimate of the final R-matrix parameters for the lithium and boron reaction systems, and the e^0_P (the σ of Ref. 4) are the best pointwise* cross section parameter estimates of Poenitz, for targets other than ^{6}Li and ^{10}B, together with various experimental data set normalization parameters. [Later we employ e_L and e_B. The vector $e^0_L(e^0_{LR})$ is the set of pointwise estimates for the lithium system that is obtained from the R-matrix parameters e^0_{LR}. The vector e^0_B of pointwise estimates is similarly obtained from e^0_{BR}. However, since for Li and B the R-matrix parameters are sought, e^0_L and e^0_B are derived quantities.]

Note that the R-matrix parameterization generates neutron cross sections covering a wider energy range than that for which it has been applied in the ENDF/B system. Moreover, the ratio and other data in use with GMA for ^{6}Li+n and ^{10}B+n, which we wish to include in the R-matrix evaluation, does not cover the whole range of data types already included in the R-matrix evaluation.

The parameter vector δe of Eq. (1) corresponds to a change from the base parameter vector e^0.

$$\delta e \equiv \varepsilon = \begin{pmatrix} \varepsilon_{LR} \\ \varepsilon_{BR} \\ \varepsilon_P \end{pmatrix} , \tag{3}$$

where $\varepsilon_{LR} = e_{LR} - e^0_{LR}$, $\varepsilon_{BR} = e_{BR} - e^0_{BR}$, and ε_P ($\equiv \delta p$ of Ref. 4) has as components the relative differences $(e_{P,i} - e^0_{P,i})/e^0_{P,i}$ utilized by the GMA code of Poenitz,[4] in the present case only for variables other than the lithium and boron cross sections. The output parameters from an iteration of the grand system are the vector segments e_{LR}, e_{BR}, and e_P.

---

* "Pointwise" is a modest misnomer, since the GMA system now utilizes in the energy region below 100 keV some parameter definitions corresponding to cross section averages or integrals.

The (δy_i) vector of eq (1) is a stacked difference vector including both segment 1 and segment 2 of the data base.

$$\delta y \equiv \eta = \begin{pmatrix} \eta_{1L} \\ \eta_{1B} \\ \eta_2 \end{pmatrix} . \tag{4}$$

The vector $\eta_{1L} = \bar{y}_{1L} - y_{1L}(e^0_{LR})$ the difference between the segment 1L measurement vector and the calculated vector from the best-guess R-matrix parameters for lithium. The vector segment η_{1B} is defined similarly for the segment 1B boron data and R-matrix computed values. The vector segment η_2 has components

$$\eta_{2i} = \bar{y}_{2i} - y_{2i}(e^0) \quad . \tag{5}$$

The element $y_{2i}(e^0)$ is the value comparable to $\bar{y}_{2i}$ but calculated from the base parameter vector eq (2). Recall that the information of ^{7}Li and ^{11}B reaction systems are contained in R-matrix parameters. The η_{2i} are M_i of Ref. 4 multiplied by the standard deviations of the corresponding observations.

4. SEGMENTING THE DERIVATIVE AND VARIANCE-COVARIANCE MATRICES

The derivative matrix $G \equiv (\partial y_i/\partial \varepsilon_\alpha)|_{\varepsilon=0}$ can be expanded as follows:

$$G = \begin{pmatrix} G_{1LR} & 0 & 0 \\ 0 & G_{1BR} & 0 \\ G_{2L}S_L & G_{2B}S_B & G_{2P} \end{pmatrix} . \tag{6}$$

This matrix has as many columns as the number of output parameters e_α, and as many rows as the elements of the global data base. It is evaluated at the best known parameter set e^0. There are large null submatrices because the interpolated cross sections from the R-matrix fit for the lithium system are not explicit functions of the R-matrix parameters of the boron system or the pointwise cross section parameters for ^{239}Pu, ^{238}U, etc.

In eq (6) the matrix G_{LR} elements are obtained from the R-matrix program

$$G_{1LR,i\alpha} = \frac{\partial y_{1L,i}}{\partial e_{LR,\alpha}}\bigg|_{e_{LR}=e^0_{LR}} , \tag{7}$$

and the elements of G_{BR} are similarly obtained. The matrices G_{1LR} and G_{1BR} are generated in the R-matrix analysis of the segment 1 data.

The elements of G_{2L}, G_{2B}, and G_{2P} take into account the relative nature of the fitting variables of Ref. 4 and correspond to the derivatives of Ref. 4 for the portions of the pointwise data base for ^{6}Li, ^{10}B, and all others, respectively. For example, going back to the definition in Eq. (5)

$$G_{2P,i\alpha} = e_{P\alpha}\,\frac{\partial y_{2i}(e)}{\partial e_{P\alpha}}\bigg|_{e=e^0} , \tag{8}$$

and

$$G_{2B,i\alpha} = e_{B\alpha}\,\frac{\partial y_{2i}(e)}{\partial e_{B\alpha}}\bigg|_{e=e^0} . \tag{9}$$

Recall that e_B is a set of pointwise parameters for the ^{11}B reaction system, values of which are computed from the R-matrix parameters for the boron system. In the case of interest to CSEWG, G_{2L}, G_{2B}, and G_{2P} are inherent in the ANL analysis of the segment 2 data. Indeed, the matrix (G_{2L}, G_{2B}, G_{2P}) is the matrix A of Ref. 4 with each element multiplied by the standard deviation of the corresponding observed value, when only segment 2 data is included in the computation of the matrix elements.

Finally, the elements of the matrices S_L and S_B in Eq. (6) are the derivatives of the pointwise relative cross section parameters ε_P with respect to the corresponding R-matrix parameters. For example,

$$S_{L,\alpha\beta} = \frac{1}{e^0_{L,\alpha}}\left(\frac{de_{L,\alpha}}{de_{LR,\beta}}\right)\bigg|_{e=e^0} . \tag{10}$$

The e_L and e_B are just interpolated values from the R-matrix analysis, and so the elements given by Eq. (10) can be computed in a modification of that program. Note from Eqs. (9) and (10) that the product matrices $G_{2L}S_L$ and $G_{2B}S_B$ just yield the derivatives like $\partial y_{2i}/\partial e_{LR,\beta}$ required for Eq. (6).

Because the data segments 1L, 1B, and 2 are each free of observations correlated with observations in either of the other two segments, the data covariance matrix V of Eq. (1) is "block diagonal" and one can directly write V^{-1} in terms of the inverses of submatrices that are the variance-covariance matrices of each of the data segments.

$$V^{-1} = \begin{bmatrix} V_{1L}^{-1} & 0 & 0 \\ 0 & V_{1B}^{-1} & 0 \\ 0 & 0 & V_2^{-1} \end{bmatrix} . \tag{11}$$

5. THE GLOBAL LEAST-SQUARES PROBLEM EXPRESSED IN SEGMENTED FORM

Equation (1) can now be expanded in terms of the segmented vectors and matrices defined above.

$$\begin{bmatrix} G_{1LR}^t & 0 & S_L^t G_{2L}^t \\ 0 & G_{1BR}^t & S_B^t G_{2B}^t \\ 0 & 0 & G_{2P}^t \end{bmatrix} \begin{bmatrix} V_{1L}^{-1} & 0 & 0 \\ 0 & V_{1B}^{-1} & 0 \\ 0 & 0 & V_2^{-1} \end{bmatrix} \begin{bmatrix} G_{1LR} & 0 & 0 \\ 0 & G_{1BR} & 0 \\ G_{2L}S_L & G_{2B}S_B & G_{2P} \end{bmatrix} \begin{bmatrix} \varepsilon_{LR} \\ \varepsilon_{BR} \\ \varepsilon_P \end{bmatrix}$$

$$= \begin{bmatrix} G_{1LR}^t & 0 & S_L^t G_{2L}^t \\ 0 & G_{1BR}^t & S_B^t G_{2B}^t \\ 0 & 0 & G_{2P}^t \end{bmatrix} \begin{bmatrix} V_{1L}^{-1} & 0 & 0 \\ 0 & V_{1B}^{-1} & 0 \\ 0 & 0 & V_2^{-1} \end{bmatrix} \begin{bmatrix} \eta_{1L} \\ \eta_{1B} \\ \eta_2 \end{bmatrix} . \tag{12}$$

Equation (12) may be rewritten using the following matrix definition

$$W_{1L} \equiv G_{1LR}^t \, V_{1L}^{-1} \, G_{1LR} \quad ,$$

$$W_{1B} \equiv G_{1BR}^t \, V_{1B}^{-1} \, G_{1BR} \quad ,$$

$$W_2 = \begin{bmatrix} G_{2L}^t \\ G_{2B}^t \\ G_{2P}^t \end{bmatrix} V_2^{-1} \left(G_{2L}, G_{2B}, G_{2P}\right) \quad , \text{ and} \tag{13}$$

$$S = \begin{bmatrix} S_L & 0 & 0 \\ 0 & S_B & 0 \\ 0 & 0 & 1 \end{bmatrix} .$$

Similarly define the following vectors:

$$R_{1L} \equiv G_{LR}^{t}\, V_{1L}^{-1}\, \eta_{1L} \quad ,$$
$$R_{1B} \equiv G_{BR}^{t}\, V_{1B}^{-1}\, \eta_{1B} \quad , \quad \textit{and}$$
$$R_2 = \begin{pmatrix} G_L^t \\ G_B^t \\ G_P^t \end{pmatrix} V_2^{-1}\, \eta_2 \quad . \tag{14}$$

Based on all the definitions of Eqs. (13) and (14), the global least-squares equation becomes

$$\left[\begin{pmatrix} W_{1L} & 0 & 0 \\ 0 & W_{1B} & 0 \\ 0 & 0 & 0 \end{pmatrix} + S^t\, W_2\, S \right] \begin{pmatrix} \varepsilon_{LR} \\ \varepsilon_{BR} \\ \varepsilon_P \end{pmatrix} = \begin{pmatrix} R_{1L} \\ R_{1B} \\ 0 \end{pmatrix} + S^t\, R_2 \quad . \tag{15}$$

This may be solved for ε, and the decision then made whether additional iterations are required.

6. OBTAINING THE VECTORS AND MATRICES REQUIRED FOR THE GLOBAL LEAST-SQUARES FIT

It is believed that the vectors and sums in Eq. (15) can be obtained from relatively simple modifications to the programs that separately perform the R-matrix fits at LANL and the simultaneous evaluation fits at ANL. This might be accomplished without actually performing iterative fits to the separate segments of the data base.

The S-matrix contains derivatives with respect to R-matrix parameters of interpolated values from the R-matrix formula in EDA. That program has been trained to output the needed values.

The matrix W_2 is the matrix C_δ^{-1} in Eq. (20) of Ref. 4, when the latter is obtained using the estimated parameter set e^0 and only segment 2 of the input data base. (Note that the matrix inversion to obtain C_δ is not required.) R_2 is the vector $A^t\, C^{-1}\, M$ of Ref. 4 when obtained under the same circumstances. Therefore, W_2 and R_2 are readily available.

If the EDA program were based on the usual general least-squares approach, W_{1L} and R_{1L} would be the least-squares matrix and right-hand side of the equation

expressing an iteration starting with the parameter set e^0_{LR} and using only segment 1L of the data base. However, this is not the basis of the search in EDA, which is based on the following relation[6] for the change in the parameter vector δp:

$$\delta p = -G^{-1} g \quad ,$$

where

$$g_i = \frac{\partial \chi^2}{\partial p_i}$$

and

$$G_{ij} = \frac{\partial^2 \chi^2}{\partial p_i \, \partial p_j} \quad .$$

The gradient vector $g_L = 2R_{1L}$ under the conditions indicated above; it is readily available. However, G^{-1} is directly obtained in EDA as part of the iterative process and in the EDA program it is not defined except at the solution point.

At least three options remain if all the matrices of Eq. (15) are to be available for the global least-squares approach.

(a) One may use for e^0_{LR} and e^0_{BR} the iterated EDA solutions obtained from the segment 1 data set. This choice of e^0 is not apt to be our actual best estimate. This option would permit only one full iteration of the global problem. In this case one is using the G matrices relating R_{1L} and R_{1B} to δp of Eq. (16) (ε of earlier sections here) from EDA rather than from least-squares theory. G. Hale has shown that for this problem the matrices do differ, and has indicated that G^{-1} is a more general approximation to the parameter covariance matrix.

(b) One could modify the EDA program to give W_{1L} (and W_{1B}) just for this application, computed at any selected parameter vector e^0_{LR} (and e^0_{BR}). This approach negates any advantage from the EDA formulation of the equations, but does permit (rather clumsy multilab) iteration.

(c) Again for a single iteration, one could choose for e^0_{LR} and e^0_{BR} the parameters from the R-matrix analyses of unsegmented data sets, as is likely to be favored. One could then compute the W_1 just for that portion of the neutron data being "given up" in the data base segmentation, and subtract this from the G computed via EDA. This approach assumes that the contribution to G from this part of the neutron data is the same as would be obtained in least-squares theory. While this approach would be relatively simple, this author believes that numerical problems are apt to ensue.

The author believes that approach (b) is the most promising because it gives the most options for the completion of the global analysis. The initial 1986 results have been obtained using option (a).

7. INCLUSION OF THE THERMAL FISSILE CONSTANTS

At present the CSEWG Standards Committee has access to the results of the thermal fissile standards.[7,8] These overlap the information in the pointwise file. The situation is:

(a) The output ^{239}Pu and ^{235}U "thermal" fission cross sections from Ref. 7 are included as input data to GMA.

(b) The thermal parameter measurements utilized in Ref. 7, for ^{6}Li, ^{10}B, ^{197}Au, are also employed as input to GMA.

(c) The output values from GMA may differ from inputs in the cases of ^{6}Li, ^{10}B, ^{235}U, and ^{239}Pu.

In addition to these problems, the output cross sections and *g*-factors from Ref. 7 may be inconsistent with R-matrix fits to the resonance regions of the fissile nuclides.

Recent R-matrix fits to the fissile nuclide cross sections do not exist now, but may well exist by the time ENDF/B-VI is being assembled. It is recommended that for ENDF/B-VI such R-matrix fits be employed in file construction if the 2.2 km/s value lies within ~ 1/2 standard deviation of the thermal parameters recommended by the Standards Subcommittee. Otherwise, the Standards Subcommittee should review any proposed resolution of the conflict.

Whenever the *g* factors derived from fissile resonance parameterizations differ from the values assumed in the derivation of the fissile thermal parameters, the Standards Subcommittee should consider the impact of such changes on the thermal parameter outputs. This would be facilitated by earlier documentation of the sensitivity to such inputs.

The overlap between the GMA analysis and the traditional thermal fissile constant fit has been handled in the May 1986 results by including all the traditional thermal constants as variables in GMA along with the covariance data obtained by Axton in his analysis of the thermal data.[8]

REFERENCES

1. Letter to W. P. Poenitz from R. W. Peelle dated October 20, 1981, revised June 1983, on Evaluation Strategy for Standards and Other Important Cross Sections for Which the "Simultaneous Evaluation" Approach May be Applicable.

2. A. D. Carlson, W. P. Poenitz, G. M. Hale, and R. W. Peelle, "The Neutron Cross Section Standards Evaluations for ENDF/B-VI," Proc. of Advisory Group Meeting on Nuclear Standard Reference, Geel, Belgium, November 12-18, 1984. Also Proc. Intern. Conf. on Nuclear Data for Basic and Applied Science, Santa Fe, New Mexico, May 13-17, 1985, (1986) pp. 1429.

3. G. M. Hale, *et al.*, "ENDF/B-IV Summary Documentation for $^{6}Li(^{10}B)$," in ENDF-201 (BNL-17541) "ENDF/B Summary Documentation," compiled by R. Kinsey (1979). Also, G.M. Hale, "R-Matrix Analysis of the ^{7}Li System," Proc. of International Specialists Symp. on Neutron Standards and Applications, National Bureau of Standards (Eds. C. D. Bowman, A. D. Carlson, H. O. Liskien, and L. Stewart), NBS Spec. Publ. 493, p. 30 (1977).

4. W. P. Poenitz, "Data Interpretation, Objective Evaluation Procedures and Mathematical Techniques for the Evaluation of Energy-Dependent Ratio, Shape and Cross Section Data," Proc. Conf. on Nuclear Data Evaluation Methods and Procedures, Brookhaven National Laboratory (Eds. B. A. Magurno and S. Pearlstein) BNL-NCS-51363, vol. 1, p. 249 (1981).

5. R. W. Peelle, "Uncertainty in Nuclear Data Used for Reactor Calculations," in *Advances in Nuclear Science and Technology*, vol. 14, Chapter 2, p. 11-84, Eds. Lewins and Becker, Plenum Publishing Corp., 1982. .

6. W. P. Poenitz, "The Simultaneous Evaluation of Interrelated Cross Sections by Generalized Least-Squares and Related Data File Requirements," Proc. International Atomic Energy Agency (IAEA) Advisory Group Meeting on Nuclear Standard Reference Data, November 12-18, 1984, Geel, Belgium, IAEA-TEDOC-335 (1985) pp. 426-430.

7. M. Divadeenam and J. R. Stehn, Ann. Nucl. Energy 11, No. 8, 375 (1984).

8. E. J. Axton, "Evaluation of the Thermal Constants of ^{233}U, ^{235}U, ^{239}Pu, and ^{241}Pu, and the Fission Neutron Yield of ^{252}Cf," Central Bureau for Nuclear Measurements report CBNM/PH/I/82, May 1986.

APPENDIX D. Complete Results of the Combination Process

August 31, 1987

MEMORANDUM To: C. Dunford

From: A. Carlson, G. Hale, R. Peelle, W. Poenitz

Subject: Results of the ENDF/B-VI Standards Evaluation

The following are the complete output listings from the standards evaluation process, plus an extension to low energies of the ^{238}U fission cross section by the evaluator, W. Poenitz, for completeness. Note that cross sections such as the integral scattering cross sections for the light elements are included though they are not useful as standards.

This is the smoothed output of the combination of the generalized least squares (using segment 2 data) and R-matrix (using segment 1 data) evaluations. The uncertainties are not yet final. In some cases, points have been added to improve the definition of the cross section shape and to ease interpolation thereby. The comments before each data set are important and should be distributed with the data.

For ^{10}B and ^{6}Li at all energies the cross sections are point values. Though in some cases they were obtained in part with data having moderate neutron energy resolution, its effect on the evaluation is probably not significant. Except for the range up to 20 keV, for the heavy elements, the cross sections are low resolution smooth point values. The 9.4 eV value for the ^{235}U fission cross section is the integral cross section over the range from 7.8 to 11 eV. The cross sections listed for the heavy elements with tags from 0.15 keV through 15 keV represent decimal interval average values labeled at the center energies for intervals starting at 0.1 to 0.2 keV and ending with the interval 10 to 20 keV.

It should be noted that data inconsistencies exist which can cause false cross section structure. For example, the energy grid chosen in some energy ranges because of local structure in one cross section causes few experimental values to be available for other cross sections and consequently leads to lack of correlation restraint. Therefore the combination output has been smoothed to remove such structure if evidence indicates that it is very improbable that the fluctuations are real. In some cases, e.g., $^{235}U(n,f)$, structure has been left in since there is a reasonable probability that it is remnant of real structure.

The data have been finalized only in certain energy regions in order to give the assigned ENDF/B file evaluators for these nuclides sufficient freedom in the evaluation process. For the heavy elements the evaluators may superimpose structure on the cross sections below the "finalized" energy limits given here. In these cases the committee recommends that evaluators try to impose structure that maintains the average values given to about 0.5 standard deviations. It is also recommended that the values of the thermal constants used in the ^{233}U, ^{235}U, ^{239}Pu and ^{241}Pu evaluations agree within 0.5 standard deviations of the values listed here. For the light element standards, the evaluator G. Hale may need to revise values above the upper limit given in order to take into account information required for extending the evaluation to 20 MeV.

Appendix D (Continued)

$^{6}Li(n,t)$

Proposed final cross sections below 1 MeV
uncertainties are not final
Log-log interpolation up to 500 keV
Linear-linear interpolation above 500 keV
The values with *'s are points added for ease in interpolation

E_n(MeV)	σ(b)	Uncertainty(%)	E_n(MeV)	σ(b)	Uncertainty(%)
0.2530E-07	940.9827	0.14	0.2410E+00	3.2539*	0.23
0.9400E-05	48.7928	0.14	0.2420E+00	3.2485*	0.23
0.1500E-03	12.1957	0.14	0.2430E+00	3.2403*	0.23
0.2500E-03	9.4428	0.14	0.2440E+00	3.2297*	0.23
0.3500E-03	7.9777	0.14	0.2450E+00	3.2164	0.23
0.4500E-03	7.0337	0.14	0.2500E+00	3.1145	0.24
0.5500E-03	6.3613	0.14	0.2600E+00	2.7896	0.26
0.6500E-03	5.8502	0.14	0.2700E+00	2.4026	0.28
0.7500E-03	5.4454	0.14	0.2800E+00	2.0366	0.29
0.8500E-03	5.1137	0.14	0.3000E+00	1.4743	0.31
0.9500E-03	4.8371	0.14	0.3100E+00	1.2746*	0.32
0.1500E-02	3.8470	0.14	0.3250E+00	1.0498	0.32
0.2500E-02	2.9791	0.14	0.3350E+00	0.9365*	0.32
0.3500E-02	2.5181	0.14	0.3500E+00	0.8056	0.32
0.4500E-02	2.2214	0.14	0.3600E+00	0.7376*	0.32
0.5500E-02	2.0110	0.14	0.3750E+00	0.6565	0.31
0.6500E-02	1.8516	0.14	0.3850E+00	0.6128*	0.31
0.7500E-02	1.7243	0.14	0.4000E+00	0.5591	0.31
0.8500E-02	1.6221	0.14	0.4100E+00	0.5294*	0.31
0.9500E-02	1.5358	0.14	0.4250E+00	0.4919	0.31
0.1500E-01	1.2301	0.14	0.4350E+00	0.4706*	0.31
0.2000E-01	1.0737	0.15	0.4500E+00	0.4431	0.31
0.2400E-01	0.9867	0.15	0.4600E+00	0.4273*	0.31
0.3000E-01	0.8930	0.16	0.4750E+00	0.4065	0.31
0.3500E-01	0.8359*	0.17	0.4850E+00	0.3944*	0.31
0.4500E-01	0.7562	0.18	0.5000E+00	0.3782	0.31
0.5500E-01	0.7052	0.20	0.5200E+00	0.3597	0.31
0.6500E-01	0.6725	0.22	0.5400E+00	0.3441	0.32
0.7500E-01	0.6532	0.24	0.5700E+00	0.3249	0.32
0.8500E-01	0.6450	0.26	0.6000E+00	0.3093	0.33
0.9500E-01	0.6468	0.29	0.6500E+00	0.2891	0.34
0.1000E+00	0.6515	0.30	0.7000E+00	0.2740	0.35
0.1100E+00	0.6687*	0.32	0.7500E+00	0.2623	0.36
0.1200E+00	0.6976	0.33	0.8000E+00	0.2529	0.37
0.1300E+00	0.7406*	0.34	0.8500E+00	0.2454	0.38
0.1400E+00	0.8013*	0.35	0.9000E+00	0.2391	0.39
0.1500E+00	0.8843	0.36	0.9400E+00	0.2349	0.39
0.1600E+00	0.9968*	0.36	0.9600E+00	0.2331	0.40
0.1700E+00	1.1485	0.35	0.9800E+00	0.2313	0.40
0.1800E+00	1.3522	0.35	0.1000E+01	0.2297	0.41
0.1900E+00	1.6207	0.34	0.1100E+01	0.2232	0.43
0.2000E+00	1.9653	0.32	0.1250E+01	0.2171	0.47
0.2100E+00	2.3763	0.30	0.1400E+01	0.2143	0.51
0.2200E+00	2.8047	0.27	0.1600E+01	0.2143	0.56
0.2300E+00	3.1393	0.25	0.1800E+01	0.2184	0.64
0.2350E+00	3.2311	0.24	0.2000E+01	0.2184	0.67
0.2360E+00	3.2416*	0.24	0.2200E+01	0.2108	0.63
0.2370E+00	3.2495*	0.24	0.2400E+01	0.2006	0.68
0.2380E+00	3.2546*	0.24	0.2600E+01	0.1896	0.75
0.2390E+00	3.2571*	0.24	0.2800E+01	0.1774	0.85
0.2400E+00	3.2568	0.23			

^{6}Li(n,n)

Cross sections are not final
Uncertainties are not final
Linear-linear interpolation

E_n(MeV)	σ(b)	Uncertainty(%)	E_n(MeV)	σ(b)	Uncertainty(%)
0.2530E-07	0.6717	1.27	0.2350E+00	7.7537	0.35
0.9400E-05	0.6713	1.27	0.2400E+00	8.0351	0.32
0.1500E-03	0.6701	1.27	0.2450E+00	8.1469	0.30
0.2500E-03	0.6696	1.27	0.2500E+00	8.0949	0.29
0.3500E-03	0.6692	1.27	0.2600E+00	7.6053	0.30
0.4500E-03	0.6689	1.27	0.2700E+00	6.8402	0.32
0.5500E-03	0.6686	1.27	0.2800E+00	6.0288	0.34
0.6500E-03	0.6683	1.27	0.3000E+00	4.6619	0.38
0.7500E-03	0.6681	1.27	0.3250E+00	3.5376	0.39
0.8500E-03	0.6679	1.27	0.3500E+00	2.8498	0.40
0.9500E-03	0.6676	1.27	0.3750E+00	2.4095	0.41
0.1500E-02	0.6666	1.27	0.4000E+00	2.1125	0.41
0.2500E-02	0.6651	1.27	0.4250E+00	1.9013	0.41
0.3500E-02	0.6639	1.27	0.4500E+00	1.7443	0.42
0.4500E-02	0.6629	1.27	0.4750E+00	1.6258	0.43
0.5500E-02	0.6619	1.27	0.5000E+00	1.5319	0.43
0.6500E-02	0.6611	1.27	0.5200E+00	1.4706	0.43
0.7500E-02	0.6604	1.27	0.5400E+00	1.4191	0.44
0.8500E-02	0.6597	1.27	0.5700E+00	1.3536	0.44
0.9500E-02	0.6590	1.27	0.6000E+00	1.3020	0.44
0.1500E-01	0.6561	1.26	0.6500E+00	1.2332	0.45
0.2000E-01	0.6545	1.26	0.7000E+00	1.1821	0.45
0.2400E-01	0.6537	1.25	0.7500E+00	1.1428	0.45
0.3000E-01	0.6531	1.24	0.8000E+00	1.1123	0.45
0.4500E-01	0.6565	1.21	0.8500E+00	1.0876	0.45
0.5500E-01	0.6628	1.19	0.9000E+00	1.0688	0.45
0.6500E-01	0.6732	1.15	0.9400E+00	1.0561	0.45
0.7500E-01	0.6889	1.11	0.9600E+00	1.0497	0.45
0.8500E-01	0.7114	1.06	0.9800E+00	1.0454	0.45
0.9500E-01	0.7425	1.01	0.1000E+01	1.0410	0.45
0.1000E+00	0.7622	0.98	0.1100E+01	1.0239	0.45
0.1200E+00	0.8800	0.83	0.1250E+01	1.0141	0.46
0.1500E+00	1.2710	0.62	0.1400E+01	1.0194	0.49
0.1700E+00	1.8420	0.54	0.1600E+01	1.0464	0.51
0.1800E+00	2.3028	0.53	0.1800E+01	1.0972	0.54
0.1900E+00	2.9411	0.52	0.2000E+01	1.1729	0.56
0.2000E+00	3.8025	0.50	0.2200E+01	1.2564	0.57
0.2100E+00	4.9038	0.48	0.2400E+01	1.3437	0.57
0.2200E+00	6.1593	0.43	0.2600E+01	1.4398	0.57
0.2300E+00	7.3212	0.38	0.2800E+01	1.5072	0.59

Appendix D (Continued)

$^{10}B(n,\alpha_0)$

Proposed final cross sections below 250 keV
Uncertainties are not final
Log-log interpolation up to 500 keV
Linear-linear interpolation above 500 keV

E_n(MeV)	σ(b)	Uncertainty(%)	E_n(MeV)	σ(b)	Uncertainty(%)
0.2530E-07	241.2677	0.21	0.1900E+00	0.1434	0.76
0.9400E-05	12.5002	0.21	0.2000E+00	0.1438	0.76
0.1500E-03	3.1169	0.21	0.2100E+00	0.1439	0.77
0.2500E-03	2.4105	0.21	0.2200E+00	0.1439	0.78
0.3500E-03	2.0347	0.21	0.2300E+00	0.1439	0.79
0.4500E-03	1.7928	0.21	0.2350E+00	0.1438	0.80
0.5500E-03	1.6199	0.21	0.2400E+00	0.1438	0.81
0.6500E-03	1.4889	0.21	0.2450E+00	0.1437	0.82
0.7500E-03	1.3850	0.21	0.2500E+00	0.1436	0.82
0.8500E-03	1.3000	0.21	0.2600E+00	0.1435	0.83
0.9500E-03	1.2290	0.21	0.2700E+00	0.1432	0.84
0.1500E-02	0.9748	0.21	0.2800E+00	0.1431	0.84
0.2500E-02	0.7519	0.21	0.3000E+00	0.1431	0.86
0.3500E-02	0.6333	0.22	0.3250E+00	0.1442	0.91
0.4500E-02	0.5571	0.22	0.3500E+00	0.1471	0.99
0.5500E-02	0.5028	0.23	0.3750E+00	0.1533	1.08
0.6500E-02	0.4617	0.25	0.4000E+00	0.1638	1.10
0.7500E-02	0.4291	0.26	0.4250E+00	0.1787	1.07
0.8500E-02	0.4025	0.28	0.4500E+00	0.1951	1.05
0.9500E-02	0.3804	0.30	0.4750E+00	0.2062	1.08
0.1500E-01	0.3017	0.40	0.5000E+00	0.2072	1.05
0.2000E-01	0.2613	0.50	0.5200E+00	0.2011	0.98
0.2400E-01	0.2390	0.57	0.5400E+00	0.1913	0.91
0.3000E-01	0.2148	0.66	0.5700E+00	0.1747	0.87
0.4500E-01	0.1796	0.81	0.6000E+00	0.1592	0.87
0.5500E-01	0.1662	0.86	0.6500E+00	0.1396	0.86
0.6500E-01	0.1572	0.87	0.7000E+00	0.1261	0.87
0.7500E-01	0.1510	0.87	0.7500E+00	0.1170	1.01
0.8500E-01	0.1467	0.87	0.8000E+00	0.1106	1.30
0.9500E-01	0.1440	0.87	0.8500E+00	0.1062	1.70
0.1000E+00	0.1431	0.86	0.9000E+00	0.1031	2.16
0.1200E+00	0.1412	0.87	0.9400E+00	0.1014	2.56
0.1500E+00	0.1417	0.84	0.9600E+00	0.1008	2.77
0.1700E+00	0.1426	0.80	0.9800E+00	0.1003	2.99
0.1800E+00	0.1431	0.78	0.1000E+01	0.0999	3.21

Appendix D (Continued)

$^{10}B(n,\alpha_1)$

Proposed final cross sections below 250 keV
Uncertainties are not final
Log-log interpolation up to 500 keV
Linear-linear interpolation above 500 keV

E_n(MeV)	σ(b)	Uncertainty(%)	E_n(MeV)	σ(b)	Uncertainty(%)
0.2530E-07	3598.2280	0.16	0.1900E+00	1.3340	0.59
0.9400E-05	186.4350	0.16	0.2000E+00	1.2876	0.60
0.1500E-03	46.5003	0.16	0.2100E+00	1.2417	0.61
0.2500E-03	35.9671	0.16	0.2200E+00	1.1972	0.62
0.3500E-03	30.3659	0.16	0.2300E+00	1.1543	0.62
0.4500E-03	26.7516	0.16	0.2350E+00	1.1338	0.62
0.5500E-03	24.1756	0.16	0.2400E+00	1.1127	0.62
0.6500E-03	22.2287	0.16	0.2450E+00	1.0928	0.63
0.7500E-03	20.6811	0.16	0.2500E+00	1.0732	0.63
0.8500E-03	19.4130	0.17	0.2600E+00	1.0346	0.64
0.9500E-03	18.3446	0.17	0.2700E+00	0.9976	0.65
0.1500E-02	14.5603	0.17	0.2800E+00	0.9623	0.67
0.2500E-02	11.2352	0.17	0.3000E+00	0.8967	0.73
0.3500E-02	9.4717	0.17	0.3250E+00	0.8243	0.82
0.4500E-02	8.3353	0.18	0.3500E+00	0.7636	0.87
0.5500E-02	7.5254	0.18	0.3750E+00	0.7163	0.89
0.6500E-02	6.9123	0.18	0.4000E+00	0.6833	0.91
0.7500E-02	6.4260	0.18	0.4250E+00	0.6634	0.96
0.8500E-02	6.0296	0.18	0.4500E+00	0.6494	1.02
0.9500E-02	5.6981	0.18	0.4750E+00	0.6282	1.04
0.1500E-01	4.5194	0.20	0.5000E+00	0.5910	1.04
0.2000E-01	3.9090	0.21	0.5200E+00	0.5515	1.03
0.2400E-01	3.5682	0.23	0.5400E+00	0.5082	1.02
0.3000E-01	3.1959	0.25	0.5700E+00	0.4452	1.01
0.4500E-01	2.6285	0.30	0.6000E+00	0.3901	1.00
0.5500E-01	2.3943	0.33	0.6500E+00	0.3182	1.00
0.6500E-01	2.2203	0.35	0.7000E+00	0.2659	1.04
0.7500E-01	2.0844	0.38	0.7500E+00	0.2267	1.14
0.8500E-01	1.9745	0.40	0.8000E+00	0.1965	1.28
0.9500E-01	1.8835	0.43	0.8500E+00	0.1727	1.44
0.1000E+00	1.8420	0.44	0.9000E+00	0.1535	1.62
0.1200E+00	1.7031	0.49	0.9400E+00	0.1405	1.76
0.1500E+00	1.5330	0.55	0.9600E+00	0.1348	1.84
0.1700E+00	1.4303	0.57	0.9800E+00	0.1294	1.91
0.1800E+00	1.3817	0.58	0.1000E+01	0.1244	1.99

Appendix D (Continued)

$^{10}B(n,n)$

Cross sections are not final
Uncertainties are not final
Linear-linear interpolation

E_n(MeV)	σ(b)	Uncertainty(%)	E_n(MeV)	σ(b)	Uncertainty(%)
0.2530E-07	2.1413	1.42	0.1900E+00	3.3303	0.38
0.9400E-05	2.1386	1.42	0.2000E+00	3.3935	0.37
0.1500E-03	2.1312	1.42	0.2100E+00	3.4529	0.36
0.2500E-03	2.1283	1.42	0.2200E+00	3.5076	0.36
0.3500E-03	2.1265	1.42	0.2300E+00	3.5578	0.36
0.4500E-03	2.1245	1.41	0.2350E+00	3.5813	0.35
0.5500E-03	2.1236	1.41	0.2400E+00	3.6027	0.35
0.6500E-03	2.1216	1.41	0.2450E+00	3.6241	0.35
0.7500E-03	2.1206	1.41	0.2500E+00	3.6444	0.35
0.8500E-03	2.1197	1.40	0.2600E+00	3.6812	0.35
0.9500E-03	2.1187	1.40	0.2700E+00	3.7130	0.35
0.1500E-02	2.1156	1.39	0.2800E+00	3.7401	0.35
0.2500E-02	2.1122	1.36	0.3000E+00	3.7821	0.35
0.3500E-02	2.1107	1.34	0.3250E+00	3.8119	0.35
0.4500E-02	2.1101	1.31	0.3500E+00	3.8191	0.35
0.5500E-02	2.1114	1.29	0.3750E+00	3.8083	0.36
0.6500E-02	2.1117	1.26	0.4000E+00	3.7833	0.37
0.7500E-02	2.1141	1.24	0.4250E+00	3.7475	0.39
0.8500E-02	2.1154	1.22	0.4500E+00	3.7065	0.41
0.9500E-02	2.1187	1.19	0.4750E+00	3.6590	0.42
0.1500E-01	2.1349	1.08	0.5000E+00	3.6044	0.42
0.2000E-01	2.1548	0.99	0.5200E+00	3.5538	0.42
0.2400E-01	2.1725	0.93	0.5400E+00	3.4994	0.42
0.3000E-01	2.2025	0.85	0.5700E+00	3.4121	0.43
0.4500E-01	2.2854	0.71	0.6000E+00	3.3228	0.44
0.5500E-01	2.3478	0.66	0.6500E+00	3.1765	0.46
0.6500E-01	2.4135	0.62	0.7000E+00	3.0380	0.49
0.7500E-01	2.4826	0.59	0.7500E+00	2.9093	0.52
0.8500E-01	2.5539	0.57	0.8000E+00	2.7902	0.55
0.9500E-01	2.6272	0.55	0.8500E+00	2.6819	0.58
0.1000E+00	2.6652	0.54	0.9000E+00	2.5813	0.62
0.1200E+00	2.8178	0.50	0.9400E+00	2.5069	0.64
0.1500E+00	3.0476	0.43	0.9600E+00	2.4722	0.66
0.1700E+00	3.1951	0.40	0.9800E+00	2.4374	0.67
0.1800E+00	3.2641	0.39	0.1000E+01	2.4046	0.68

Appendix D (Continued)

Au(n,γ)

Proposed final cross sections from 200 keV to 2.5 MeV
Structure may be imposed below 200 keV

Average cross sections are given
from the interval (2.0-3.0 keV), labelled 0.2500E-02 MeV;
to the interval (10-20 keV), labelled 0.1500E-01 MeV

Uncertainties are not final
Linear-linear interpolation

E_n(MeV)	σ(b)	Uncertainty(%)	E_n(MeV)	σ(b)	Uncertainty(%)
0.2530E-07	98.6862*	0.14	0.2800E+00	0.2141	1.31
0.2500E-02	2.4597	3.59	0.3000E+00	0.1999	1.30
0.3500E-02	2.6251	1.37	0.3250E+00	0.1877	1.23
0.4500E-02	2.2280	1.30	0.3500E+00	0.1778	1.25
0.5500E-02	1.9593	1.33	0.3750E+00	0.1689	1.25
0.6500E-02	1.7731	1.40	0.4000E+00	0.1614	1.16
0.7500E-02	1.5641	1.30	0.4250E+00	0.1538	1.21
0.8500E-02	1.3459	1.34	0.4500E+00	0.1462	1.17
0.9500E-02	1.2001	1.27	0.4750E+00	0.1389	1.27
0.1500E-01	0.8918	1.09	0.5000E+00	0.1324	1.15
0.2000E-01	0.6963	1.74	0.5200E+00	0.1270	1.22
0.2400E-01	0.6396	0.92	0.5400E+00	0.1236	1.33
0.3000E-01	0.5863	0.75	0.5700E+00	0.1186	1.64
0.4500E-01	0.4570	0.98	0.6000E+00	0.1084	1.37
0.5500E-01	0.4131	1.08	0.6500E+00	0.1002	1.73
0.6500E-01	0.3796	1.04	0.7000E+00	0.0964	1.42
0.7500E-01	0.3535	1.03	0.7500E+00	0.0928	1.66
0.8500E-01	0.3300	1.03	0.8000E+00	0.0897	1.57
0.9500E-01	0.3150	1.11	0.8500E+00	0.0869	2.10
0.1000E+00	0.3099	1.14	0.9000E+00	0.0843	3.10
0.1200E+00	0.2921	0.98	0.9400E+00	0.0825	3.10
0.1500E+00	0.2719	0.97	0.9600E+00	0.0818	3.70
0.1700E+00	0.2617	1.15	0.9800E+00	0.0810	4.00
0.1800E+00	0.2567	1.40	0.1000E+01	0.0803	2.50
0.1900E+00	0.2534	1.41	0.1100E+01	0.0772	1.80
0.2000E+00	0.2502	1.24	0.1250E+01	0.0729	1.48
0.2100E+00	0.2469	1.43	0.1400E+01	0.0694	1.75
0.2200E+00	0.2445	1.35	0.1600E+01	0.0665	1.70
0.2300E+00	0.2415	1.35	0.1800E+01	0.0596	1.78
0.2350E+00	0.2403	1.33	0.2000E+01	0.0534	2.05
0.2400E+00	0.2388	1.67	0.2200E+01	0.0433	2.01
0.2450E+00	0.2374	1.23	0.2400E+01	0.0360	3.02
0.2500E+00	0.2360	1.36	0.2600E+01	0.0311	2.40
0.2600E+00	0.2331	1.38	0.2800E+01	0.0255	2.23
0.2700E+00	0.2299	1.49			

*This value differs slightly from that of ENDF/B-VI.

Appendix D (Continued)

$^{235}U(n,f)$

Proposed final cross sections above 150 keV
Structure may be imposed below 150 keV
The 9.4 eV value is the integral cross section from 7.8 to 11 eV

Average cross sections are given
from the interval (0.1-0.2 keV), labelled 0.1500E-03 MeV;
to the interval (10-20 keV), labelled 0.1500E-01 MeV

Uncertainties are not final
Linear-linear interpolation

E_n(MeV)	σ(b)	Uncertainty(%)	E_n(MeV)	σ(b)	Uncertainty(%)
0.2530E-07	584.2522*	0.19	0.1700E+00	1.3967	0.72
0.9400E-05	246.4970#	0.42	0.1800E+00	1.3800	0.70
0.1500E-03	21.1374	0.44	0.1900E+00	1.3647	0.82
0.2500E-03	20.6721	0.46	0.2000E+00	1.3510	0.79
0.3500E-03	13.1380	0.51	0.2100E+00	1.3370	0.71
0.4500E-03	13.7862	0.52	0.2200E+00	1.3265	0.71
0.5500E-03	15.1890	0.53	0.2300E+00	1.3130	0.63
0.6500E-03	11.4739	0.54	0.2350E+00	1.3100	0.67
0.7500E-03	11.1436	0.54	0.2400E+00	1.3070	0.68
0.8500E-03	8.2481	0.54	0.2450E+00	1.3030	0.64
0.9500E-03	7.5274	0.55	0.2500E+00	1.2930	0.58
0.1500E-02	7.3465	0.49	0.2600E+00	1.2690	0.63
0.2500E-02	5.3900	0.55	0.2700E+00	1.2500	0.62
0.3500E-02	4.7822	0.53	0.2800E+00	1.2350	0.65
0.4500E-02	4.2729	0.53	0.3000E+00	1.2300	0.60
0.5500E-02	3.8012	0.61	0.3250E+00	1.2300	0.70
0.6500E-02	3.2824	0.57	0.3500E+00	1.2230	0.64
0.7500E-02	3.2558	0.52	0.3750E+00	1.2130	0.70
0.8500E-02	3.0166	0.56	0.4000E+00	1.2020	0.66
0.9500E-02	3.1130	0.56	0.4250E+00	1.1900	0.74
0.1500E-01	2.4975	0.49	0.4500E+00	1.1662	0.70
0.2000E-01	2.3932	1.81	0.4750E+00	1.1510	0.73
0.2400E-01	2.1627	0.49	0.5000E+00	1.1410	0.59
0.3000E-01	2.0908	0.60	0.5200E+00	1.1365	0.72
0.4500E-01	1.8486	0.54	0.5400E+00	1.1300	0.62
0.5500E-01	1.8029	0.54	0.5700E+00	1.1220	0.67
0.6500E-01	1.7437	0.55	0.6000E+00	1.1185	0.62
0.7500E-01	1.6766	0.53	0.6500E+00	1.1182	0.58
0.8500E-01	1.5909	0.56	0.7000E+00	1.1135	0.59
0.9500E-01	1.5665	0.61	0.7500E+00	1.1120	0.58
0.1000E+00	1.5724	0.63	0.8000E+00	1.1100	0.56
0.1200E+00	1.4961	0.58	0.8500E+00	1.1135	0.59
0.1500E+00	1.4203	0.58	0.9000E+00	1.1372	0.57

*This value differs slightly from that of ENDF/B-VI.
#units of barn-eV

Appendix D (Continued)

$^{235}U(n,f)$ (Continued)

E_n(MeV)	σ(b)	Uncertainty(%)	E_n(MeV)	σ(b)	Uncertainty(%)
0.9400E+00	1.1691	0.60	0.6000E+01	1.0985	0.85
0.9600E+00	1.1876	0.64	0.6200E+01	1.1817	0.87
0.9800E+00	1.1992	0.72	0.6500E+01	1.3481	0.87
0.1000E+01	1.1969	0.52	0.7000E+01	1.5467	0.89
0.1100E+01	1.1938	0.54	0.7500E+01	1.6964	0.94
0.1250E+01	1.2020	0.51	0.7750E+01	1.7300	1.05
0.1400E+01	1.2200	0.54	0.8000E+01	1.7606	1.01
0.1600E+01	1.2435	0.52	0.8500E+01	1.7800	0.89
0.1800E+01	1.2619	0.54	0.9000E+01	1.7700	0.99
0.2000E+01	1.2714	0.51	0.1000E+02	1.7415	1.06
0.2200E+01	1.2699	0.53	0.1100E+02	1.7219	1.11
0.2400E+01	1.2561	0.55	0.1150E+02	1.7170	1.26
0.2600E+01	1.2442	0.59	0.1200E+02	1.7347	1.14
0.2800E+01	1.2220	0.62	0.1300E+02	1.9002	0.90
0.3000E+01	1.2010	0.58	0.1400E+02	2.0600	0.59
0.3600E+01	1.1473	0.62	0.1450E+02	2.0800	0.51
0.4000E+01	1.1295	0.63	0.1500E+02	2.0890	0.84
0.4500E+01	1.1011	0.64	0.1600E+02	2.0890	1.10
0.4700E+01	1.0923	0.70	0.1700E+02	2.0413	1.27
0.5000E+01	1.0617	0.70	0.1800E+02	1.9748	1.26
0.5300E+01	1.0502	0.72	0.1900E+02	1.9325	1.25
0.5500E+01	1.0388	0.72	0.2000E+02	1.9343	1.52
0.5800E+01	1.0408	0.78			

Appendix D (Continued)

$^{238}U(n,f)$

Average cross sections proposed as final in the full energy range
Structure may be imposed below 4 MeV
Uncertainties are not final
Linear-linear interpolation

The values with †'s were supplied by the ENDF evaluator (W. Poenitz)
but are not part of the present evaluation process

The values with *'s are points added for ease in interpolation

E_n(MeV)	σ(b)	Uncertainty(%)	E_n(MeV)	σ(b)	Uncertainty(%)
0.3000E+00	0.0001133†	10.00	0.1100E+01	0.03004	1.41
0.3500E+00	0.0001852†	9.39	0.1130E+01	0.03600†*	1.38
0.3800E+00	0.0002329†	9.03	0.1140E+01	0.03810†*	1.37
0.4000E+00	0.0002513†	8.78	0.1150E+01	0.03920†*	1.36
0.4200E+00	0.0002758†	8.54	0.1170E+01	0.04025†*	1.34
0.4300E+00	0.0002758†	8.42	0.1200E+01	0.04209†*	1.31
0.4400E+00	0.0002830†	8.30	0.1230E+01	0.04030†*	1.28
0.4500E+00	0.0002849†	8.18	0.1240E+01	0.04000†*	1.28
0.4600E+00	0.0002908†	8.06	0.1250E+01	0.03912	1.27
0.4700E+00	0.0003037†	7.93	0.1280E+01	0.05020†*	1.24
0.5000E+00	0.0003764†	7.57	0.1300E+01	0.06500†*	1.22
0.5500E+00	0.0006295†	6.96	0.1350E+01	0.1119†*	1.17
0.5800E+00	0.0006908†	6.60	0.1400E+01	0.1855	1.13
0.5900E+00	0.0007588†	6.48	0.1450E+01	0.2822†*	1.08
0.6000E+00	0.0008226†	6.36	0.1480E+01	0.3310†*	1.05
0.6200E+00	0.0009277†	6.11	0.1500E+01	0.3560†*	1.03
0.6400E+00	0.001128†	5.87	0.1525E+01	0.3805†*	1.01
0.6500E+00	0.001239†	5.75	0.1550E+01	0.3990†*	0.98
0.6600E+00	0.001294†	5.63	0.1575E+01	0.4125†*	0.96
0.6800E+00	0.001574†	5.39	0.1600E+01	0.4226	0.94
0.7000E+00	0.001717†	5.14	0.1700E+01	0.4550†*	0.84
0.7500E+00	0.002574†	4.54	0.1800E+01	0.4820	0.75
0.7800E+00	0.003578†	4.17	0.1900E+01	0.5070†*	0.75
0.8000E+00	0.004470†	3.93	0.2000E+01	0.5250	0.72
0.8500E+00	0.007168†	3.32	0.2100E+01	0.5355†*	0.73
0.8800E+00	0.01077†	2.96	0.2200E+01	0.5391	0.73
0.9000E+00	0.01362†	2.71	0.2400E+01	0.5373	0.75
0.9300E+00	0.01549†	2.35	0.2600E+01	0.5328	0.73
0.9500E+00	0.01654†	2.11	0.2800E+01	0.5270	0.79
0.9700E+00	0.01582†	1.86	0.3000E+01	0.5160	0.75
0.1000E+01	0.01398	1.50	0.3200E+01	0.5210†*	0.75
0.1020E+01	0.01570†*	1.48	0.3600E+01	0.5354	0.78
0.1030E+01	0.01693†*	1.47	0.4000E+01	0.5483	0.81
0.1050E+01	0.02000†*	1.45	0.4500E+01	0.5496	0.82
0.1080E+01	0.02700†*	1.43	0.4700E+01	0.5470	0.89

Appendix D (Continued)

$^{238}U(n,f)$ (Continued)

E_n(MeV)	σ(b)	Uncertainty(%)	E_n(MeV)	σ(b)	Uncertainty(%)
0.5000E+01	0.5404	0.87	0.9000E+01	0.9979	1.15
0.5300E+01	0.5430	0.92	0.1000E+02	0.9868	1.21
0.5500E+01	0.5500	0.90	0.1100E+02	0.9830	1.36
0.5800E+01	0.5731	0.95	0.1150E+02	0.9830	1.50
0.6000E+01	0.6153	1.03	0.1200E+02	0.9850	1.33
0.6200E+01	0.6859	1.04	0.1300E+02	1.0130	1.04
0.6500E+01	0.8257	1.01	0.1400E+02	1.1300	0.76
0.6700E+01	0.8860*	1.02	0.1450E+02	1.1555	0.70
0.7000E+01	0.9403	1.04	0.1500E+02	1.1980	0.94
0.7300E+01	0.9680*	1.08	0.1600E+02	1.2593	1.26
0.7500E+01	0.9807	1.11	0.1700E+02	1.2561	1.40
0.7750E+01	0.9910	1.23	0.1800E+02	1.2493	1.44
0.8000E+01	0.9935	1.16	0.1900E+02	1.2954	1.49
0.8500E+01	1.0000	1.07	0.2000E+02	1.3521	1.74

Appendix D (Continued)

$^{238}U(n,\gamma)$

Proposed final from 150 keV to 2 MeV
Structure may be imposed below 150 keV

Average cross sections are given
from the interval (0.1-0.2 keV), labelled 0.1500E-03 MeV;
to the interval (10-20 keV), labelled 0.1500E-01 MeV

Uncertainties are not final
Interpolation rules to be determined

E_n(MeV)	σ(b)	Uncertainty(%)	E_n(MeV)	σ(b)	Uncertainty(%)
0.2530E-07	2.7081	0.35	0.2300E+00	0.1210	1.59
0.1500E-03	16.1260	2.24	0.2350E+00	0.1201	3.03
0.2500E-03	8.1332	2.12	0.2400E+00	0.1194	2.49
0.3500E-03	2.7346	2.11	0.2450E+00	0.1192	1.85
0.4500E-03	2.5204	2.12	0.2500E+00	0.1184	2.02
0.5500E-03	4.2754	3.48	0.2600E+00	0.1173	1.58
0.6500E-03	3.3746	1.94	0.2700E+00	0.1162	2.90
0.7500E-03	1.6737	1.88	0.2800E+00	0.1158	1.92
0.8500E-03	2.7942	1.94	0.3000E+00	0.1150	1.59
0.9500E-03	3.7471	1.95	0.3250E+00	0.1140	2.44
0.1500E-02	1.7843	1.92	0.3500E+00	0.1138	1.82
0.2500E-02	1.3305	2.07	0.3750E+00	0.1128	1.77
0.3500E-02	1.0917	2.24	0.4000E+00	0.1119	1.36
0.4500E-02	0.8671	2.36	0.4250E+00	0.1112	2.55
0.5500E-02	0.8445	2.17	0.4500E+00	0.1106	1.66
0.6500E-02	0.7639	2.22	0.4750E+00	0.1098	5.66
0.7500E-02	0.7246	2.13	0.5000E+00	0.1093	1.37
0.8500E-02	0.6240	2.41	0.5200E+00	0.1095	2.08
0.9500E-02	0.6430	2.03	0.5400E+00	0.1101	1.83
0.1500E-01	0.5656	1.54	0.5700E+00	0.1102	1.90
0.2000E-01	0.5035	1.77	0.6000E+00	0.1113	2.40
0.2400E-01	0.4686	1.16	0.6500E+00	0.1160	5.70
0.3000E-01	0.4264	1.03	0.7000E+00	0.1189	6.30
0.4500E-01	0.3494	1.15	0.7500E+00	0.1192	4.10
0.5500E-01	0.2802	1.22	0.8000E+00	0.1205	1.90
0.6500E-01	0.2411	1.22	0.8500E+00	0.1217	5.16
0.7500E-01	0.2116	1.27	0.9000E+00	0.1228	2.51
0.8500E-01	0.1924	1.27	0.9400E+00	0.1248	2.35
0.9500E-01	0.1796	1.25	0.9600E+00	0.1260	2.76
0.1000E+00	0.1746	1.27	0.1000E+01	0.1251	2.17
0.1200E+00	0.1585	1.16	0.1100E+01	0.1143	2.14
0.1500E+00	0.1415	1.26	0.1250E+01	0.0927	1.98
0.1700E+00	0.1336	1.63	0.1400E+01	0.0782	2.06
0.1800E+00	0.1313	2.42	0.1600E+01	0.0640	2.01
0.1900E+00	0.1285	1.81	0.1800E+01	0.0560	2.58
0.2000E+00	0.1274	1.67	0.2000E+01	0.0461	3.17
0.2100E+00	0.1244	1.71	0.2200E+01	0.0376	2.81
0.2200E+00	0.1226	2.58			

Appendix D (Continued)

^{239}Pu(n,f)

Proposed final cross sections above 150 keV
Structure may be imposed below 150 keV

Average cross sections are given
from the interval (0.1-0.2 keV), labelled 0.1500E-03 MeV;
to the interval (10-20 keV), labelled 0.1500E-01 MeV

Uncertainties not final
Interpolation rules to be determined

E_n(MeV)	σ(b)	Uncertainty(%)	E_n(MeV)	σ(b)	Uncertainty(%)
0.2530E-07	747.9861*	0.25	0.2000E+00	1.4766	1.01
0.1500E-03	18.6664	0.69	0.2100E+00	1.4820	1.14
0.2500E-03	17.8794	0.67	0.2200E+00	1.4880	1.02
0.3500E-03	8.4301	0.70	0.2300E+00	1.4920	0.84
0.4500E-03	9.5697	0.69	0.2400E+00	1.4950	1.33
0.5500E-03	15.5569	0.70	0.2450E+00	1.4980	0.92
0.6500E-03	4.4593	0.83	0.2500E+00	1.5040	0.99
0.7500E-03	5.6301	0.72	0.2600E+00	1.5090	1.02
0.8500E-03	4.9794	0.77	0.2700E+00	1.5150	0.84
0.9500E-03	8.2969	0.81	0.2800E+00	1.5200	0.85
0.1500E-02	4.4659	0.71	0.3000E+00	1.5255	0.85
0.2500E-02	3.3041	0.76	0.3250E+00	1.5348	0.84
0.3500E-02	3.0000	0.77	0.3500E+00	1.5380	0.79
0.4500E-02	2.3830	0.75	0.3750E+00	1.5400	0.90
0.5500E-02	2.3007	0.78	0.4000E+00	1.5405	0.83
0.6500E-02	2.0083	0.84	0.4250E+00	1.5450	1.39
0.7500E-02	2.0536	0.68	0.4500E+00	1.5500	0.84
0.8500E-02	2.2164	0.79	0.4750E+00	1.5520	0.87
0.9500E-02	1.8641	0.78	0.5000E+00	1.5558	0.76
0.1500E-01	1.7637	0.63	0.5200E+00	1.5630	1.09
0.2000E-01	1.7683	1.86	0.5400E+00	1.5670	0.77
0.2400E-01	1.5947	0.72	0.5700E+00	1.5800	0.95
0.3000E-01	1.6587	0.74	0.6000E+00	1.5880	0.94
0.4500E-01	1.4900	0.67	0.6500E+00	1.6100	0.71
0.5500E-01	1.5350	0.74	0.7000E+00	1.6243	0.76
0.6500E-01	1.5300	0.71	0.7500E+00	1.6420	0.69
0.7500E-01	1.5280	0.78	0.8000E+00	1.6580	0.70
0.8500E-01	1.5220	0.73	0.8500E+00	1.6752	0.73
0.9500E-01	1.5150	1.00	0.9000E+00	1.6850	0.72
0.1000E+00	1.5150	0.83	0.9400E+00	1.6900	0.81
0.1200E+00	1.5058	0.71	0.9600E+00	1.6940	0.78
0.1500E+00	1.4820	0.67	0.9800E+00	1.7020	0.98
0.1700E+00	1.4800	0.85	0.1000E+01	1.7128	0.64
0.1800E+00	1.4747	0.93	0.1100E+01	1.7420	0.70
0.1900E+00	1.4780	1.06	0.1250E+01	1.8241	0.62

*This value differs slightly from that of ENDF/B-VI.

Appendix D (Continued)

^{239}Pu(n,f) (Continued)

E_n(MeV)	σ(b)	Uncertainty(%)	E_n(MeV)	σ(b)	Uncertainty(%)
0.1400E+01	1.8894	0.64	0.7000E+01	2.0813	1.04
0.1600E+01	1.9137	0.64	0.7500E+01	2.1691	1.08
0.1800E+01	1.9262	0.67	0.7750E+01	2.1974	1.16
0.2000E+01	1.9400	0.67	0.8000E+01	2.2110	1.36
0.2200E+01	1.9350	0.65	0.8500E+01	2.2030	1.07
0.2400E+01	1.9030	0.69	0.9000E+01	2.1917	1.13
0.2600E+01	1.8762	0.72	0.1000E+02	2.1778	1.21
0.2800E+01	1.8567	0.74	0.1100E+02	2.1742	1.28
0.3000E+01	1.8204	0.68	0.1150E+02	2.1850	1.48
0.3600E+01	1.7802	0.74	0.1200E+02	2.1980	1.34
0.4000E+01	1.7517	0.74	0.1300E+02	2.2674	1.16
0.4500E+01	1.7210	0.79	0.1400E+02	2.3877	0.86
0.4700E+01	1.7100	0.82	0.1450E+02	2.3753	0.64
0.5000E+01	1.6920	0.81	0.1500E+02	2.3600	1.21
0.5300E+01	1.6722	0.86	0.1600E+02	2.3038	1.35
0.5500E+01	1.6699	0.86	0.1700E+02	2.2443	1.56
0.5800E+01	1.6860	0.91	0.1800E+02	2.1855	1.51
0.6000E+01	1.7776	0.97	0.1900E+02	2.1808	1.67
0.6200E+01	1.8409	1.03	0.2000E+02	2.1850	1.88
0.6500E+01	1.9497	0.98			

Thermal (2200 m/s) Constants with Uncertainties in Percent

Quantity	^{233}U	^{235}U	^{239}Pu	^{241}Pu
σ_{nf}	531.1396 ± 0.25%	584.2522 ± 0.19%	747.9861 ± 0.25%	1012.6840 ± 0.65%
$\sigma_{n\gamma}$	45.5095 ± 1.50%	98.9649 ± 0.75%	271.4265 ± 0.79%	361.290 ± 1.37%
σ_{nn}	12.1309 ± 5.48%	15.4557 ± 6.87%	7.8835 ±12.30%	12.1738 ±21.50%
g_f	0.9955 ± 0.14%	0.9771 ± 0.08%	1.0563 ± 0.21%	1.0450 ± 0.53%
g_a	0.9996 ± 0.11%	0.9790 ± 0.08%	1.0782 ± 0.22%	1.0440 ± 0.19%
$\bar{\nu}$	2.4946 ± 0.16%	2.4320 ± 0.15%	2.8815 ± 0.18%	2.9453 ± 0.20%

^{252}Cf $\bar{\nu}$ 3.7676 ± 0.13%

The evaluation by Axton (CBNM Report GE/PH/01/86) was used as input